National Library of Canada
Bibliothèque nationale du Canada

Canadian Theses Service
Service des thèses canadiennes

Ottawa, Canada
K1A 0N4

NOTICE

The quality of this microform is heavily dependent upon the quality of the original thesis submitted for microfilming. Every effort has been made to ensure the highest quality of reproduction possible.

If pages are missing, contact the university which granted the degree.

Some pages may have indistinct print especially if the original pages were typed with a poor typewriter ribbon or if the university sent us an inferior photocopy.

Previously copyrighted materials (journal articles, published tests, etc.) are not filmed.

Reproduction in full or in part of this microform is governed by the Canadian Copyright Act, R.S.C. 1970, c. C-30.

AVIS

La qualité de cette microforme dépend grandement de la qualité de la thèse soumise au microfilmage. Nous avons tout fait pour assurer une qualité supérieure de reproduction.

S'il manque des pages, veuillez communiquer avec l'université qui a conféré le grade.

La qualité d'impression de certaines pages peut laisser à désirer, surtout si les pages originales ont été dactylographiées à l'aide d'un ruban usé ou si l'université nous a fait parvenir une photocopie de qualité inférieure.

Les documents qui font déjà l'objet d'un droit d'auteur (articles de revue, tests publiés, etc.) ne sont pas microfilmés.

La reproduction, même partielle, de cette microforme est soumise à la Loi canadienne sur le droit d'auteur, SRC 1970, c. C-30.

NL-339 (r. 88/04)

Canada

THE UNIVERSITY OF ALBERTA

MODELING AND DIAGNOSTIC OF PLASMA ETCHING PROCESSES

BY

© PHILIPPE SCHOENBORN

A THESIS

SUBMITTED TO THE FACULTY OF GRADUATE STUDIES AND RESEARCH

IN PARTIAL FULFILMENT OF THE REQUIREMENTS FOR THE DEGREE

OF MASTER OF SCIENCE

DEPARTMENT OF ELECTRICAL ENGINEERING

EDMONTON, ALBERTA

FALL 1987

Permission has been granted to the National Library of Canada to microfilm this thesis and to lend or sell copies of the film.

The author (copyright owner) has reserved other publication rights, and neither the thesis nor extensive extracts from it may be printed or otherwise reproduced without his/her written permission.

L'autorisation a été accordée à la Bibliothèque nationale du Canada de microfilmer cette thèse et de prêter ou de vendre des exemplaires du film.

L'auteur (titulaire du droit d'auteur) se réserve les autres droits de publication; ni la thèse ni de longs extraits de celle-ci ne doivent être imprimés ou autrement reproduits sans son autorisation écrite.

ISBN 0-315-40971-1

THE UNIVERSITY OF ALBERTA

RELEASE FORM

NAME OF AUTHOR : PHILIPPE SCHOENBORN

TITLE OF THESIS : MODELING AND DIAGNOSTIC OF PLASMA ETCHING PROCESSES

DEGREE : MASTER OF SCIENCE

YEAR THIS DEGREE GRANTED : 1987

Permission is hereby granted to THE UNIVERSITY OF ALBERTA LIBRARY to reproduce single copies of this thesis and to lend or sell such copies for private, scholarly or scientific research purposes only.

The author reserves other publication rights, and neither the thesis nor extensive extracts from it may be printed or otherwise reproduced without the author's written permission.

Schoenborn

(student's signature)

3, Côte aux Vignes
1097 RIEX (VAUD)
SWITZERLAND
(student's permanent address)

Date : Sept. 9, 1987

THE UNIVERSITY OF ALBERTA

FACULTY OF GRADUATE STUDIES AND RESEARCH

The undersigned certify that they have read, and recommend to the Faculty of Graduate Studies and Research for acceptance, a thesis entitled, 'Modeling and Diagnostic of Plasma Etching Processes',
submitted by Philippe Schoenborn
in partial fulfilment of the requirements for the degree of Master of Science.

(Supervisor)

Date : 2 Sept 87

Abstract

The optimization, the modeling and the experimental diagnostic of plasma etching processes using a commercial parallel plate single wafer etcher are presented. Firstly, polysilicon and SiO_2 etch rates in fluorocarbon chemistries have been measured for various combinations of the process parameters according to the statistical design of experiments methodology. The use of empirical modeling of etch rates in a multidimensional parameter space is discussed. Secondly, a numerical simulation of the gas phase chemistry of a CF_4/O_2 plasma is presented. The calculated concentrations of free fluorine and oxygen atoms in the plasma are found to be in agreement with spectroscopic analyses of their emission line intensity. Calculated etch rates of crystalline silicon are compared with measured etch rates for various plasma conditions. It is found that a competition between F and O atoms for the production of SiF_2 alone does not provide a satisfactory explanation for the etch rate dependence on the O_2 percentage in the feed. Yet, Si etch rates are well predicted by the model when pressure, power and load are varied.

ACKNOWLEDGEMENTS

I am deeply grateful to my supervisor, Dr. Henry P. Baltes, Tory Professor, for providing continuous guidance and motivation throughout my thesis program as well as helping me set the direction of my research work. I would also like to thank him for the financial support he provided through NSERC funds.

It was a great pleasure to work with Dr. Roger Patrick, LSI Logic Corp., to whom I express my utmost appreciation for his help in setting specific milestones and discussing all technical aspects of my research work.

I wish to thank Dr. Conrad Dell'Oca, Vice President Research of LSI Logic, for providing access to their R&D facilities. It is also a pleasure to thank the staff members of LSI Logic's R&D Department, in particular Paul Poenisch, Dr. Peter Byrne, Laura Macias, Marcia Woodward, and Larry Budnick for their most appreciated help and suggestions.

I acknowledge the Swiss National Funds for Scientific Research and the Alberta Microelectronic Centre for the financial support they provided during the course of my thesis program.

TABLE OF CONTENTS

CHAPTER	PAGE
1. INTRODUCTION	1
2. PLASMA ETCHING PROCESSES	6
2.1 Plasma etching mechanisms	6
2.2 Plasma etchers	11
2.3 Film characterization	15
3. STATISTICAL DESIGN OF EXPERIMENTS	17
3.1 Empirical modeling	17
3.2 The Response Surface Methodology (RSM)	20
3.2.1 Mathematical model	20
3.2.2 Experimental error	23
3.2.3 Parameter range	23
3.2.4 LSIFIT's features	24
3.2.5 Contour plots	25
3.3 The applications of the RSM	25
3.3.1 Optimization of plasma etching processes	25
3.3.2 Characterization of plasma etching processes	31
3.3.3 Application to research	34
3.4 Summary	34
4. PLASMA DIAGNOSTIC	39
4.1 Methods	39
4.2 Experimental setup	40
4.3 Spectroscopic diagnostic	42
4.3.1 General principle	42
4.3.2 Quantitative approach	44

4.4 Experimental results 47

4.4.1 Optical spectroscopy 47

4.4.2 Mass spectrometry 54

4.5 Plasma electrical properties 56

5. NUMERICAL SIMULATION OF A

CF_4/O_2 PLASMA ETCHING SILICON 58

5.1 Previous studies 58

5.2 Numerical simulation 61

5.2.1 The model 61

5.2.2 The simulation program 62

5.2.3 Steady state 63

5.2.4 Flow rates 67

5.3 Computed and measured relative concentrations 70

5.4 Silicon etch rates 80

5.5 Discussion 90

6. CONCLUSIONS 96

7. REFERENCES 99

APPENDIX A, LSIFIT & MAPPING LISTINGS AND USER-GUIDE 104

APPENDIX B, FCC & NESTED FCC-BOX-BEHNKEN DESIGNS 174

APPENDIX C, GLOW DISCHARGE LUMINESCENT INTENSITY 175

APPENDIX D, CHEMICAL KINETICS REACTION SCHEME 179

LIST OF TABLES

Table	Description	Page
I	3-parameter 3-level Box-Behnken design.	22
II	Model terms correlation coefficients.	52
III	Species traced by mass spectrometry.	55

LIST OF FIGURES

Figure		Page
2.1.1	Schematic of plasma etching processes in a parallel plate reactor with RF voltage applied to the top electrode. The dissociation of CF_4 by direct electron impact produces free fluorine atoms available for etching the silicon wafer sitting on the grounded bottom electrode in this example.	6
2.1.2	Schematic illustration of the potential in a parallel plate RF discharge.	9
2.2.1	Schematic of a batch barrel hexode-type plasma etcher.	11
2.2.2	Schematic drawing of the parallel plate single wafer etcher from Lam Research Corp. used in this thesis (not on scale).	13
2.3.1	General locations for measurement sites on a 5-inch wafer.	15
3.1.1	Cross section showing the structure of integrated contact holes in a borophosphosilicate (BPSG) and low-temperature oxide (LTO) film.	17
3.1.2	This figure represents a response versus two parameters. A single dimension search along parameter X_1 (fat line) leads to a local maximum instead of the true maximum.	18
3.2.1	3-parameter 3-level Box-Behnken design requiring 13 experiments plus replicates.	22
3.3.1	Contour plot of the selectivity of etch oxide:poly as a function of added CHF_3 and Ar in the feed gas at constant power. The CF_4 flow rate is fixed.	28

3.3.2 Contour plot of the uniformity of etch of oxide as a function of added CHF_3 and Ar in the feed gas at constant power. The CF_4 flow rate is fixed. 29

3.3.3 Contour plot of the oxide etch rate in μm/min as a function of added CHF_3 and Ar in the feed gas at constant power. The CF_4 flow rate is fixed. The shaded area represents the region of the parameter space where the uniformity is within ±5% while the blackened area is the region where the selectivity is above 10:1. 30

3.3.4 Contour plot of the specification response function as a function of added CHF_3 and Ar in the feed at constant power. The CF_4 flow rate is fixed. A value of 1.0 corresponds to 12:1 selectivity and ±2% uniformity while a value of 0.74 corresponds to 10:1 selectivity and ±5% uniformity. 31

3.3.5 Contour plot of the oxide etch rate in μm/min as a function of power and pressure at 150 sccm CF_4, 50 sccm He. Gap is fixed at 0.35 cm. 32

3.3.6 Oxide etch rate in μm/min as a function of pressure at 150 sccm CF_4, 50 sccm He, 900 Watts and 0.35 cm gap. Comparison between mathematical model (diamonds) and subsequent measurements (black & white triangles,squares). 33

4.2.1 Schematic representation of the experimental setup for the diagnostic of CF_4/O_2 plasmas using spectroscopic and mass spectrometric analyses. 41

4.3.1 The argon emission line intensity is a calibrant for the fluorine emission line intensity because the direct electron impact excitations taking place between the ground states and the excited states have comparable energies. 43

4.4.1 Argon emission line intensity (750.4 nm) versus pressure in a CF_4/O_2 plasma with argon. This graph represents the variations of the discharge excitation efficiency for a constant absolute amount of argon as a function of pressure. The squares represent the corrected experimental values while the solid line is a least-squares fit showing an almost perfect 1/p dependence. 48

4.4.2 Oxygen (O) emission line intensity at 777.4 nm as a function of pressure. The dotted squares are the raw oxygen readings while the black diamonds are those readings corrected by the excitation efficiency. It represents the relative behavior of the O concentration versus pressure. The process parameters have the same values as in Fig. 4.4.1. 49

4.4.3 Fluorine emission line intensity at 703.7 nm as a function of pressure. The dotted squares are the raw fluorine readings while the black diamonds are those readings corrected by the excitation efficiency. It represents the relative behavior of the F concentration versus pressure. The process parameters have the same values as in Fig. 4.4.1. 49

4.4.4 Fluorine emission line intensity at 703.7 nm and F/Ar intensity ratio as a function of the percentage of O_2 in the feed CF_4/O_2 gas mixture. The total flow of CF_4 and O_2 is fixed at 100 sccm. 5 sccm of argon are added. The power is 900 Watts, the pressure is 1.4 Torr and the gap is 0.8 cm. 50

4.4.5 F(703.7)nm/Ar(750.4nm) intensity ratio as a function of the percentage of O_2 in the feed CF_4/O_2 mixture, pressure and power (vertical axis). The total flow of CF_4 and O_2 is fixed at 100 sccm. 5 sccm of argon are added. The gap is 0.8 cm. Statistical tests: F-ratio=102.8, 3.88 corresponds to 99% level of confidence, R^2=0.98. 51

4.4.6 Section of the contour plot of Fig. 4.4.5 as a function of the O_2 content in the feed at 1.4 Torr and 900 Watts. The circles indicate subsequent measurements. 53

4.4.7 Section of the contour plot of Fig. 4.4.5 as a function of pressure at 900 Watts and with 50% O_2 in the feed. The circles indicate subsequent measurements. 53

4.4.8 Section of the contour plot of Fig. 4.4.5 as a function of power at 1.4 Torr and with 50% O_2 in the feed. The circles indicate subsequent measurements. 54

4.4.9 Mass spectra downstream of a 80/20 sccm CF_4/O_2 plasma with a 5 inch silicon wafer in the reactor at 800 Watts, 200 mTorr and 0.8 cm gap. 55

4.5.1 Maxwell-Boltzmann distribution. 56

4.5.2 Measured DC self-bias versus pressure at 50/50 sccm CF_4/O_2, 900 Watts and 0.8 cm gap. 57

5.2.1 Computed total concentration in a 50/50% CF_4/O_2 plasma as a function of time for various gas flow modes. The initial pressure is 1.0 Torr, the power is 900 Watts and the plasma volume 259 cm^3. 64

5.2.2 Computed total concentration in a 50/50% CF_4/O_2 plasma as a function of time for various total gas flow rates. The initial and steady state pressure is 1.0 Torr, the power is 900 Watts and the plasma volume 259 cm^3. The arrows indicate the residence time corresponding to each flow rate. 65

5.2.3 Mass spectra signals of the 69 line (CF_3^+ parent to CF_4), the 66 line (COF_2^+ & SiF_2^+ parent to COF_2 & SiF_4) and the 85 line (SiF_3^+ parent to SiF_4) as a function of time during silicon etching (6 inch wafer) in a 87.5/50/5 sccm CF_4/O_2/Ar plasma, at 1.4 Torr, 900 Watts, 0.8 cm gap. The power is turned on at time 0 and off after 180 sec. The signals are not calibrated. 67

5.2.4 Pumping rate required to maintain a constant total pressure of 1.0 Torr as a function of the percentage of O_2 in the CF_4/O_2 input mixture, with 100 sccm total feeding rate. The power is 900 Watts and the plasma volume 259 cm^3. 69

5.3.1 Computed concentrations of some species as a function of the percentage of O_2 in the CF_4/O_2 input mixture, with 100 sccm total feeding rate. The pressure is 1.0 Torr, the power is 900 Watts and the plasma volume 259 cm^3. 71

5.3.2 Comparison of computed [F]/[Ar] concentration ratio with measured F(703.7nm)/Ar(750.4nm) emission intensities versus the O_2 content in the feed. The process parameters are : 100 sccm CF_4/O_2 input gas mixture with 5 sccm Ar, 1.4 Torr pressure, 900 Watts power, 259 cm^3 plasma volume corresponding to 0.8 cm electrode gap. The measurements are related to the calculation by the relationship : $F(703.7nm)/Ar(750.4nm) = (k_F/k_{Ar})[F]/[Ar]$ where k_F and k_{Ar} are respectively the F and Ar electron impact excitation rates. 72

5.3.3 Comparison of computed [O]/[Ar] concentration ratio with measured O(777.4nm)/Ar(750.4nm) emission intensities versus the O_2 content in the feed at 1.4 Torr, 900 Watts, 0.8 cm gap. The measurements are related to the calculation by the relationship: 73

O(777.4nm)/Ar(750.4nm)=(k_O/k_{Ar})[O]/[Ar], where k_O and k_{Ar} are respectively the O and Ar electron impact excitation rates.

5.3.4 Comparison of computed [O]/[F] concentration ratio with measured O(777.4nm)/F(703.7nm) emission intensities versus the O_2 content in the feed at 1.4 Torr, 900 Watts, 0.8 cm gap. The measurements are related to the calculation by the relationship : O(777.4nm)/F(703.7nm) =(k_O/k_F)[O]/[F] , where k_O and k_F are respectively the O and F electron impact excitation rates. 73

5.3.5 Comparison of computed [F]/[Ar] concentration ratio with measured F(703.7nm)/Ar(750.4nm) emission intensities versus pressure in a 50/50 sccm CF_4/O_2 input gas mixture with 5 sccm Ar at 900 Watts, 0.8 cm gap. 74

5.3.6 Comparison of computed [O]/[Ar] concentration ratio with measured O(777.4nm)/Ar(750.4nm) emission intensities versus pressure in a 50/50 sccm CF_4/O_2 input gas mixture with 5 sccm Ar at 900 Watts, 0.8 cm gap. 74

5.3.7 Comparison of computed [O]/[F] concentration ratio with measured O(777.4nm)/F(703.7nm) emission intensities versus pressure in a 50/50 sccm CF_4/O_2 input gas mixture with 5 sccm Ar at 900 Watts, 0.8 cm gap. The measurements are related to the calculation by the relationship : O(777.4nm)/F(703.7nm)=(k_O/k_F) [O]/[F] , where k_O and k_F are respectively the O and F electron impact excitation rates. 75

5.3.8 Comparison of computed [F]/[Ar] concentration ratio with measured F(703.7nm)/Ar(750.4nm) emission intensities versus power in a 50/50 sccm CF_4/O_2 input gas mixture with 5 sccm Ar at 1.4 Torr, 0.8 cm gap. The measurements are related to the 75

calculation by the relationship : F(703.7nm)/Ar(750.4nm) = $(k_F/k_{Ar})[F]/[Ar]$ where k_F and k_{Ar} are respectively the F and Ar electron impact excitation rates.

5.3.9 Comparison of computed [O]/[Ar] concentration ratio with measured O(777.4nm)/Ar(750.4nm) emission intensities versus power in a 50/50 sccm CF_4/O_2 input gas mixture with 5 sccm Ar at 1.4 Torr, 0.8 cm gap. The measurements are related to the calculation by the relationship: O(777.4nm)/Ar(750.4nm) = $(k_O/k_{Ar})[O]/[Ar]$ where k_O and k_{Ar} are respectively the O and Ar electron impact excitation rates. 76

5.3.10 Comparison of computed [O]/[F] concentration ratio with measured O(777.4nm)/F(703.7nm) emission intensities versus power in a 50/50 sccm CF_4/O_2 input gas mixture with 5 sccm Ar at 1.4 Torr, 0.8 cm gap. The measurements are related to the calculation by the relationship : O(777.4nm)/F(703.7nm) = $(k_O/k_F)[O]/[F]$, where k_O and k_F are respectively the O and F electron impact excitation rates. 76

5.3.11 Measured F/Ar intensity ratio keeping the total flow to gap ratio F/g and the power to gap ratio W/g constant. The pressure is 1.4 Torr, the proportion of CF_4/O_2/Ar is 47.6/47.6/4.8 %. The solid line represents a least-squares fit to data. Under those conditions the calculated [F]/[Ar] concentration ratio would be constant. 78

5.3.12 Measured O/Ar intensity ratio keeping the total flow to gap ratio F/g and the power to gap ratio W/g constant. The pressure is 1.4 Torr, the proportion of CF_4/O_2/Ar is 47.6/47.6/4.8 %. The solid line represents a least-squares fit to data. Under those conditions the calculated [O]/[Ar] concentration ratio would be constant. 78

5.3.13 Measured O/F intensity ratio keeping the total flow to gap ratio F/g and the power to gap ratio W/g constant. The pressure is 1.4 Torr, the proportion of CF_4/O_2/Ar is 47.6/47.6/4.8 %. The solid line represents a least-squares fit to data. Under those conditions the calculated [O]/[F] concentration ratio would be constant. 79

5.4.1 Comparison of computed and measured silicon etch rates versus the O_2 content in a 100 sccm CF_4/O_2 input gas mixture with 5 sccm Ar at 900 Watts, 1.4 Torr, 0.8 cm gap. The silicon exposed area is 126 cm^2 (5 inch wafers). 83

5.4.2 Comparison of computed and measured silicon etch rates versus the O_2 content in a 100 sccm CF_4/O_2 input gas mixture with 5 sccm Ar at 900 Watts, 1.4 Torr, 0.8 cm gap. The silicon exposed area is 126 cm^2 (5 inch wafer). Competition between F and O atoms for the formation of SiF_4 is included and ß=8. 85

5.4.3 Comparison of computed and measured silicon etch rates versus the O_2 content in a 100 sccm CF_4/O_2 input gas mixture with 5 sccm Ar at 900 Watts, 1.4 Torr, 0.8 cm gap. The silicon exposed area is 182 cm^2 (6 inch wafer). Competition between F and O atoms for the formation of SiF_4 is included and ß=8. 85

5.4.4 Comparison of computed atomic fluorine concentrations with and without silicon in the system versus the O_2 content in a 100 sccm CF_4/O_2 input gas mixture with 5 sccm Ar at 900 Watts, 1.4 Torr, 259 cm^3 plasma volume. In the presence of silicon, the active exposed area is 126 cm^2 and competition between F and O atoms for the formation of SiF_4 is included along with ß=8. 86

5.4.5 Comparison of F(703.7nm)/Ar(750.4nm) emission intensities with and without silicon wafer in the system versus the O_2 content in a 87

100 sccm CF_4/O_2 input gas mixture with 5 sccm Ar at 900 Watts, 1.4 Torr, 0.8 cm gap. It can be seen that the relative concentration of fluorine with silicon present in the system does not correlate with that computed and shown in Fig. 5.4.4.

5.4.6 Comparison of measured and calculated silicon etch rate versus pressure with 182 cm^2 load (6 inch wafer), in a 87.5/50/5 sccm CF_4/O_2/Ar input gas mixture at 900 Watts, 0.8 cm gap. The simulation includes "competition for sites" between F and O atoms and ß=8. 88

5.4.7 Comparison of measured and calculated silicon etch rate versus power with 182 cm^2 load (6 inch wafer), in a 50/50/5 sccm CF_4/O_2/Ar input gas mixture at 1.4 Torr, 0.8 cm gap. The simulation includes "competition for sites" between F and O atoms and ß=8. 89

5.4.8 Comparison of measured and calculated silicon etch rate versus silicon exposed area (load : 2,3,4,5,6 inch wafers), in a 70/30/5 sccm CF_4/O_2/Ar input gas mixture at 900 Watts, 1.4 Torr, 0.8 cm gap. The simulation includes "competition for sites" between F and O atoms and ß=8. The solid lines represent logarithmic least-squares fits showing a $1/A^{0.69}$ dependence of the experimental etch rate on the silicon exposed area and a $1/A^{0.6}$ dependence for the computed etch rate. 89

'C1 Position of the tip of the fiber optic (optical "sensor") with respect to the glow region (dotted area) contained between two parallel plates. 175

C2 Top view of the reactor showing the position of the optical sensor with respect to the electrodes. 177

C3 Top view of the reactor showing the position of the optical sensor with respect to the electrodes. 177

C4 Top view of the reactor showing the position of the optical sensor with respect to the electrodes. 178

LIST OF SYMBOLS

Symbol	Description	Units
Chapter 3. :		
a_j	model coefficient j	
A_j	average value of T_j	
E_k	experimental error	
r_{jk}	intercorrelation of model terms T_j, T_k	
RF_{sel}	response function for the selectivity S	
S	selectivity of etch SiO_2/Poly	
S_p	specification response function	
T_j	model term j	
T_{ji}	i^{th} experimental value of T_j	
UN	uniformity of etch of SiO_2	
V_j	model term T_j variance	
X_j	independent parameter j	
X_{ji}	i^{th} experimental value of X_j	
y_j	model response function j	
y_{ji}	i^{th} experimental value of y_j	
Y_j	experimental response function j	
Y_{ji}	i^{th} experimental value of Y_j	
χ^2	residual sum of squares	

Chapter 4. & appendix C

a	angle	rad
A	optical detector sensitive area	m^2
$C(\mu)$	optical spectrometer sensitivity at frequency μ	unitless
$d(\varnothing)$	distance	m
D	distance	m
e	denotes an electron	
E	distance	m
f_μ	density of photons escaping the discharge	$m^{-3}sec^{-1}$
G	constant	$m^{-3}sec^{-1}$
H	plasma height	m
I_{x^*}	optical emission intensity	arbitrary
$I_\mu, \Delta i_{d(\varnothing)}$	fluxes of energy at the optical detector	Watts m^{-2}
Δi	intensity	Watts
k_q	relaxation rate by collision	sec^{-1}
k_r	relaxation rate by spontaneous emission	sec^{-1}
k_x	excitation rate of species X by electron impact	sec^{-1}
L	distance	m
L_μ	glow discharge luminescent intensity	Watts
M	denotes a third body	
[M]	total gas density	cm^{-3}
n_e	electron density	cm^{-3}
N_μ	optical spectrometer readings at frequency μ	unitless
N_{x^*}	density of photons from the optical transition	
	$X^* \dashrightarrow X$	m^{-3}
P	distance	m
R	electrode radius	m
t_s	sampling time	sec
Δt	lifetime of an excited state	sec
S	integration constant	m^{-2}
V	plasma volume	m^3

X	a chemical species in its electronic ground state	
X^*	species X in an excited state	
$[X]$	concentration of species X	cm^{-3}
Ω	frequency of a photon	sec^{-1}
$\emptyset$	angle	rad
ΔI_μ	plasma surface emission intensity	Watts m^{-2}
μ, μ_o	frequencies	sec^{-1}

Chapter 5.

A	silicon exposed area	cm^2
$C(\mu)$	optical spectrometer sensitivity at frequency μ	unitless
e	denotes an electron	
E	crystalline silicon etch rate	$\mu m/min$
ΔE_j	bond energy	ev
f_j	constant	unitless
F	total flow rate	sccm
g	gap	cm
Γ_s	impingement rate	$cm^{-2}sec^{-1}$
k_B	Boltzmann constant	$J\,K^{-1}$, $ev\,K^{-1}$
k_c	second order competition rate	cm^3sec^{-1}
k_e	first order electron impact dissociation rate	sec^{-1}
k_E	first order fluorine consumption rate	sec^{-1}
k_f	zero order feeding rate	$cm^{-3}sec^{-1}$
k_j	second order dissociation rate of X_j	cm^3sec^{-1}
k_o	rate	$cm^3Watts^{-1}sec^{-1}$
k_{out}	second order pumping rate	cm^3sec^{-1}
k_x	excitation rate of species X by electron impact	sec^{-1}
m_F	mass of the fluorine atom	Kg
$\bar{n}_e$	average electron density	cm^{-3}

[M]	total gas density	cm^{-3}
N_μ	optical spectrometer readings at frequency μ	unitless
p	total pressure	Torr, Pascal
q	second order pumping rate	cm^3sec^{-1}
r_j	second order rate	J cm^3sec^{-1}
T	gas temperature	K
T_e	electron temperature	K
V	plasma volume	cm^3
W	power injected in the plasma	Watts
X_j	chemical species j	
$[X_j]$	species X_j concentration	cm^{-3}
ß	correction factor	unitless
ρ	atomic density in crystalline silicon	cm^{-3}
Θ	reaction probability of atomic fluorine on silicon	unitless

Appendix D

A	rate constants	consistent
A1	rate constant	cm^3sec^{-1}
	plasma volume	cm^3
F	constant	unitless
k_o	rate constant	cm^6sec^{-1}
k_∞	rate constant	cm^3sec^{-1}
[M]	total gas density	cm^{-3}
R	second order rate	cm^3sec^{-1}
S	activation energy	K
S1	power injected in the plasma	Watts
TEMP	temperature	K

1. INTRODUCTION

With the recent opening of a 2 µm metallization line for Application Specific Integrated Circuits (ASIC) by the Alberta Microelectronic Centre at the University of Alberta, an interest arose in the research of microelectronic technology steps. A constant effort in this direction is required in order to contribute to the technological evolution of this fast changing industry. In this study, plasma etching processes are investigated and both a development-oriented and a research-oriented approach are illustrated.

The goals were, (1) to develop a software package for computer-aided optimization of microelectronic processes based on the statistical design of experiments, application to plasma etching of silicon dioxide, and (2) to investigate the applicability of a chemical kinetics, tubular reactor model of a CF_4/O_2 plasma etching silicon, to the modeling of silicon etch rates in the commercial parallel plate single wafer etcher used in this study. To our knowledge, this is the first attempt to apply a chemical simulation to the systematic modeling of production plasma-etching equipment performances.

The manufacturing of microelectronic components consists essentially of depositing or growing thin films on a silicon substrate (wafer) and then removing them in some places in order to reproduce fine patterns. It also consists of diffusing materials such as phosphorus or boron in small quantities in the structure in order to modify its electrical properties.

The removing of a layer is called etching. Etching serves to open windows through a thin film in order to expose the underlying material for ion implantation or to make a contact with a subsequent layer deposited on the wafer surface. It also serves to delineate transistor's gate and metal lines in order to interconnect electrically the devices laid in the integrated circuit.

When several layers of metal are used, etching may be used to planarize the wafer surface between two metal layers. Finally, etching is used for stripping an entire film from the surface or the back of the wafer.

The applications of etching are not limited to integrated circuit manufacturing. The micromachining of integrated sensors in silicon for example, requires to precisely reproduce small structures [1].

The speed, cost and to some extent reliability of an integrated circuit depend on the size of the transistor itself. For instance, the performance of the Metal-Oxide-Semiconductor (MOS) transistor is related to the distance separating the source and drain, that is the gate length. This distance should be as small as possible. Therefore, the milestone of integration is determined by how small the gate can be made repeatably with the desired properties. The size of the smallest pattern that can be reproduced repeatably is referred to as the minimum feature size and it sets the level of integration and precision for the manufacturing of any kind of microstructure, not only MOS transistors. Today's typical minimum feature size is 1µm or more depending on the application. Structures of that size must be reproduced in a thin film sometimes a few hundred Angströms thick (1 Angström = 10^{-10} m) and throughout a silicon wafer up to 8 inch (20.3 cm) in diameter.

The other key factor of microelectronic device manufacturing, beside (very) large scale integration, is the ability to produce them at high throughput and low cost. Fabrication processes must always be designed with those two aspects in mind. As far as etching is concerned, it has been achieved using chemical or physico-chemical processes. The simplest etching method consists of dipping the wafer into a liquid reacting chemically with the surface (wet etch). Wet etching processes tend to etch uniformly in all directions (isotropic processes). Due to the isotropic nature

of wet etching of noncrystalline materials, it is not appropriate for the fabrication of features below 3 μm.

The use of reactive gases, instead of reactive liquids, allows a tighter control of the isotropy or anisotropy of etch. Molecules of nonreactive gases are dissociated in a radio frequency (RF) discharge, creating reactive gaseous species. Those processes are referred to as dry etching or plasma etching, because the discharge produces an ionized gas. The anisotropy of etch can be achieved either by the directionality of ion bombardment onto the wafer or by passivation of the walls [2,3].

The basic types of materials used in the fabrication of integrated devices can be etched by dry processes : insulators such as silicon dioxide (SiO_2) and silicon nitride (Si_3N_4), semiconductors such as silicon (Si), conductors such as doped polysilicon (poly Si), aluminum ($Al_{98\%}Si_{2\%}$) and tungsten silicide (WSi_2), and photoresist mask (polymeric material).

The task of the dry-etch process engineer is to develop a suitable process for each application. The etching process, or recipe, must meet certain requirements which translate into a number of specifications. The requirements are typically :

(1) Precision ((an)isotropy, undercut, sloped etch).
(2) Process repeatability in time.
(3) Uniformity across a wafer (etch rates within ±5% of their average value for example).
(4) Selectivity of etch between different materials.
(5) Throughput.

From the point of view of the process engineer, plasma etching is much more complex than wet etching because of the great number of parameters

affecting the process. The theory of plasma etching processes is based on the understanding of RF discharges, gas phase chemistry of charged and neutral particles, transport processes by convective flow, diffusion and ambipolar diffusion of ions, and last but not least, surface chemistry. Because of this complexity, plasma etching processes have been empirically developed and the understanding of them is quite limited.

In chapter 2, a brief description of plasma etching principles is made, the plasma etcher used in this work is presented, and some useful quantities, to which it will be referred throughout the thesis, are defined.

In chapter 3, an empirical method is presented, that allows the characterization and the optimization of plasma etching processes. It is based on the statistical design of experiments and it is often referred to in the literature as the Response Surface Methodology (RSM) [4]. In this thesis, the use of the RSM is demonstrated for the etching of polysilicon and silicon dioxide in a fluorocarbon chemistry. Those experiments illustrate the use of the software developed in this work for the optimization and characterization of multiparameter processes.

In chapter 4, the experimental procedure for characterizing the plasma is described. It includes the spectroscopic diagnostic as reported in the literature, and mass spectrometric data. An expression has been derived, that relates the optical spectrometer readings with the concentration of an emitting species in its ground state. The fluorine emission line intensity has been characterized as a function of injected power, pressure and gas composition in a CF_4/O_2 plasma, using the RSM.

In chapter 5, a numerical simulation of the gas phase chemistry of a CF_4/O_2 plasma is presented. The reaction scheme and the simulation program

come from different sources. In this study, they have been adapted as much as possible to the particular conditions of experiments. The calculated concentrations of free fluorine and oxygen atoms are correlated with spectroscopic measurements of their excited state emission line intensity. Crystalline silicon etch rates in the same plasma are related with the gas phase composition and compared with etch rate measurements.

The empirical method illustrates how industry may approach plasma etching processes while the theoretical model gives an insight of what happens in the plasma. In both cases, the goal is to relate the process parameters, such as operating pressure and gas flow rates, with etch rates or other quantities of interest. The empirical method provides a direct link between the cause and the effect while the theoretical approach helps us understand the process.

2. PLASMA ETCHING PROCESSES

2.1 Plasma etching mechanisms

The principle of plasma etching is to form reactive gaseous species, or reactants, from a nonreactive gas mixture [3]. The reactants must attack the film to be etched and form volatile products that will be pumped out of the reactor. Reactive species are produced by electron impact dissociation of the inert gaseous molecules in a radio frequency (RF) discharge. This is illustrated in Fig. 2.1.1 for the production of free fluorine from freon 14 (CF_4) in a parallel plate reactor.

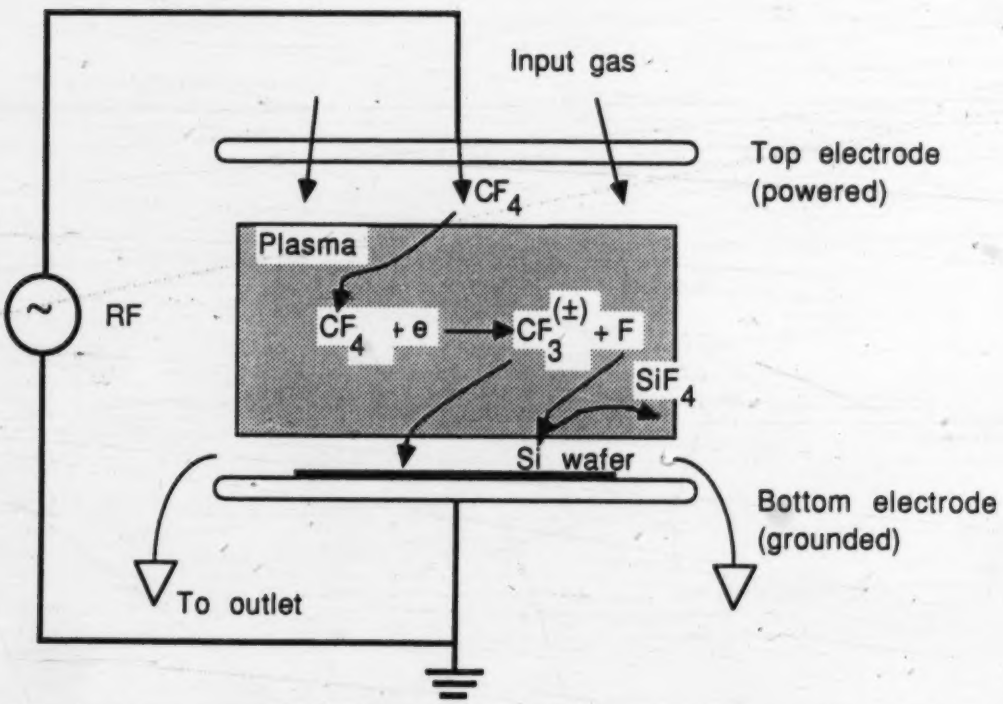

Fig. 2.1.1) Schematic of plasma etching processes in a parallel plate reactor with RF voltage applied to the top electrode. The dissociation of CF_4 by direct electron impact produces free fluorine atoms available for etching the silicon wafer sitting on the grounded bottom electrode in this example.

The RF voltage, at 13.56 MHz and a few hundred volts peak to peak typically, is applied between two electrodes. Electrons are pulled out of the atoms and energized by the electric field, creating a chain reaction. The gaseous volume between the electrodes is rapidly ionized and energetic electrons are available for breaking molecules such as CF_4 in the example. The dissociated CF_4 molecules leave positively and negatively charged CF_3 ions as well as neutral CF_3 radicals. Free fluorine atoms are also created which can react with the silicon wafer sitting on the bottom electrode. Fluorine is known as an etchant for silicon because it forms volatile SiF_4 molecules [5].

There are two kinds of discharges, DC and AC discharges [6]. AC discharges used in plasma etching are referred to as RF discharges because they operate at a frequency of several MHz. In a DC discharge, a constant voltage is applied at the electrodes. If the voltage is sufficiently high, electrons will be extracted from the atoms leaving positively charged particles. The steady polarity of the system makes it inappropriate for etching. Usually, at some point of the manufacturing process, wafers are coated with insulating material. In a DC discharge, charges would pile up on the wafer until the discharge is extinguished [7]. This problem is overcome by using AC discharges. Charges accumulated on the wafer during one half of the cycle are removed during the other half and so the discharge can be sustained.

In a 13.56 MHz RF discharge, heavy charged particles like ionized atoms or molecules do not respond to the electric field AC variations. Electrons, to the contrary, are light enough to follow the electrical force AC variations. As a result of the difference in ion and electron mobility, the positively charged electrode draws a larger electron current than ion current for a given

voltage. This asymmetry is automatically balanced and the interelectrode region, or plasma, self-biases itself at a positive DC voltage with respect to the electrodes so that a quasi constant ion current flowing from the plasma toward the electrodes compensates the electron current excess. The plasma region is electric field free and is separated from solid surfaces by a positive space charge region called sheath (Fig. 2.1.2). Energized electrons not only dissociate molecules, they also excite electronically the atoms and molecules which relax by emitting photons. As a result, the plasma region is bright and it is also called glow region. The sheaths being virtually electron free, they appear dark on both sides of the glow region. The glow region is therefore the place where dissociation occur. The plasma potential is always higher than the electrode potentials. A theoretical argument indicates that its potential with respect to ground is about half the peak to peak voltage applied to the electrodes [7]. Electrodes with different areas or made out of different materials cause a net DC bias to form between the two plates as indicated by V_b in Fig. 2.1.2. Unlike the plasma DC potential offset, the plate to plate bias can be readily measured with a voltmeter. The voltage drop between the plasma and the electrodes is typically a few tens of volts to several hundreds of volts depending on the type of reactor, the plasma chemistry and other operating conditions. As ions enter the sheath, they are accelerated toward the electrode and bombard its surface. The ion bombardment contributes to the physical part of the etching process. A strong ion bombardment can knock atoms off the wafer surface, physically etching the material exposed to the plasma. Such etching is referred to as sputter etching because of the similarity with sputtering. Reactive Ion Etching (RIE) is another type of ion-enhanced etching. RIE is a combination of sputter etching and plasma etching.

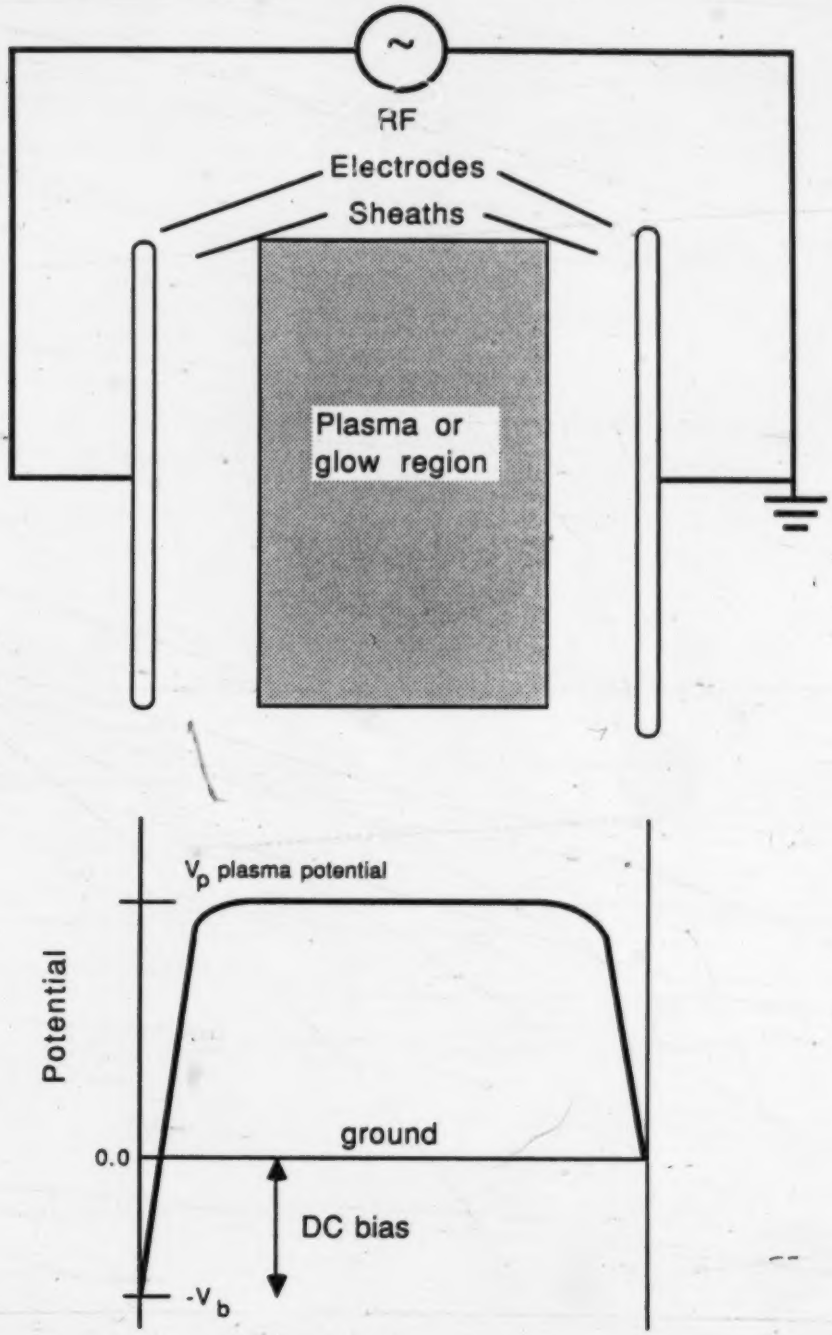

Fig. 2.1.2) Schematic illustration of the potential in a parallel plate RF discharge.

Here, plasma etching is used in the sense of chemical etching, although in a parallel plate reactor, ion bombardment cannot be separated from chemical etching. The ion contribution to the etching process is enhanced by placing the wafer on the powered electrode and by making that electrode smaller than the grounded electrode. This will increase the plate to plate DC bias so that ions experience a greater voltage drop when striking the wafer surface.

Neutral species, on the other hand, are transported to the wafer surface by diffusion. During the etching process, the plasma is constantly fed with new gas and only a fraction is converted into reactive species. High gas flow rates help remove the reaction by-products from the reactor chamber. The total input gas flow rate also determines the residence time of species in the plasma. The residence time is affected by the plasma volume too. The gas pressure determines the amount of reactant in the gas phase. At operating pressures below 500 mTorr, ion bombardment participates actively to the etching process (RIE). Above 1 Torr, collisions between molecules and ions reduce the ion contribution and the etching is mostly a chemical process (plasma etching). The plasma is sustained by the power the generator delivers to the electrodes.

The total gas flow rate, the total pressure in the chamber and the power deposited in the plasma are the typical process parameters of plasma etching. The electrode spacing, when it can be adjusted in a parallel plate reactor, and the individual gas flow rates, when a mixture of gases is used, are other examples of process parameters. The process parameters can be adjusted continuously within their operating range from the reactor control panel.

In the plasma, the electron temperature can be as high as 10^5 K [8] but ions and neutrals remain at room temperature, thus, providing the ion bombardment is not too strong, plasma etching is not detrimental to

microstructures. Etching at room temperature avoids a too rapid erosion of the resist as well. Although, the reactor temperature can be controlled, it is usually not a process parameter.

The choice of reactor geometry, gases and process parameter values translates into etch rate of materials exposed to the plasma. The directionality of etch affects the isotropy or anisotropy of etch while etch rates determine the throughput. When removing a silicon oxide layer on top of a polysilicon transistor gate for example, one must make sure that the poly etch rate is much slower than the oxide etch rate so that the gate is not altered by the oxide etching process. The ratio of etch rates of different materials exposed to the same process is the selectivity of etch. The etch rate must be uniform throughout the wafer, throughout the reactor if it holds several wafers at a time, batch to batch and day after day. In other words, uniformity of etch and repeatability of the process must be achieved.

2.2 Plasma etchers

There are several kinds of plasma etching reactors [2,3,9]. The earliest type is the barrel reactor, shown in Fig. 2.2.1, which can hold 25 to 50 wafers

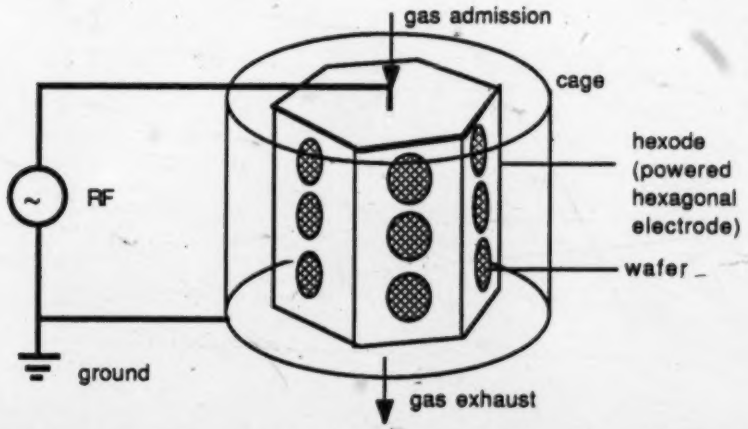

Fig. 2.2.1) Schematic of a batch barrel hexode-type plasma etcher.

depending on their size.

Wafers are placed on the inner, powered, barrel-shaped electrode. The cage serves as the grounded electrode. Because barrel reactors operate at low pressures (10-100 mTorr) and because the wafer carrier is smaller than the outer electrode, those reactors are Reactive Ions Etchers.

The parallel plate reactor configuration has been mentioned above. The Lam AutoEtch from Lam Research Corporation is the etcher used in this work. The same machine is currently used at the Alberta Microelectronic Centre for SiO_2 contact etching (Fig. 2.2.2). It is a commercial plasma etcher with parallel 8 inch electrodes. One wafer at a time is processed in the plasma chamber. The front control panel allows the programming of etching recipes. The process parameters are then automatically controlled by a computer. Current status and recipes are displayed on the CRT screen.

Wafers to be etched are loaded on the left side of the machine. A cassette, or boat, holding up to 25 wafers is placed on the left indexer. One by one, wafers are automatically conveyed from the boat to the entrance loadlock via a conveyor belt. Then they are lifted up and deposited in the entrance arm. Once in the loadlock, the pressure is lowered from atmosphere down to about 60 mTorr of nitrogen. During the etching, the wafer sits on the grounded bottom anodized aluminum electrode. For oxide etching, a graphite top electrode is used whereas, for polysilicon etching the etcher is equipped with an anodized aluminum electrode. After etch, the wafer is transported through the exit loadlock, and via the exit conveyor belt, to the receive cassette on the right side of the machine. At all times the reactor chamber is isolated from atmosphere in order to keep the chamber as clean as possible. The advantage of an automated etcher is that manual wafer handling is suppressed, which limits the contamination of the wafers and the risk of breaking them.

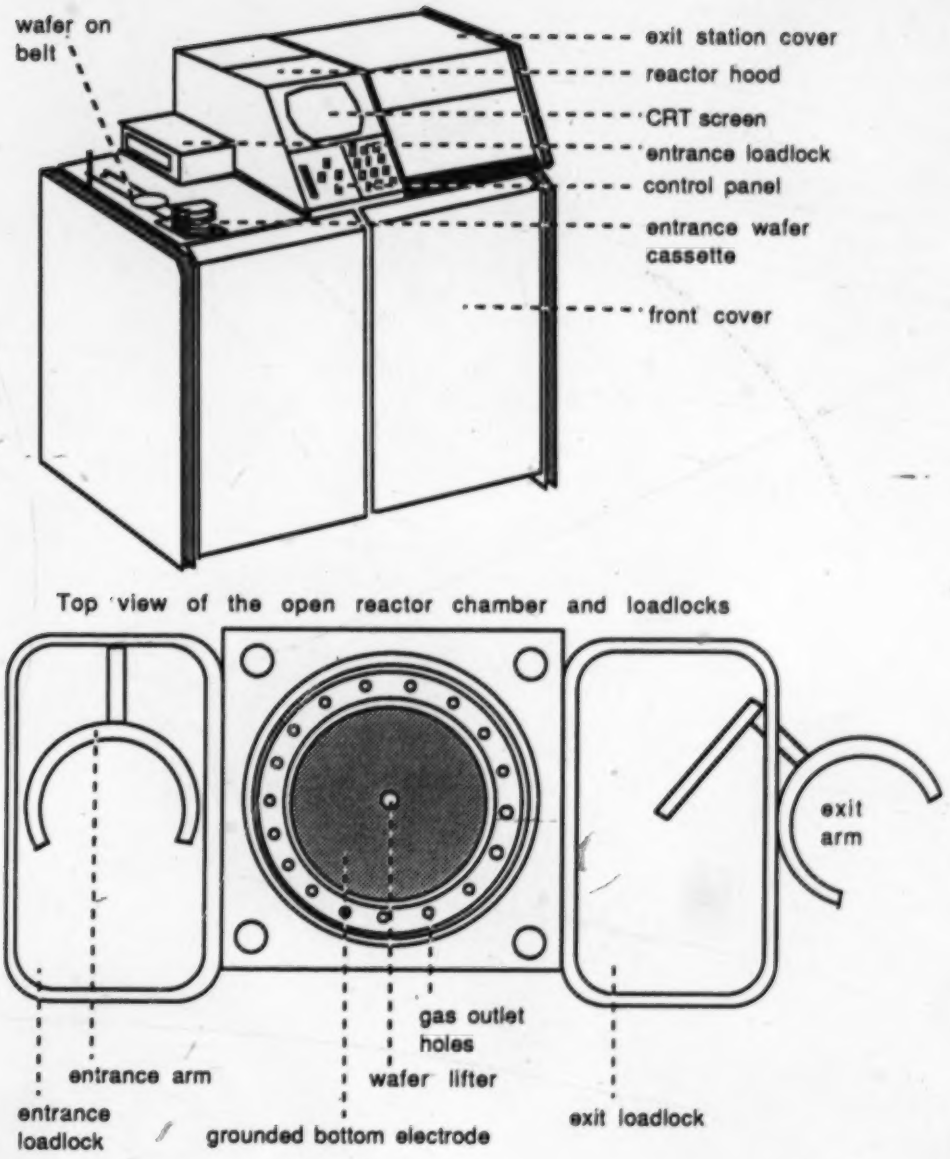

Fig. 2.2.2) Schematic drawing of the parallel plate single wafer etcher from Lam Research Corp. used in this thesis (not on scale).

Single wafer reactors allow a better control of the uniformity of etch across the wafer as opposed to a barrel reactor which requires control of the uniformity over a much longer distance. Unlike batch reactors, single wafer reactor throughputs are insensitive to wafer size. They are also more suitable for research and development as well as for small production purposes. Endpoint of the etching process, using optical emission techniques for example, is easier with single wafer reactors since each wafer is treated separately. On the other hand, higher etch rates are required in single wafer reactors than in batch systems in order to achieve comparable throughputs.

In the Lam etchers, gases are fed through the shower-head type top electrode and pumped out at the bottom of the chamber. The five input gas lines have individual control mass flow meters calibrated for each specific gas. The gas flow rates can be programmed between 0 and 200 sccm (sccm = standard cubic centimeter per minute, cc/min at 760 Torr and 20 ^{o}C). A capacitance manometer located at the chamber outlet monitors the pressure variations that the computer corrects by controlling the angle of the valve situated at the chamber vacuum manifold. The chamber base pressure is about 10 mTorr. Operating pressures range from 0.1 Torr to a few Torr. A water cooled RF generator delivering up to 1250 Watts in the model 590, and 650 Watts in the model 490, powers the top electrode. In the model 590, the cathode and the anode are cooled by deionized water. The electrode spacing, or gap, can be adjusted and ranges from 0.2 to 2.5 cm. The impedance of the generator is matched to that of the plasma by a matching network located between the generator and the top electrode. At high powers, it prevents power from being reflected to the generator and causing damage. The impedance of the plasma varies with the gap, the pressure and the plasma chemistry.

2.3 Film characterization

The etch rate is the difference in the film thickness before and after etch divided by the etch time. It is expressed in Angströms/minute (Å/min) or in micrometers/minute (μm/min). A Nanospec/AFT model #0100180 has been used for measurements of SiO_2 and poly etch rates. The film thickness is determined by the intensity of transmission of a light beam reflected beneath the film. The Nanospec is programmed for the measurement of SiO_2 films on crystalline silicon, polysilicon films on 1000 Å SiO_2 on silicon and other materials. In order to calculate the uniformity of etch across the wafer, the etch rate is measured at different locations. 5 inch wafers have been probed at 9 sites (Fig. 2.3.1).

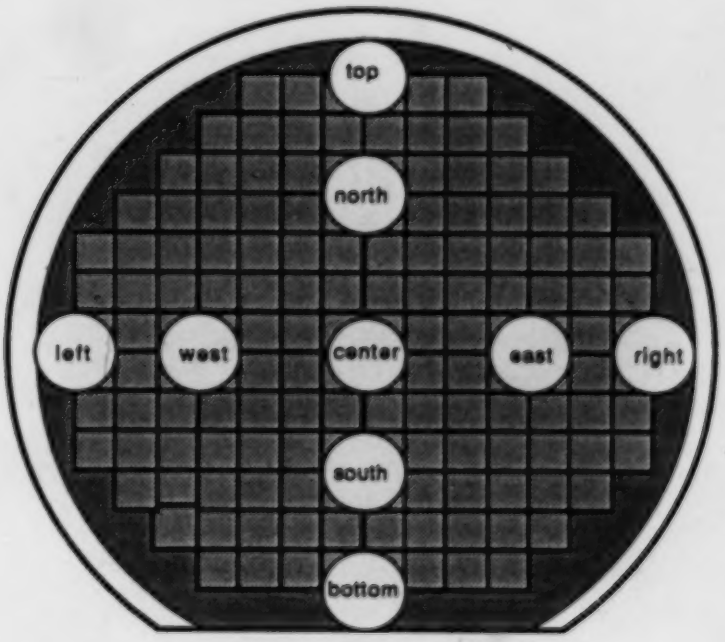

Fig 2.3.1) General locations for measurement sites on a 5-inch wafer.

The average value of those measurements is simply called the etch rate. The selectivity of etch is defined as the ratio of the average etch rates of two materials. In this thesis the uniformity is defined as follows :

uniformity = 100·(max. etch rate - min. etch rate)/(max. etch rate + min. etch rate) (2.1)

This definition accounts for the extreme readings because integrated devices are all over the wafer surface. Contrarily to what one might expect, recipes etching very uniformly have low uniformity values with this definition. A process with high uniformity means therefore that etch rates at various locations on the wafer differ significantly and that the etching is actually nonuniform.

3. STATISTICAL DESIGN OF EXPERIMENTS

3.1 Empirical modeling

Let us consider the plasma etching of silicon dioxide using the oxide etcher Lam AutoEtch 590. In an integrated circuit, contact holes are etched through the oxide layer in order to connect the metal lines with the polysilicon gates and the diffusion regions of CMOS transistors (Fig. 3.1.1).

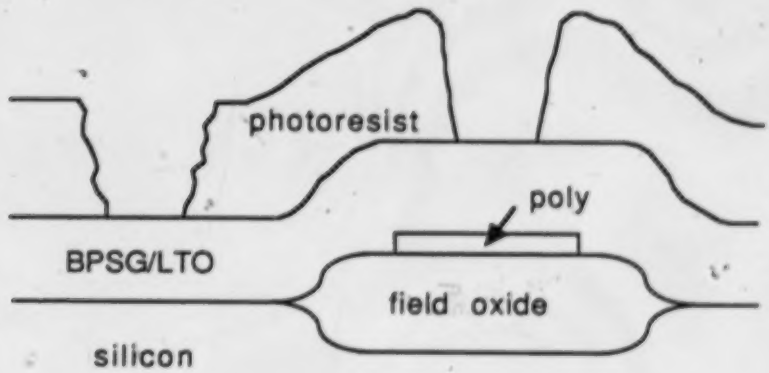

a) Before etch

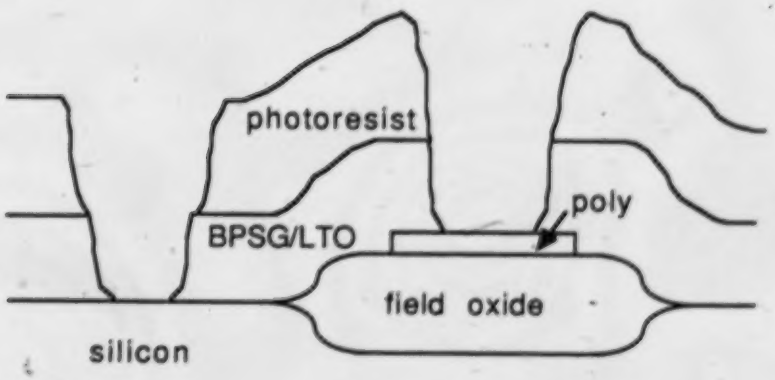

b) After etch

Fig. 3.1.1) Cross section showing the structure of integrated contact holes in a borophosphosilicate glass (BPSG) and low-temperature oxide (LTO) film.

The task of the process engineer is depicted by the following example. A process must be developed which etches the oxide at a rate of 6000 Å/min or more in order to achieve a viable throughput. The uniformity of etch rate across the wafer must be within ±5%. The selectivity oxide to poly must be as high as possible because the underlying polysilicon will be uncovered in some places before complete removal of the oxide. The process parameters are: power, pressure, gas flow rates, electrode spacing.

Firstly, a suitable chemistry must be chosen. Secondly, what values of the process parameters make the etch rate, uniformity and selectivity meet the specifications ? As illustrated in Fig. 3.1.2, varying one parameter at a time may not allow the location of the true optimum.

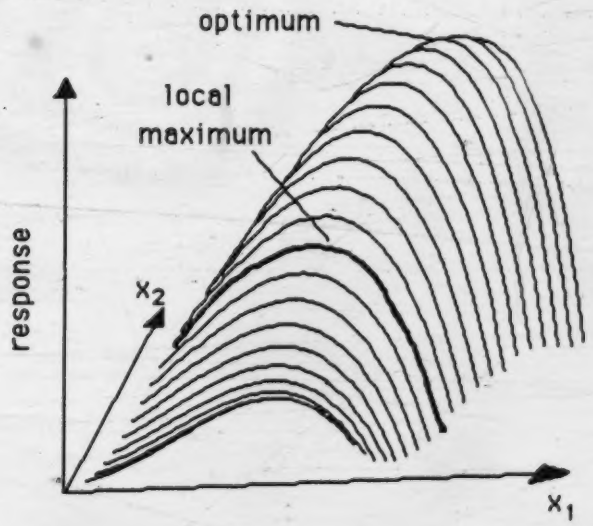

Fig. 3.1.2) This figure represents a response versus two parameters. A single dimension search along parameter X_1 (fat line) leads to a local maximum instead of the true maximum.

The orthogonal matrix method determines a response's dependence on a given parameter by randomizing the other parameter values [4]. Hence it

indicates only the average trends of a response (etch rate, uniformity...) as a function of one parameter (pressure, power...). It is useful for determining what are the general trends or what are the most important parameters and it requires only the use of a pocket calculator.

The Response Surface Methodology (RSM) is a statistical method allowing the optimization of a multiparameter process by conducting the experimenter toward the optimal operating point more efficiently than the single dimension search. Similarly with the orthogonal matrix, it is based on the statistical design of experiments which means that instead of measuring response values for arbitrary settings of the process parameters, the responses are measured for designed values of those parameters. In other words, it is a strategic search toward the optimal process. As a result, not only is the process optimized, but also a maximum of information is obtained with a minimum of experiments. As opposed to the one-parameter at a time method, or a random search, the statistical design of experiments is a scientific alternative providing better results in less time and with less work.

The RSM has been developed by Box *et al.* [4]. Its advantage over the other methods is that it provides a direct link between the process parameters and the responses, it also gives the correlations between the responses and the process parameters. The RSM requires that the process parameters can be varied continuously and have a continuous effect on all observed responses. It also requires the help of a computer to fit experimental data with a mathematical function and to display the results. A typical RSM output is a two-dimensional map of the response versus two of the process parameters.

Technically speaking, the RSM is an all-computed search toward a maximum in the response. It starts with a multifactorial linear fit of the response surface in a subregion of the parameter space. A computer program

then conducts the experimenter toward the maximum by following the steepest ascent. When the linear fit fails to improve the experimental results, the fit is extended to a quadratic surface, which shows the local response surface topology. When no more than three parameters are used simultaneously, the quadratic fit may be refined by a cubic fit (a cubic fit with more than three parameters would be rather cumbersome and of no practical use). In this work, the term RSM refers in general to nonlinear multifactorial statistical design of experiments.

3.2 The Response Surface Methodology (RSM)

3.2.1 Mathematical model

The responses are related to the process parameters with a polynomial function called a multiple regression equation. For example, the etching of silicon dioxide in a CF_4/He plasma can be related to pressure, power and helium percentage in the feed by a quadratic polynomial :

etch rate :

$$y_1 = a_1 + a_2X_1 + a_3X_1^2 + a_4X_2 + a_5X_1X_2 + a_6X_2^2 + a_7X_3 + a_8X_1X_3 + a_9X_2X_3 + a_{10}X_3^2$$

$$y_1 = a_1 + \Sigma\, a_jT_j \qquad j=2,\ldots,10 \qquad (3.1)$$

uniformity :

$$y_2 = b_1 + b_2X_1 + b_3X_1^2 + b_4X_2 + b_5X_1X_2 + b_6X_2^2 + b_7X_3 + b_8X_1X_3 + b_9X_2X_3 + b_{10}X_3^2$$

$$y_2 = b_1 + \Sigma\, b_jT_j \qquad j=2,\ldots,10 \qquad (3.2)$$

where y_1 the oxide etch rate, and y_2 the uniformity are functions of power X_1, pressure X_2 and helium percentage X_3. Model terms T_j are combinations of

independent parameters X_j , j=1,2,3. The model coefficients $a_1,....,a_{10}$ and $b_1,....,b_{10}$ must now be determined. Since there are 10 coefficients in this model we need at least 10 experimental points Y_{1i}, Y_{2i} i=1,...,10 , corresponding to 10 different combinations of X_{1i}, X_{2i}, X_{3i} i=1,...,10 , where the index i now denotes the i^{th} experimental value.

A FORTRAN program, named LSIFIT (appendix A), for the least-squares fitting of multiparameter nonlinear functions has been developed. The algorithm is from reference [10]. LSIFIT calculates the a's and b's such that the residual sum of squares $\chi^2 = \sum_i (y_{ji}-Y_{ji})^2$ j=1,2 , be minimum, where y_{ji} is response y_j i^{th} calculated value and Y_{ji} its corresponding experimental value. However, the X_{ji} j=1,2,3 ; i=1,...,10 must be chosen adequately. In other words the experiment must be designed in order to minimize intercorrelations between X_{1i}, X_{2i}, X_{3i}. The intercorrelation (also called simply correlation or covariance) $r_{jk} = \sum_i (T_{ji}-A_j)(T_{ki}-A_k)/ (V_j V_k)^{1/2}$ measures the amount - comprised between -1 and +1 - by which two model terms T_j, T_k are dependent to each other. A_j and V_j denote respectively the average and variance of model term T_j. When two terms are perfectly correlated ($r_{jk}=\pm 1$) their effect on the response cannot be distinguished. Finally, a n^{th} order polynomial requires independent parameters having at least n+1 levels.

The Box-Behnken design meets these requirements [11]. In our example it

could be as shown in Table I. + denotes the upper level, - the lower level and 0 the intermediate level. + and - are at equal distance from the intermediate level.

Table I :

	Run #	X_1	X_2	X_3
	+	950 W	2.5 T	37.5 %
Levels :	0	900	2.0	25
	-	850	1.5	12.5
	1	+	+	0
	2	+	-	0
	3	-	+	0
	4	-	-	0
	5	+	0	+
	6	+	0	-
	7	-	0	+
	8	-	0	-
	9	0	+	+
	10	0	+	-
	11	0	-	+
	12	0	-	-
	13	0	0	0

In three dimensions, it is possible to visualize the design (Fig. 3.2.1).

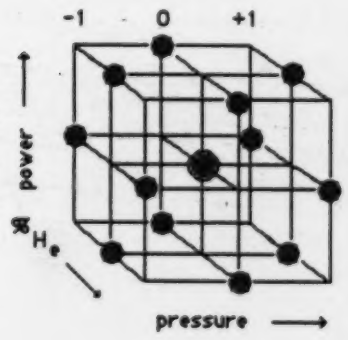

Fig. 3.2.1) 3-parameter 3-level Box-Behnken design requiring 13 experiments plus replicates.

3.2.2 Experimental error

There are various sources of error. In our example uncertainty is associated with film thickness measurement which itself splits into two parts. The intrinsic inaccuracy of the Nanospec contributes for one part. The etch rate is related to the difference between the film thickness before and after etching. When unpatterned wafers are used those measurements may not be done exactly on the same spot, which accounts for the second part. The etcher itself controls the parameters within some uncertainty. Most of all, the process repeatability is not perfect. To be consistent one would like to account for all those sources of error in a simple and experimental manner. This is achieved by replicating several times the center point (X_1=900 W, X_2=2.0 Torr, X_3=25%). The experimental error associated to the response Y_k is calculated according to :

$$E_k = \sum_{ij}(Y_{ki}-Y_{kj})^2/(2m) \qquad (3.3)$$

where the summation is taken on all pairs i,j $i \neq j$ of replicates and m is their number.

3.2.3 Parameter range

The range over which a parameter is varied must be determined so that the response at + or - levels is different from the response at the center point by far more than the experimental error. On the other hand, the larger the range the higher must be the order of the polynomial. A trade-off must be found depending on the goal. Measuring the response for four values of the most important parameter, if known, may help determine a suitable order of

polynomial. If the curvature of the response seems monotonic (concave or convex only) a second order polynomial is adequate, if the curvature seems to have an inflection point (concave to convex) a third order fit is required.

3.2.4 LSIFIT's features

Given the parameter values (pressure, power...) and the corresponding responses (etch rate, uniformity...), LSIFIT calculates the model coefficients and outputs various statistical tests allowing the user to judge the quality of the fit. In this thesis, the least-squares fit algorithm from reference [10] has been completed to provide the model coefficients individual F-ratios which allow the user to identify the important terms. Model coefficients with low F-ratios can be dropped out of the model, leaving a reduced polynomial. The program also outputs the correlations between the parameters and the responses themselves, and between responses and parameters. Data, fit, residual and relative residual are displayed as well as current statistical tests such as the fit F-ratio, the adjusted R-square and the experimental error F-ratio [4,11,12,13]. Linear and quadratic fits for any number of independent parameters can be generated as well as cubic fits for up to three parameters. For quadratic fits, the program indicates whether an extremum in the response (maximum or minimum) is reached within the experimental window of the parameter space. This is useful when the experimenter deals with more than three parameters at a time which makes it impossible to visualize the response surface. Customized functions can be defined in the source code as well. The software runs on any computer that supports FORTRAN, involving only minor modifications. A personal computer is suitable to run LSIFIT for most practical applications and typical run times range from 15 seconds to 2 minutes.

3.2.5 Contour plots

A FORTRAN program, named MAPPING (appendix A), for displaying two-dimensional contour plots of the responses versus two parameters has been developed on a Macintosh from Apple Computer. Because of the use of the Macintosh's ROM, MAPPING is restricted to this computer. MAPPING maps out the response contour lines as a function of two of the process parameters. For that, it uses LSIFIT output model coefficients. The user can choose interactively the parameters, their range and the responses to be displayed. Several responses can be seen simultaneously and regions where a response takes specific values can be highlighted which makes the program suitable for process optimization. Contour plots presented in this thesis have been drawn by MAPPING.

3.3 The applications of the RSM

The statistical design of experiments is useful for :

- Optimization of manufacturing processes.
- Characterization of manufacturing processes.
- Application to research.

References [11,14-19] illustrate the use of RSM applied to various problems.

3.3.1 Optimization of plasma etching processes

The optimization of plasma etching processes does not necessarily consist of finding the maximum etch rate or selectivity alone. The goal is rather to find a set of operating conditions for which several responses meet together the experimenter's specifications referred to as the target. As an example, the etching of contact holes in SiO_2 on top of polysilicon illustrates the use of

RSM.

An actual process for contact etching of SiO_2 on Si uses CF_4, CHF_3 and He. It is a two-step process. The first of which, referred to as the low-selectivity step, has a relatively high SiO_2 etch rate (about 6000 Å/min) and a low selectivity of etch between oxide and underlying silicon. Their etch rates is in the ratio of about 2:1. The second step, referred to as the high-selectivity step, is used for etching down the remaining oxide without etching too much of the underlying silicon. It has a low SiO_2 etch rate (less than 3000 Å/min) and a higher selectivity (above 7:1).

When etching silicon, free fluorine atoms arriving on the silicon surface are first consumed to form volatile CF_4 from CF_n ($n < 4$) molecules on the surface [20]. The remaining fluorine atoms are available for etching the silicon. Selective etching of silicon dioxide versus (poly)silicon is due to the preferential deposition of polymer on (poly)silicon rather than on SiO_2. The build-up of polymer from CF_n radicals in the plasma competes with the actual etching mechanism. The selectivity oxide to poly raises when the flow rate of CHF_3 is increased. Optimizing the selectivity consists of working at the onset of polymerization which, in the conditions of that experiment, occurred when the $[CHF_3]/[CF_4]$ flow rate ratio exceeded 1.2 [21].

It was proposed that adding argon to this process allows etching with larger $[CHF_3]/[CF_4]$ ratios without depositing polymer, which in turn should increase the selectivity.

21 5-inch SiO_2 and poly wafers, patterned with a contact mask, have been etched in order to test the argon process during the high-selectivity step. The

poly wafers were doped at 20 to 30 Ω/Square. The photoresist (type ONPR800, Tokyo Ohka, positive) has been hardbaked for 30 minutes at 140 ^{o}C. In order to simulate at best the flow of events during production, the sequence of etch was as follows : 1) blank crystalline silicon wafer (dummy wafer) etched for 2 minutes with the low-selectivity step followed by 5 seconds of the high-selectivity step. Then 2) Thermal oxide and 3) poly wafer etched during 1 minute with the high-selectivity step.

A Box-Behnken design was chosen for characterizing the process as a function of 3 parameters : CHF_3 and Ar flow rates, power. The pressure and the gap were held constant. The purpose of this experiment was not to optimize the entire set of parameters but rather verify statistically the assumption that adding argon allows addition of CHF_3 without depositing polymer. Also a 3-level 3-parameter Box-Behnken design requires only 13 different recipes and the intercorrelations between model terms can be kept low so that unambiguous information can be obtained.

The oxide etch rate, the uniformity of etch of oxide and the selectivity, oxide to polysilicon, have been fitted by quadratic polynomials.

Etching recipes with $[CHF_3]/[CF_4]$ ratios up to 2.0 have been used without observing polymer deposition on the wafers. Whether polymer forms on the wall of the reactor or not has not been investigated. Polymer formation on the walls can affect the process repeatability after hundreds of runs. As expected, increasing the relative amount of CHF_3 raises the selectivity (Fig. 3.3.1). For $[CHF_3]/[CF_4]$ ratios above 1.7, the map indicates a decrease in selectivity. The explanation is the following : the response function RF_{sel} for the selectivity S is a gaussian function tending toward 1.0 as the selectivity

approaches 12:1 by superior or inferior limit.

$$RF_{sel} = \exp(-(S-12)^2/32) \qquad (3.4)$$

That way, very high, and therefore nonrepeatable selectivities found at high CHF_3 contents, are disregarded by the fit. In the figures those responses have been converted in actual units. It is also observed that the selectivity improves with increasing amounts of argon. This experiment confirms that adding argon to the process allows one to slightly increase the selectivity.

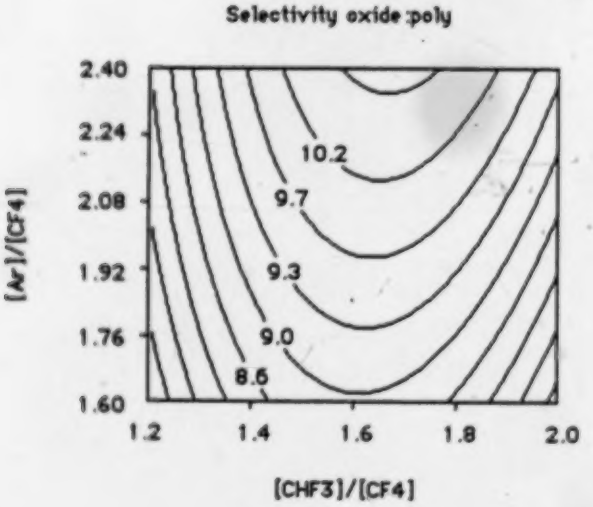

Fig. 3.3.1) Contour plot of the selectivity of etch oxide:poly as a function of added CHF_3 and Ar in the feed gas at constant power. The CF_4 flow rate is fixed.

Under the same conditions the uniformity (Fig. 3.3.2) depends essentially on the relative amount of CHF_3. It is usually correlated to the etch rate. When the etch rate increases, the uniformity decreases, which means that, relative

to the etch rate, fast etching recipes tend to etch more uniformly than slow etching recipes (see definition of uniformity in section 2.3).

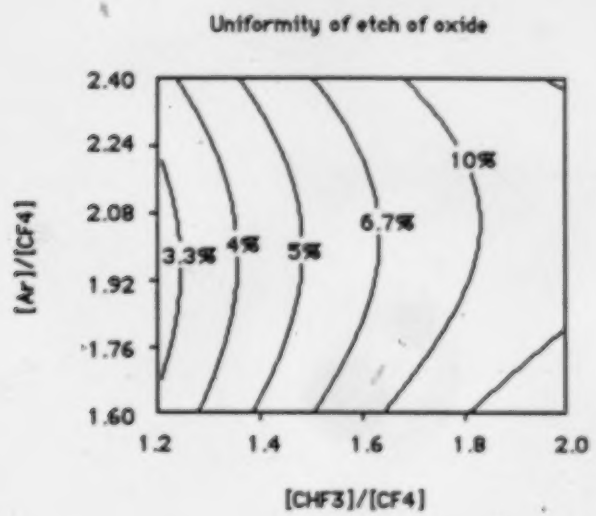

Fig. 3.3.2) Contour plot of the uniformity of etch of oxide as a function of added CHF_3 and Ar in the feed gas at constant power. The CF_4 flow rate is fixed.

As CHF_3 is added, the etch rate decreases (Fig. 3.3.3) indicating that polymer formation slows down the etching of SiO_2. In Fig. 3.3.3, regions where the selectivity is above 10:1 (black) and where the uniformity is within ±5% (shaded) have been highlighted. It can be seen that they do not overlap, which means that a process with the required specifications cannot be achieved in this region of the parameter space. Another way to optimize simultaneously several quantities at a time is to write a function accounting for all the responses.

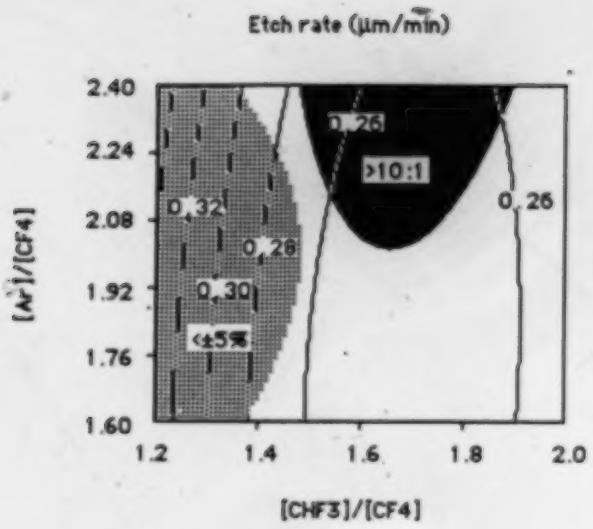

Fig. 3.3.3) Contour plot of the oxide etch rate in µm/min as a function of added CHF_3 and Ar in the feed gas at constant power. The CF_4 flow rate is fixed. The shaded area represents the region of the parameter space where the uniformity is within ±5% while the blackened area is the region where the selectivity is above 10:1.

Imposing the specifications stated above, we can write the following specification response function :

$$S_p = \exp(-(S-12)^2/32)\cdot\exp(-(UN-2)^2/50) \qquad (3.5)$$

S_p tends toward 1.0 as the selectivity S approaches 12:1 and the uniformity UN approaches 2%. It is a gaussian function with standard deviations of 4.0 for S and 5.0 for UN. Taking the product of two gaussian curves acts as a logical AND and imposes that both responses be optimized together. If one response OR the other were to be optimized, a sum of gaussian would be used.

Figure 3.3.4 shows the response function for the specifications. The target

is Sp=0.74 corresponding to 10:1 selectivity and ±5% uniformity.

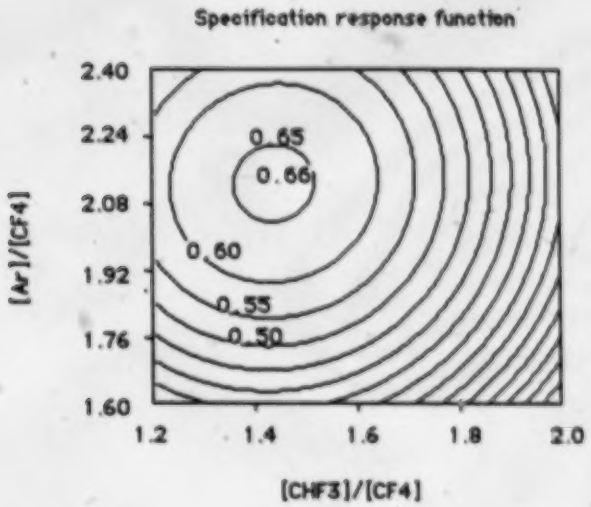

Fig. 3.3.4) Contour plot of the specification response function as a function of added CHF_3 and Ar in the feed at constant power. The CF_4 flow rate is fixed. A value of 1.0 corresponds to 12:1 selectivity and ±2% uniformity while a value of 0.74 corresponds to 10:1 selectivity and ±5% uniformity.

This figure indicates that, although it does not meet the specifications, an optimum exists in the range of experiment. This optimum is at S_p=0.66 , where $[CHF_3]/[CF_4]$=1.44 and $[Ar]/[CF_4]$ =2.12 . Predicted etch rate, uniformity and selectivity are respectively 2755 Å/min, 4.8% and 9.6:1 . One concludes that the target should be searched in another window of the parameter space with a different CF_4 flow rate.

3.3.2 Characterization of plasma etching processes

Once a process has been developed, it is useful to characterize it with the statistical design of experiments. The etch rate, uniformity and other quantities of interest are characterized around the process operating point.

Whenever a response drifts out of specification, the contour plot of that response can help the experimenter pinpoint the problem. The map indicates at what operating conditions, and how far from the normal process, the new response value lies. A systematic characterization of various responses and for various processes provides a fingerprint of the equipment's performances, allowing troubleshooting by cross comparisons. For instance, an off-calibration pressure gauge will affect differently each response in each process and the availability of a data base can help identify the problem.

Therefore, as opposed to process optimization, where only trends matter, process characterization requires a precise and quantitative modeling of the response surface. As a result, the experimental range for a quadratic fit will be relatively narrow, or, as shown in Fig. 3.3.5, a cubic fit will be necessary.

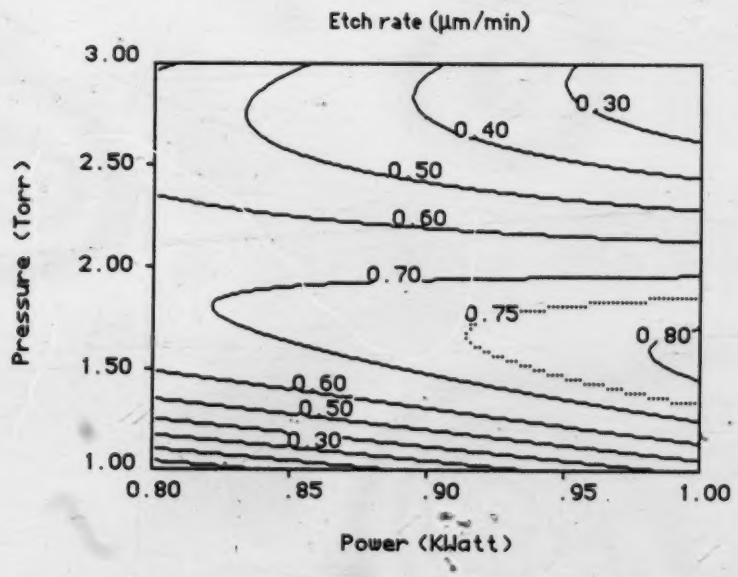

Fig. 3.3.5) Contour plot of the oxide etch rate in µm/min as a function of power and pressure at 150 sccm CF_4, 50 sccm He. Gap is fixed at 0.35 cm.

This figure shows SiO_2 etch rates in a CF_4/He plasma as a function of pressure and power. As third parameter, the fraction of helium in the feed was varied from 0 to 50%. The total flow of CF_4 and He was fixed at 200 sccm while the gap was held constant at 0.35 cm. Nested Box-Behnken (pressure from 1.5 to 2.5 Torr, power from 850 to 950 Watts, He flow from 12.5 to 37.5 %) and FCC (pressure from 1.0 to 3.0 Torr, power from 800 to 1000 Watts, He flow from 0 to 50 %) designs were used which corresponds to 27 different etching recipes with 5-level parameter values (appendix B).

In order to verify the validity of the fit, subsequent SiO_2 etch rate measurements have been collected. An example is shown in Fig. 3.3.6 where a

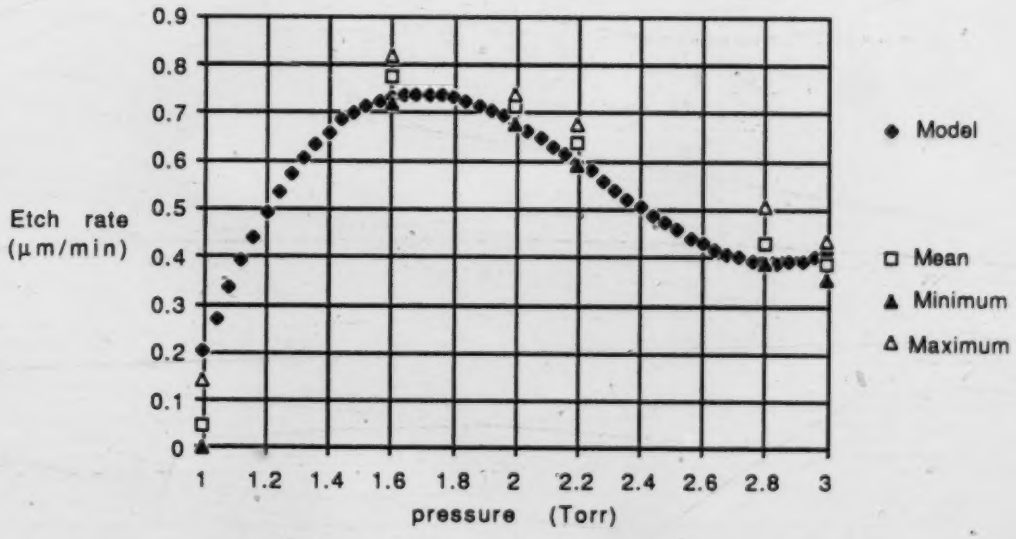

Fig. 3.3.6) Oxide etch rate in µm/min as a function of pressure at 150 sccm CF_4, 50 sccm He, 900 Watts and 0.35 cm gap. Comparison between mathematical model (diamonds) and subsequent measurements (black & white triangles, squares).

section of the map along the pressure axis is compared with experimental

data. The section is at 900 Watts power and 25% He in the feed. The black diamonds represent the mathematical model while the squares are the average etch rates on the wafers. White and black triangles indicate the spread in etch rate across the wafers. Along that section, only three points, at 1.0, 2.0 and 3.0 Torr pressure, belong to the design used for that experiment. Although the model is based on experiments done several weeks prior to the check, both are in good agreement, except for the point at 1.0 Torr which proved not to be repeatable.

3.3.3 Application to research

Nowadays, theoretical models for physical or chemical processes rely heavily on computer numerical simulation. Numerical techniques lack the simplicity of a mathematical formula and do not allow the simulated optimization of a process depending on several theoretical parameters. In this respect, the statistical design of experiments is useful in establishing a data base for comparison with numerical simulations as will be illustrated in the next chapter.

3.4 Summary

As the minimum feature size shrinks, dry etch, as opposed to wet etch, becomes a must for microelectronic devices manufacturing. Consequently, a tighter control and a better understanding of plasma etching processes is required. In order to achieve viable throughputs with a single wafer etcher, one requires relatively high etch rates of 5000-8000 Å/min for SiO_2 contact etch during the low-selectivity step for example. The etch rate uniformity and the process repeatability must be within ±5%.

The optimization and the characterization of microelectronic processes

consist of relating physical quantities of importance to a set of operating conditions. With regard to SiO_2 etching, the purpose is typically to find how process responses, such as the SiO_2 etch rate, the uniformity of the etch across the wafer and the selectivity of the etch between the oxide and underlying materials can be affected by the power injected in the plasma, the pressure, the gas composition and flow rates and the electrode spacing.

This information is necessary for improving existing processes (optimization) and developing new processes. Since the physics and chemistry of plasma etching is not well understood yet, the only straightforward way to model plasma processes is to rely on experiments. Therefore it is desirable to get maximum information with minimum experimentation. The statistical design of experiments (RSM) consists of designing experiments so that unambiguous information can be experimentally obtained. Firstly, responses (etch rate etc) are measured for designed values of the process parameters. Then the responses are related to the process parameters by a polynomial with coefficients that are determined by a least-squares fit. As opposed to the orthogonal matrix method, the RSM accounts for simultaneous variations of several parameters at a time, allowing thus to eventually find the "true" optimum.

The RSM is useful for improving existing or new processes and characterizing production processes which enables the process engineer to identify eventual problems. It can also serve to create a data base for further theoretical modeling.

For those purposes, two FORTRAN programs have been written, the first of which performs a least-squares fit to experimental data. Various statistical tests allowing the user to judge the validity of the fit are output. The second

program is for displaying contour plots of response functions. The software can be used for characterizing any kind of processes. A user-guide for RSM analyses with this software has been written (appendix A).

The use of RSM has been demonstrated for the optimization of contact etch in a CF_4/CHF_3/He/Ar plasma. 15 5-inch thermal oxide and polysilicon wafers have been etched after a 3-level 3-parameter Box-Behnken design. It is shown how the addition of argon in this chemistry allows etching with lower F/C ratios in the feed without depositing polymer. It has been demonstrated how the simultaneous optimization of uniformity of oxide etch and selectivity of etch oxide to poly can be conducted with the software.

To illustrate process characterization, the SiO_2 etch rate has been measured in a CF_4/He plasma for 27 different combinations of power, pressure and fraction of helium corresponding to a 5-level 3-parameter nested Box-Behnken-FCC design. Cross sections in the etch rate surface shows that model predictions within the experimental range are in excellent agreement with subsequent measurements.

The SiO_2 etch rate and uniformity of etch, the oxide:poly selectivity have been measured in a C_2F_6/He plasma for 25 combinations of power (0.76-0.84-0.92 kWatt), pressure (0.75-1.25-1.75 Torr), helium (50-70-90 sccm) and C_2F_6 (86-100-114 sccm) flow rates and gap (0.3-0.5-0.7 cm) on 3 levels. The responses were fitted by quadratic polynomials. Although the fit is statistically good and estimates accurately the experimental observations, the limited amount of data points did not yield good predictions in terms of major trends. More data should be collected in order to characterize this process. Also, process repeatability with C_2F_6 is not as good as with CF_4 which makes it

difficult to get a realistic fit. The relatively poor performances of the C_2F_6/He chemistry obtained at that time are attributed to polymer which may be deposited on the wafers or in the etcher, leading to nonrepeatable results. The same remarks apply to C_3F_8/He chemistry. With about 23 sccm of C_3F_8 and 120 sccm of He, some oxygen (5 sccm of O_2) must be added in order to trigger the etching.

The RSM is most suitable when limited to three parameters. This makes it possible to visualize three-dimensional response surfaces. Also, with a limited number of parameters, the experimental observations are only weakly correlated to each other, therefore providing unambiguous information. With five parameters and quadratic fits, as was experienced with the C_2F_6 process and other chemistries, only a subregion of the parameter space can be modeled or a large number of wafers (about 50) may be required in order to get a representative fit. Furthermore, it becomes difficult to interpret 2D maps when dealing with four parameters or more. Ironically enough, as the number of parameters increases, one tends to use less variables in the graphs. With two parameters, a 3D picture (Fig. 3.1.2) shows at a glance the response surface. With two, three and four parameters, 2D maps are suitable. With four, five and more parameters the tendency is to look at 1D sections of the response surface.

With four parameters and more (only quadratic fits in this case), the fitting program's ability to search for an extremum in the response is very useful. A quick look at the contour plot around the extremum determines whether it is a minimum or a maximum. When dealing with several responses, it is advantageous defining a specification response function as described in section 3.3.1, so that if an optimal process exists inside of the

experimental window, it will be located by the fitting program.

So far a fully automated search toward the maximum, as described by Box [4], has not been implemented in the fitting program. However, it is not really required for the optimization of plasma etching processes on the Lam etcher, since the practical parameter space can be completely covered by only a few experimental designs.

4. PLASMA DIAGNOSTIC

4.1 Methods

Since the development of a theoretical model for process simulation depends critically on experimental verifications, it is essential to compare the results of simulations with plasma diagnostics and etch rate measurements. While etch rates can be easily measured, the experimental diagnostic of a plasma is much more complicated.

The plasma is characterized by its electrical properties, namely the electron concentration and temperature, the potential, the electric field in the sheaths, and by its chemical composition. The plasma electrical properties can be characterized using Langmuir probe techniques [8,22] and spectroscopic analyses of excited species in the glow region [23]. The probes should not disturb the plasma and the interpretation of the measurements is complex, but they offer the advantage of an in situ analysis with spatial resolution in the reactor. Spectroscopic measurements will be explained in detail later, their advantages are that they require nonintrusive tools and the results are readily interpreted. Spatial resolution in the electron density measurements can also be achieved with this technique by using optical lenses to focus the measure.

The plasma chemical composition can be analyzed using optical emission spectroscopy, mass spectrometry and gas phase titration [24]. In this case, the optical spectroscopy provides a quasi in situ measurement of the relative concentration of some species known to be in the glow region, whereas mass spectrometry indicates what species are present in the gas phase. The drawback of mass spectrometry is that downstream measurements identify only stable or long-lived products. Therefore if reactive species are to be

analyzed, the mass spectrometer must be installed as close as possible to the discharge in order to limit gas phase and wall recombination of reactive species into stable molecules. Finally, let us mention the induced optical emission spectroscopy whereby atomic and molecular optical excitations are controlled by a laser, as opposed to the passive optical emission spectroscopy which is based on the monitoring of atomic and molecular relaxation of species excited by electron impact. The induced optical emission spectroscopy requires a costly, sophisticated experimental setup.

4.2 Experimental setup

The plasma etcher has been described in section 2.2. Both electrodes were of anodized aluminum for experiments with CF_4/O_2 discharges because plasmas with large amounts of oxygen, say 1 Torr O_2 partial pressure, would etch the graphite top electrode normally installed in the Lam AutoEtch 590.

The experimental setup is shown in Fig. 4.2.1. For the spectroscopic diagnostic, a fiber optic collects the light emitted by the plasma through the rear quartz window. The emission intensity was monitored with a multichannel analyzer EG&G Plasma Monitor 1451 which has a resolution of 1024 channels.

The emission intensity spectrum was recorded on a X-Y plotter. Mass spectrometric data were obtained from a differentially pumped UTI 100C system. The ion flux intensity spectrum was recorded with a chart recorder which paper unwinding speed and sensitivity could be adjusted. Finally, silicon etch rates were determined by measuring etched step heights with a Tencor Alpha Step.

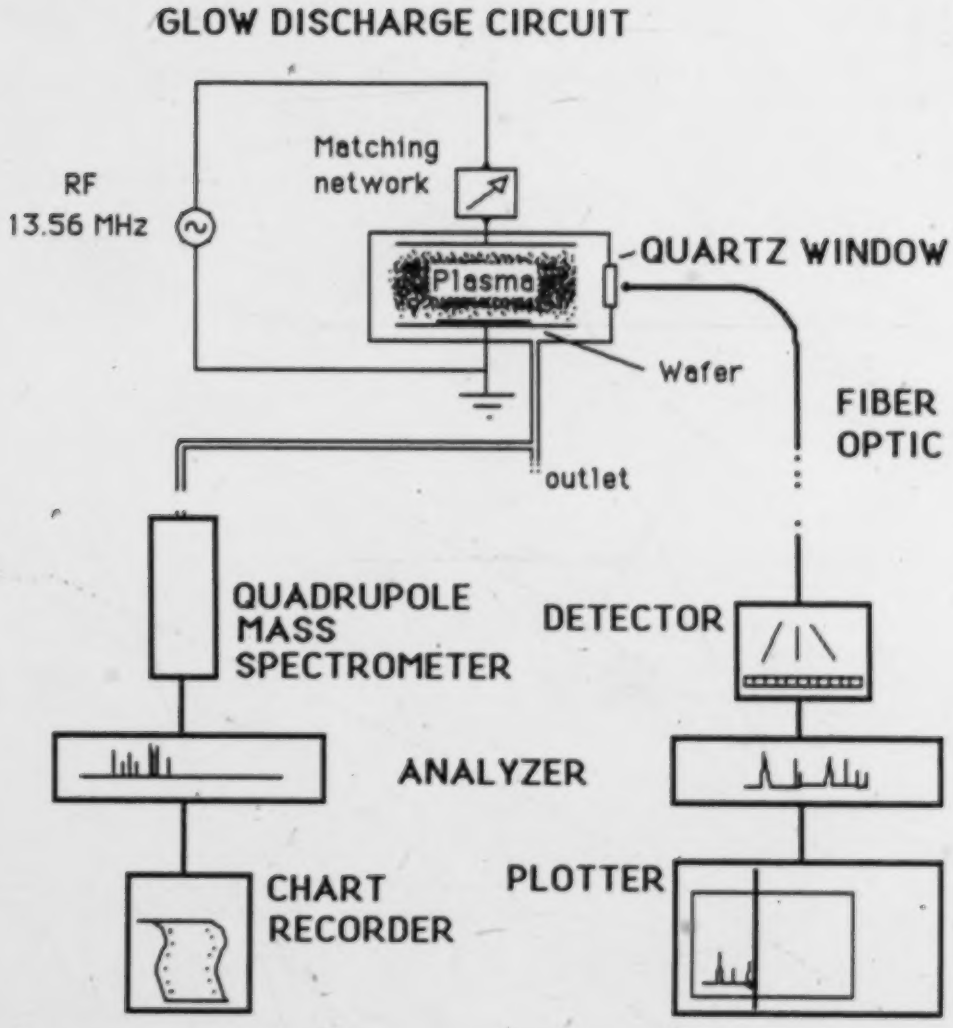

Fig. 4.2.1) Schematic representation of the experimental setup for the diagnostic of CF_4/O_2 plasmas using spectroscopic and mass spectrometric analyses.

4.3 Spectroscopic diagnostic

4.3.1 General principle

The spectroscopic diagnostic of plasmas is a simple nonintrusive method for determining the relative variations in the concentration of excited species with changing process parameters. Since, in passive spectroscopy, the atomic or molecular excitations are due to direct electron impact, the emission intensities will also be related to the electron density and energy [25]. Assuming that the most important excitation process is by electron impact, one has :

$$X + e \xrightarrow{k_x} X^* + e \qquad \text{excitation} \qquad (4.1)$$

$$X^* \xrightarrow{k_r} X + h\Omega \qquad \text{spontaneous emission} \qquad (4.2)$$

$$X^* + M \xrightarrow{k_q} X + M \qquad \text{quenching} \qquad (4.3)$$

where X is an atom and X^* denotes its excited state. e represents an electron while M is a third body (atom or molecule). X^* relaxes by emission of a photon of energy $h\Omega$. We also have $k_r = \Delta t^{-1}$ where Δt is the natural lifetime of the excited state. The emission intensity I_{x*} is related to the concentration of X atoms [X] by :

$$I_{x*} = k_x n_e \cdot [X]/(1+[M]\cdot k_q/k_r) \qquad (4.4)$$

Assuming that the deactivation due to collisions is much slower than the spontaneous emission $[M]\cdot k_q/k_r \ll 1$, one has $I_{x*} = C \cdot k_x \cdot n_e [X]$ where $k_x n_e$ is referred to as the discharge excitation efficiency and it implicitly includes

the electron energy distribution as it will be discussed in section 4.5. Under those conditions it is clear that if the discharge excitation efficiency varies with changing process parameters, I_{X^*} alone does not provide a measure for [X].

In order to account for the variation of the electron density as the process conditions are varied, Coburn and Chen [26] deliberately introduced in the plasma a small amount of an inert gas which has an excited state at an energy above the ground state close to that of the species of interest so that the electron distribution is about the same for both excitations. The optical transition itself can take place between two excited states (Fig. 4.3.1).

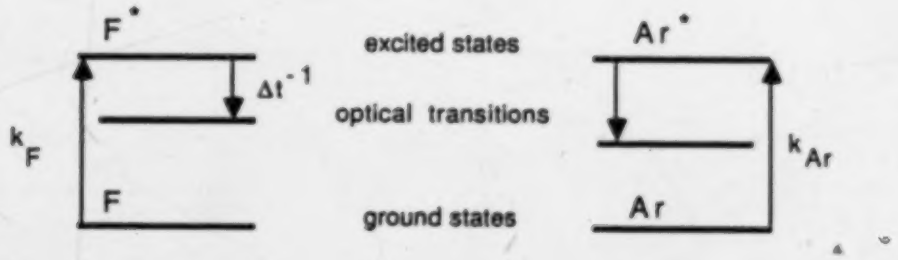

Fig. 4.3.1) The argon emission line intensity is a calibrant for the fluorine emission line intensity because the direct electron impact excitations taking place between the ground states and the excited states have comparable energies.

The content of nitrogen or argon added to the studied chemistry should not exceed 5% to not significantly disturb the plasma.

The fluorine emission line at 703.7 nm corresponding to an excited state at about 14.5 ev above ground, the oxygen line at 777.5 nm are calibrated by the argon line at 750.4 nm corresponding to an excited state at 13.5 ev above ground [26] . Therefore one also has :

$$I_{Ar^*} = k_{Ar} \cdot n_e \cdot [Ar] \qquad (4.5)$$

which gives :

$$I_{F^*} / I_{Ar^*} = (k_F / k_{Ar}) \cdot ([F]/[Ar]) \qquad (4.6)$$

since the argon does not react in the plasma its concentration is constant, thus one obtains a relative measurement for the total concentration of fluorine in the ground state by taking the ratio of both emission intensities.

Furthermore, considering the preceding example for fluorine and oxygen, we can write :

$$I_{O^*} / I_{F^*} = (k_O / k_F) \cdot ([O]/[F]) \qquad (4.7)$$

The ratio of emission line intensities of two excited reactive species gives an indication of the ratio of their total concentrations.

4.3.2 Quantitative approach

Let us calculate more thoroughly the relationship between the spectrometer reading, the concentration of an excited atom $[X^*]$ and its total concentration in the ground state [X]. The same assumptions as before with regard to the excitation and relaxation processes are made.

Firstly, in a typical parallel plate reactor such as the Lam etcher, the flux of photons per unit area per unit time through the plasma surface is related to the number of counts indicated by the spectrometer as follows :

$$\Delta I_\mu = N_\mu \cdot 4\pi h\mu/(HRAt_s C(\mu)S) \quad [Watts\,m^{-2}] \tag{4.8}$$

where ΔI_μ is the intensity of the plasma surface, N_μ the number of counts during the sampling time. Moreover the following symbols have been used :

h Planck constant.
μ transition frequency.
H plasma height = gap.
R plasma radius (8" diameter electrode).
A area of sensitive surface on the fiber optic.
t_s sampling time in seconds.
C(μ) detection response in counts per photon at frequency μ.
S in $[m^{-2}]$ is an integration constant that accounts for the fact that the sensor receives photons from different parts of the plasma surface. Therefore the factor S depends on the position of the sensor with respect to the plasma.

A detailed derivation of equation (4.8) is given in appendix C. It has been assumed that the nearest distance between the tip of the optical fiber and the plasma is much larger than half the plasma height, that is, the angle at which the sensor "sees" the plasma thickness is small. Otherwise integration along the plasma height should also be carried out.

The total luminescent intensity L_μ of the plasma is therefore given by :

$$L_\mu = 2\pi R(H+R)\ \Delta I_\mu \quad [Watts] \tag{4.9}$$

while the density of photons leaving the plasma per unit time f_μ is :

$$f_\mu = L_\mu / h\mu V \quad [m^{-3}s^{-1}] \tag{4.10}$$

where V is the plasma volume : $V = \pi R^2 H$. This leads to :

$$f_\mu = 8\pi\cdot(1/R+1/H)\cdot(HRAt_s\, C(\mu)S)^{-1} N_\mu \qquad (4.11)$$

that we will write $f_\mu = G\cdot N_\mu/C(\mu)$ since G will be constant in this study.

Let us now write the balance equations for the photon density as well as for the excited atom concentration in the plasma :

$$dN_{x*}/dt = \Delta t^{-1}[X^*] - \sum_\mu f_\mu \qquad (4.12)$$

$$d[X^*]/dt = k_x\cdot n_e[X] - \Delta t^{-1}[X^*] \qquad (4.13)$$

where N_{x*} is the photon density for the X^*--->X transition. The summation over μ accounts for the emission line width, therefore the summation should be carried out on the frequencies around μ_o, the emission line frequency. Physically it should be an integration along the frequency axis but since the multichannel analyzer digitizes the spectrum, the summation is made on the channels. At steady state, both equations equal zero and, using equation (4.12), the concentration of excited X atoms $[X^*]$ can be related to the spectrometer readings contained in f_μ :

$$[X^*] = \Delta t \sum_\mu f_\mu \qquad (4.14)$$

introducing this expression for X^* in equation (4.13), it becomes :

$$[X] = \sum_{\mu} f_{\mu}/k_x n_e = (G/k_x n_e) \sum_{\mu} N_{\mu}/C(\mu) \qquad (4.15)$$

N_{μ}, the spectrometer reading has been related to the total concentration of X in the ground state. This expression is the same as the one written at the beginning for the intensities (equ. (4.4)) :

$$\sum_{\mu} N_{\mu} = (C(\mu_o)/G)\, k_x\, n_e[X] \qquad (4.16)$$

Only now we have an absolute value for [X]. G can be calculated or at least estimated. It has been assumed that $C(\mu)$ does not change significantly over the emission line width and equals $C(\mu_o)$. We still need to know k_x and n_e.

4.4 Experimental results

4.4.1 Optical spectroscopy

The argon emission line intensity peak value has been monitored as a function of pressure in a CF_4/O_2 plasma with the Lam etcher 590 empty of wafers (Fig. 4.4.1). Since the argon concentration increases as the pressure increases at constant gas flow rates, the argon intensity readings have been divided by the pressure. This correction has been done with respect to the reading at 1.4 Torr.

As the pressure increases, the argon intensity readings did not change much, the 1/p behavior shown in the figure is therefore mainly a consequence of the correction. Under the assumptions made earlier this graph represents the variations of the discharge excitation efficiency,

namely $k_x n_e$, with pressure. This result is also in good agreement with measurements found in [27] at different plasma conditions.

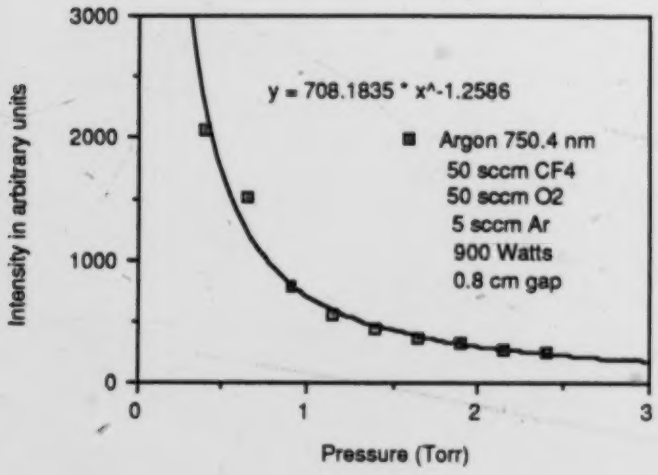

Fig. 4.4.1) Argon emission line intensity (750.4 nm) versus pressure in a CF_4/O_2 plasma with argon. This graph represents the variations of the discharge excitation efficiency for a constant absolute amount of argon as a function of pressure. The squares represent the corrected experimental values while the solid line is a least-squares fit showing an almost perfect 1/p dependence.

Figure 4.4.2 shows that raw oxygen emission intensities and intensities corrected with the excitation efficiency have opposite trends when the pressure is varied. Since the global amount of O_2 increases with increasing pressure, it is expected that the concentration of O will follow this trend as well. Therefore, this graph stresses how necessary it is to calibrate the intensity readings when the pressure is varied.

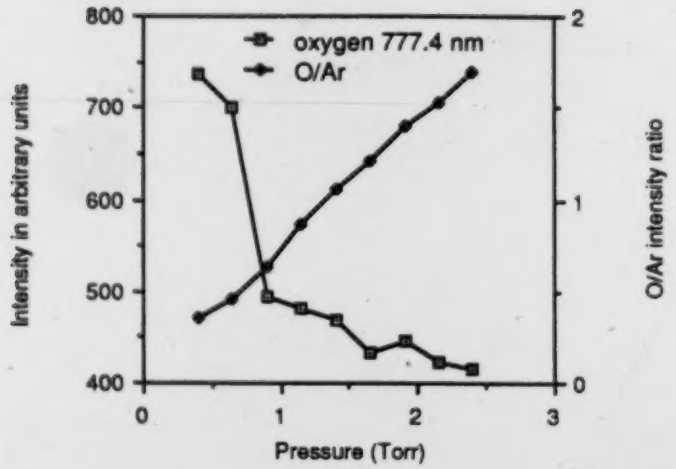

Fig. 4.4.2) Oxygen (O) emission line intensity at 777.4 nm as a function of pressure. The dotted squares are the raw oxygen readings while the black diamonds are those readings corrected by the excitation efficiency. It represents the relative behavior of the O concentration versus pressure. The process parameters have the same values as in Fig. 4.4.1.

Figure 4.4.3 shows the fluorine emission line intensity at 703.7 nm and the

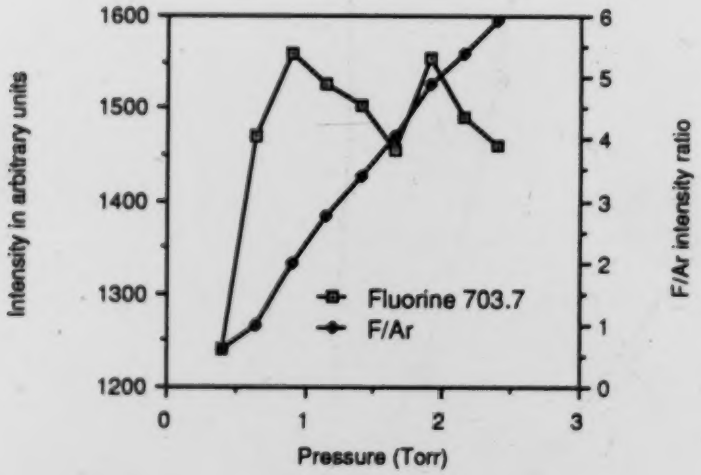

Fig. 4.4.3) Fluorine emission line intensity at 703.7 nm as a function of pressure. The dotted squares are the raw fluorine readings while the black diamonds are those readings corrected by the excitation efficiency. It represents the relative behavior of the F concentration versus pressure. The process parameters have the same values as in Fig. 4.4.1.

relative F concentration obtained by actinometry as a function of pressure. The dip in fluorine emission at about 1.6 Torr has not been observed previously. A temporary instability of the plasma or some reflected power might explain it. Anyway, it does not affect the behavior of the calibrated F concentration which increases steadily with increasing pressure.

Figure 4.4.4 shows that the corrected fluorine intensity versus percentage of O_2 in the feed gas does not change the observation much.

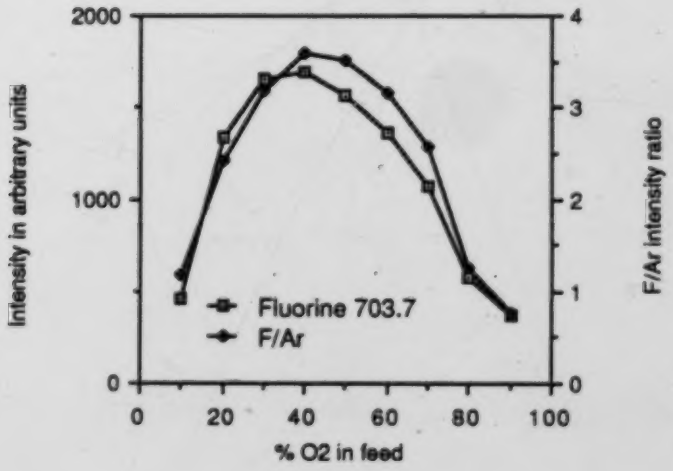

Fig. 4.4.4) Fluorine emission line intensity at 703.7 nm and F/Ar intensity ratio as a function of the percentage of O_2 in the feed CF_4/O_2 gas mixture. The total flow of CF_4 and O_2 is fixed at 100 sccm. 5 sccm of argon are added. The power is 900 Watts, the pressure is 1.4 Torr and the gap is 0.8 cm.

As O_2 is added into the feed gas, oxygen atoms from broken O_2 molecules combine with CF_n (n<4) radicals to form CO, CO_2, COF_2 and COF, leaving more free fluorine atoms in the plasma. As the amount of O_2 in the feed increases, the content of CF_4 decreases, for a fraction of O_2 exceeding 45%, the

production of F atoms from those chemical reactions does not compensate for the shortage in supply of F from the CF_4 input gas [24]. This explains the behavior of the F concentration versus the O_2 percentage shown in Fig. 4.4.4.

The major trends of the fluorine concentration as a function of the O_2 content, pressure and power, are mapped out in Fig. 4.4.5 obtained with the

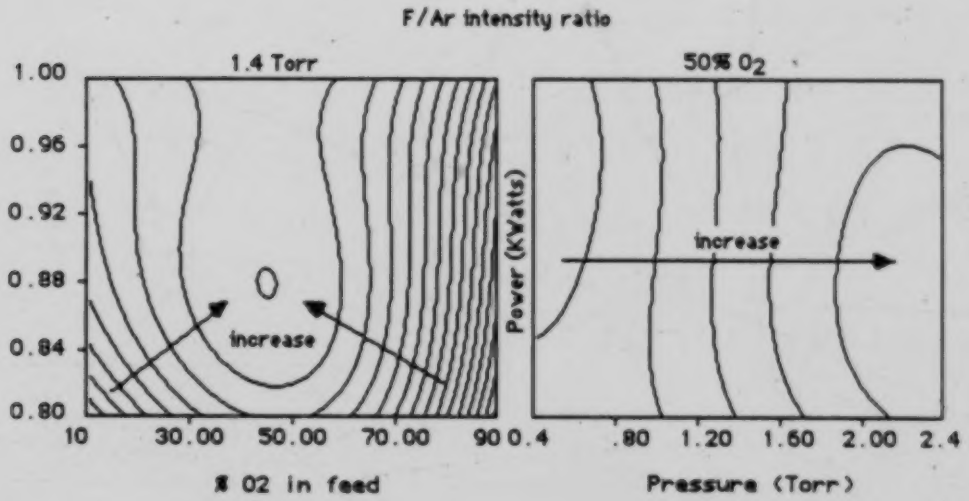

Fig. 4.4.5) F(703.7)nm/Ar(750.4nm) intensity ratio as a function of the percentage of O_2 in the feed CF_4/O_2 mixture, pressure and power (vertical axis). The total flow of CF_4 and O_2 is fixed at 100 sccm. 5 sccm of argon are added. The gap is 0.8 cm. Statistical tests: F-ratio=102.8, 3.88 corresponds to 99% level of confidence, R^2=0.98.

RSM using a 3-parameter 5-level nested FCC-Box-Behnken design (see appendix B) corresponding to 32 experiments including replicates. The F/Ar intensity ratio was fitted with a third order polynomial. The fluorine concentration is pretty much independent of the power, it reaches a maximum between 40 and 50 $\%O_2$ in the feed (see also Fig. 4.4.4) and it

increases with increasing pressure (see also Fig. 4.4.3). Similarly, the correlation coefficients between the model terms and the F/Ar intensity ratio, shown in Table II, indicate that the fluorine concentration is not correlated to the power (r=0.0) at first order but only at second order (power^2: r=-0.5). Its linear and cubic dependence on the $\%O_2$ is negligible whereas it is strongly correlated to the square term $(\%O_2)^2$ as expected from Fig. 4.4.4 .

Table II :

Model terms correlation coefficients with the F/Ar emission intensity ratio. A value of 0.41 indicates a correlation at a level of confidence of 99% according to the t-test.

corr. coeff.	model terms
-0.1	%O2
0.6	pressure
0.0	power
-0.7	(%O2)(%O2)
0.0	(%O2)(pressure)
0.0	(%O2)(power)
-0.5	(pressure)(pressure)
0.0	(pressure)(power)
-0.5	(power)(power)
-0.1	(%O2)(%O2)(%O2)
0.3	(%O2)(%O2)(pressure)
-0.1	(%O2)(pressure)(pressure)
0.5	(pressure)(pressure)(pressure)
0.0	(%O2)(%O2)(power)
-0.1	(power)(power)(%O2)
0.0	(pressure)(pressure)(power)
0.3	(pressure)(power)(power)
0.0	(%O2)(pressure)(power)
0.0	(power)(power)(power)

Subsequent measurements along three sections of the response surface were made in order to verify those trends. Those measurements are compared with the mathematical model in Fig. 4.4.6 through 4.4.8.

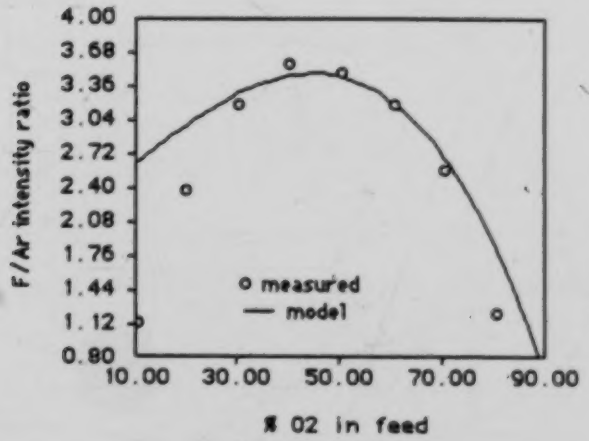

Fig. 4.4.6) Section of the contour plot of Fig. 4.4.5 as a function of the O_2 content in the feed at 1.4 Torr and 900 Watts. The circles indicate subsequent measurements.

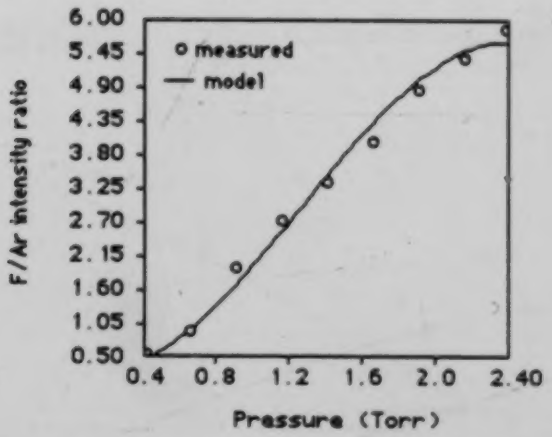

Fig. 4.4.7) Section of the contour plot of Fig. 4.4.5 as a function of pressure at 900 Watts and with 50% O_2 in the feed. The circles indicate subsequent measurements.

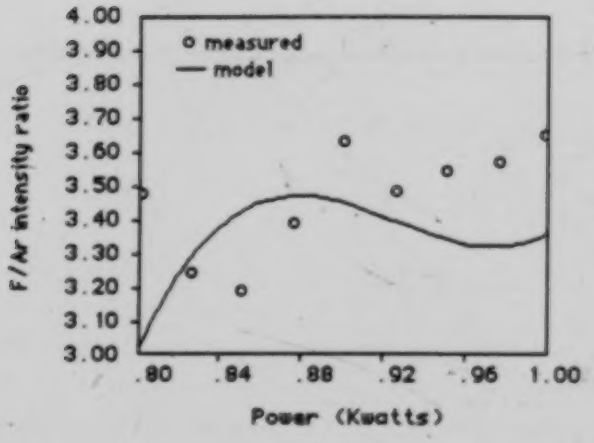

Fig. 4.4.8) Section of the contour plot of Fig. 4.4.5 as a function of power at 1.4 Torr and with 50% O_2 in the feed. The circles indicate subsequent measurements.

It can be seen that quantitative predictions at low O_2 content would be somehow inaccurate but the qualitative behavior of the fluorine concentration is correctly reproduced by the model. In Fig. 4.4.8, the model does not appear as good as it really is because of the narrow F/Ar intensity ratio scale which ranges from 3.00 to only 4.00. Measured F/Ar intensity ratios are spread over the range 3.20 to 3.60 while the model covers the range 3.00 to 3.50 . Both spreads are small as compared to those of Fig. 4.4.6 & 4.4.7.

4.4.2 Mass spectrometry

The stable products from a CF_4/O_2 plasma in presence of silicon in the system have been sampled downstream of the discharge using the mass spectrometer. The species have been identified as shown in Fig. 4.4.9 and Table III.

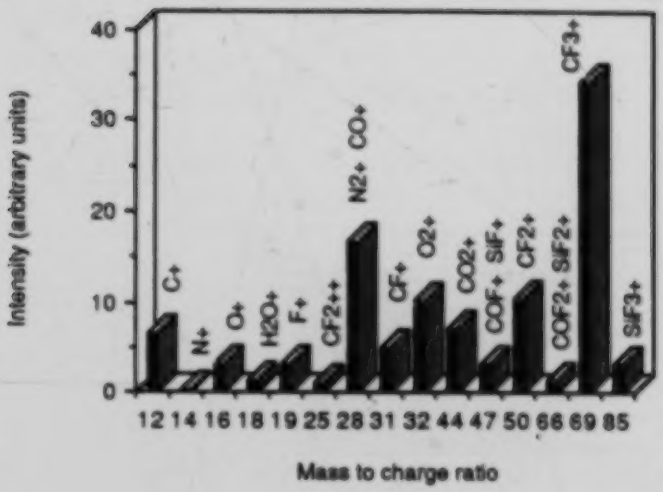

Fig. 4.4.9) Mass spectra downstream of a 80/20 sccm CF_4/O_2 plasma with a 5 inch silicon wafer in the reactor at 800 Watts, 200 mTorr and 0.8 cm gap.

Table III.

mass/charge	ion	parent molecule
12	C^+	CF_4, CO, CO_2
14	N^+	N_2
16	O^+	O_2, CO, CO_2
18	H_2O^+	H_2O
19	F^+	CF_4
25	CF_2^{++}	CF_4
28	N_2^+, CO^+	N_2, CO
31	CF^+	CF_4
32	O_2^+	O_2
44	CO_2^+	CO_2
47	COF^+, SiF^+	COF_2, SiF_4
50	CF_2^+	CF_4
66	COF_2^+, SiF_2^+	COF_2, SiF_4
69	CF_3^+	CF_4
85	SiF_3^+	SiF_4

4.5 Plasma electrical properties

It was mentioned in section 4.3 that the discharge excitation efficiency $k_x n_e$ contains implicitly the electron energy distribution (EED). According to the Maxwell-Boltzmann distribution the EED is a function of the electron temperature as shown in Fig. 4.5.1. Although the EED can be significantly

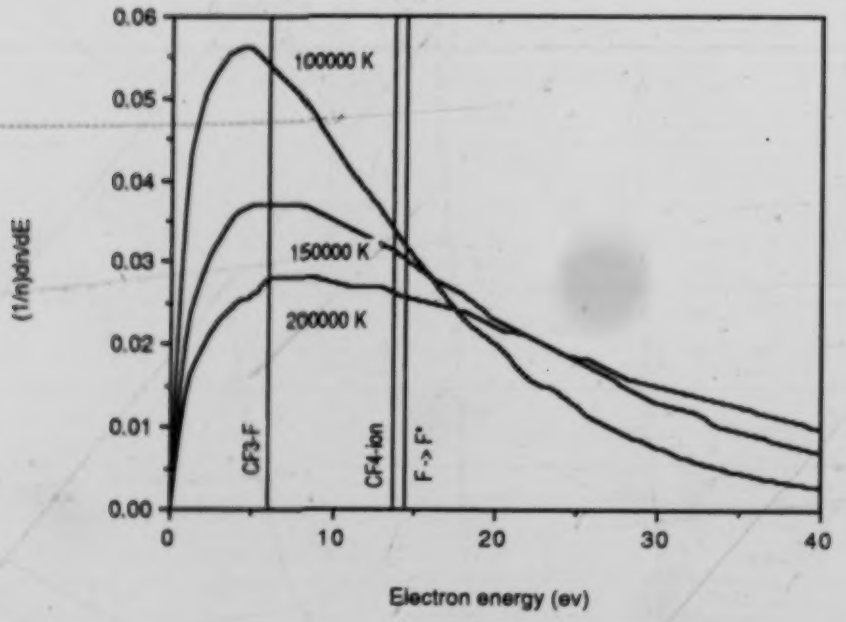

Fig. 4.5.1) Maxwell-Boltzmann distribution.

different from the Maxwell-Boltzmann distribution [8], Fig. 4.5.1 illustrates that, at typical electron temperatures of the order of 10^5 K, the electron density at energies corresponding to the CF_3-F bond (5.6 ev), the CF_4 ionization energy (13.6 ev) and the fluorine excitation energy (14.5 ev), the density of electrons available for those processes varies with the electron temperature. At those temperatures, the density of electrons for the processes

described above decreases with increasing temperature but it would increase at temperatures of the order of 10^4 K.

The variation in the discharge excitation efficiency $k_x n_e$ (Fig. 4.4.1) as pressure is varied is believed to be the result of the variation in the EED because of changing plasma electrical properties. Measurements of the DC self-bias (V_b in Fig. 2.1.2) as a function of pressure indicate changes in the plasma electrical properties (Fig. 4.5.2). This effect is accompanied by a

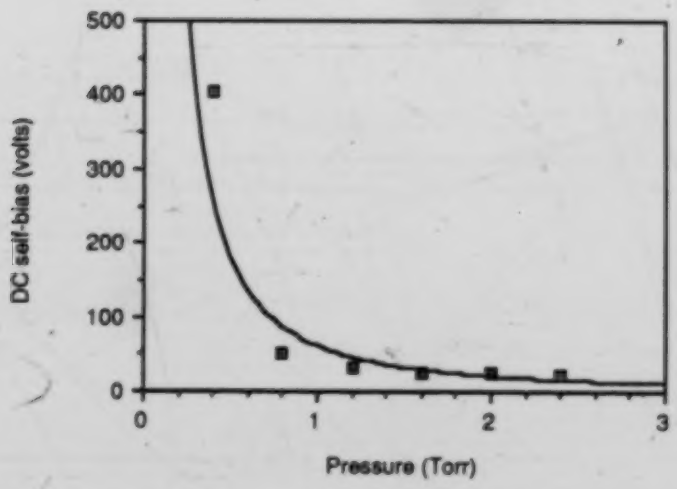

Fig. 4.5.2) Measured DC self-bias versus pressure at 50/50 sccm CF_4/O_2, 900 Watts and 0.8 cm gap.

change in either the plasma potential (V_p in Fig. 2.1.2) or the peak to peak RF voltage applied to the powered electrode or both of them [7]. The DC self-bias is also a function of power and percentage of O_2 in the CF_4/O_2 gas mixture.

5. NUMERICAL SIMULATION OF A CF_4/O_2 PLASMA ETCHING SILICON

5.1 Previous studies

The complexity of plasma etching processes has been pointed out in section 2.1. Although the etching mechanism is the result of various physical and chemical phenomena interacting with each other, each aspect of the overall process can be investigated individually. In fact, current techniques of physics and chemistry can be applied to the study of plasma etching and its understanding is rather a matter of adapting those theories to this specific problem. The least understood part of the etching mechanism is probably the surface chemistry, which depends on unknown variables such as surface cleanliness to name one.

The modeling of RF discharges has been addressed by Kushner who simulates spatially the average electron energy between the electrodes of a parallel plate reactor using the Monte-Carlo method [28]. For the same configuration, Graves and Jensen propose a continuum model for DC and RF discharges and calculate the electric field and potential as well as electron and ion currents [29]. Rogoff, Kramer and Piejak use the Boltzmann equation to calculate the time-dependent electron concentration and electric field in a parallel plate RF chlorine discharge [30]. Those are some of the references illustrating different approaches to the modeling of RF discharges.

The simulation of the gas phase chemistry aims to calculate the concentration of species in the plasma and relate it to measured concentrations and ultimately etch rates. In [31], Edelson and Flamm describe a model for the simulation of a CF_4 plasma during the etching of silicon. In their calculation a "plug-flow" reactor is assumed and the concentrations are

calculated as a function of time which is proportional to the distance the packet of gas travels along the tube. Using the same approach, Plumb and Ryan [32] have developed a reaction scheme for a CF_4/O_2 plasma and compare their results with experimental data from Smolinsky and Flamm [33]. They make a similar comparison for the simulation of a pure CF_4 plasma in presence of silicon in the system [34]. Their work shall be discussed further since it constitutes the baseline of the numerical simulation presented here.

Dalvie, Jensen and Graves have addressed the modeling of a radial flow reactor where they calculate silicon etch rates as a function of position in a CF_4 plasma [35].

A detailed understanding of the plasma electrical properties and their spatial dependence is helpful in designing reactors in order to achieve repeatability and uniformity of etch across a wafer. Chemical factors, on the other hand, determine the etch rates. Transport processes [36] influence both the etch rate, which depends on the supply of etchants, and the uniformity, which depends on how well reactive species are distributed in the plasma.

Few attempts have been made to merge the electrical and chemical problems along with the transport of species onto the surface to be etched, into a unified model. Kushner has developed a kinetic model for the etching of Si and SiO_2 in C_nF_m/H_2 and C_nF_m/O_2 mixtures [20]. In this model, the electron density is simply related to the power deposited in the plasma and to the concentration of species. The electron density determines the dissociation rates of incoming inert molecules from the feed gas. The concentrations are self-consistently computed from the chemical reaction scheme until steady-state is reached and are plotted as a function of the composition of the

feed. Si and SiO_2 etch rates are related to the supply of etchant onto the surface which accounts for diffusion processes. The same model has been adapted by Anderson, Merson and Light to calculate polysilicon etch rates in a SF_6/O_2 mixture as a function of the percentage of O_2 in the feed [37]. Kline uses Monte Carlo simulation and the Boltzmann equation along with the chemical kinetics and diffusive transport to describe a low-pressure RF discharge SF_6 plasma etching silicon [38].

In this thesis, in an attempt to improve our current understanding of the gas phase chemistry of plasma etching silicon, a numerical simulation of a CF_4/O_2 plasma has been conducted. The steady state concentrations of the most important species in the plasma have been calculated for various conditions of power, pressure and gas flow. The results of the simulation are compared with a spectroscopic analysis of fluorine and oxygen atom emission intensity and etch rate data of crystalline silicon.

Numerous numerical simulations of plasma etching processes found in the literature rely on large mainframe computers and often the results are compared with experimental data from other sources where laboratory "plug-flow" reactor setups are used. Rather than include all the physical and chemical processes taking place in plasma etching, the philosophy of the work presented here was to see how well a "plug-flow" reactor, chemical kinetics model [32,34] could apply to the simulation of etch rates in a commercial parallel plate reactor, and how it compares with experimental data obtained on that equipment. This relatively simple model, as compared to the complexity of plasma etching, allows one to understand some of the fundamental mechanisms occurring in a cold, weakly ionized plasma, such as those encountered in dry etching processes. This kind of simulation requires

only a relatively small size computer. The chemical kinetics simulation program now runs at the Alberta Microelectronic Centre.

5.2 Numerical simulation

5.2.1 The model

A reaction scheme for the CF_4/O_2 plasma published by Plumb and Ryan [32] has been simulated. The reaction scheme includes first order electron impact dissociation, where the electron density is not a computed variable but only an input parameter, and numerous chemical reactions. The RF discharge parameters show only through the power density dependent electron impact dissociation rates and is therefore not truly included in the model. The ion chemistry is not treated by this model. Other transport processes than the nonviscous "plug-flow" assumed here are not treated either.

The reaction scheme is shown in appendix D. Dissociative collisions proceeding with an electron are denoted -e-> while those reactions needing a third body are denoted -M-> and a two-body rate is used. In accord with to previous experimental results and simulations [20,39], the electron density has been made proportional to the power density W/V where W is the power deposited in the plasma and V its volume. The dissociation rates k_e have been calculated so that they equal those given by Plumb and Ryan under the plasma conditions of [33] (power : 49 Watts, volume : 14 cm^3).

$$k_e = k_0(W/V) \qquad (5.1)$$

where k_o is constant in this model. A steady room temperature (300 K) is assumed in this study. Temperature dependent reaction rates with the proper activation energy could also be used.

However simplified is this model, it already includes all the important process parameters, which are, percentage of O_2 in the feed, pressure, power and plasma volume (gap).

5.2.2 The simulation program

The simulation consists of solving the set of differential equations describing the CF_4/O_2 plasma reaction scheme. A FORTRAN program named "chemk", originally written by Gary Whitten [40], reads the chemical reactions under their symbolic forms and converts them into a system of differential equations. For instance, the reaction that produces F and COF_2 from CF_3 and O is simply described in the program input file as follows :

$$CF3 + O \text{ --k--> } COF2 + F \qquad (5.2)$$

where k is the reaction rate. This relation translates into four second order differential equations describing the time derivative of each species :

$$d[COF_2]/dt = k[CF_3][O] \qquad (5.3)$$

$$d[F]/dt = k[CF_3][O] \qquad (5.4)$$

$$d[CF_3]/dt = -k[CF_3][O] \qquad (5.5)$$

$$d[O]/dt = -k[CF_3][O] \qquad (5.6)$$

The inputs are the reactions and their reaction rates, the initial concentrations and the output attributes. "chemk" calculates the individual concentrations as a function of time. It is also possible to simulate the flow in (feeding) and flow out (pumping) of gases present in the plasma. Reactions up to the third order can be included in the reaction scheme. The reaction rates can be defined as functions of the process parameters but they are calculated at the beginning and will not be updated during the computation. In other words, the program does not perform a self-consistent computation of a system of differential equations with variable coefficients. "chemk" has been run on a Microvax II from Digital Equipment.

5.2.3 Steady state

We are not very much interested in the transient calculated concentrations inasmuch as their steady state values are reached. Preliminary transient analyses were made in order to determine at what time the concentrations reach their steady state values. A typical result is shown in Fig. 5.2.1.

In an imaginary perfectly isolated reactor without feeding, pumping or production and loss of any sort, the evolution of the total concentration would be similar to that of the curve marked with black diamonds in Fig. 5.2.1 if the initial total pressure of CF_4 and O_2 was 1.0 Torr. The increase is due to the formation of new species in the gas phase. With a constant in-out flow rate of 100 sccm, the total concentration is still higher than the initial concentration (squares in Fig. 5.2.1). In order to force the total concentration to come back to its initial value, the pumping rate must exceed the feeding rate. This mode has been called adjusted pumping (triangles in Fig 5.2.1).

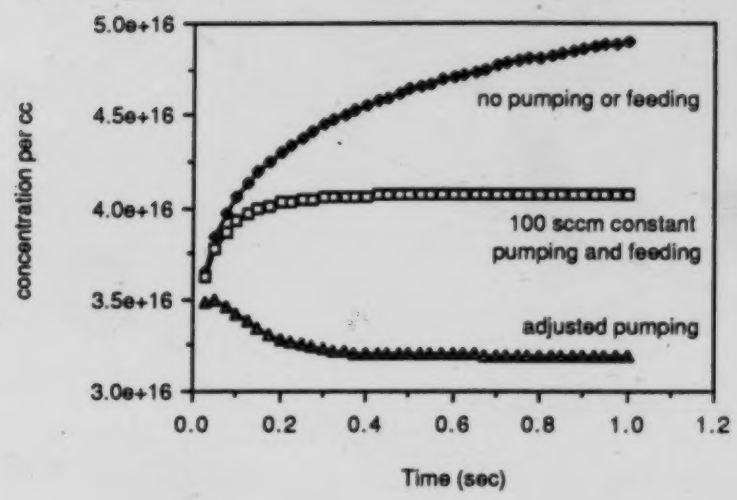

Fig. 5.2.1) Computed total concentration in a 50/50% CF_4/O_2 plasma as a function of time for various gas flow modes. The initial pressure is 1.0 Torr, the power is 900 Watts and the plasma volume 259 cm^3.

This procedure simulates what happens in the Lam etcher, since, before the plasma is ignited, the etcher adjusts the pump speed to match the pressure with its desired value. As indicated in the reaction scheme, the net pumping rate is made proportional to the total concentration. That way, the steady state is reached more quickly and to some extent the program will stabilize the total concentration automatically. A suitable pumping rate must still be found empirically since there is no built-in option in "chemk" that will keep the total gas density constant. We will see later how a suitable pumping rate can be estimated depending on the conditions.

Figure 5.2.2 shows the total concentration for various total input flow rates. It can be seen that the time needed to reach steady state is well correlated with the input flow rate. With an initial total pressure of 1.0 Torr ($3.22 \cdot 10^{16}$ particles per cc), 100 sccm total input gas flow rate of CF_4/O_2 split 50/50 %, the adjusted pumping speed required is 132 sccm. As a result of the

adjusted pumping rate, the average residence time of a species is no longer exactly given by the total input flow rate. Thus, although argon does not react in the plasma, its partial pressure can be slightly lower than that without plasma. In a 50/50 sccm CF_4/O_2 and 5 sccm Ar gas mixture, at 900 Watts and 259 cm^3 plasma volume, the calculated partial pressure of argon was found to be 3.8 % of the total pressure instead of the initial 4.8 %. The difference is therefore a significant 21% with respect to the initial value.

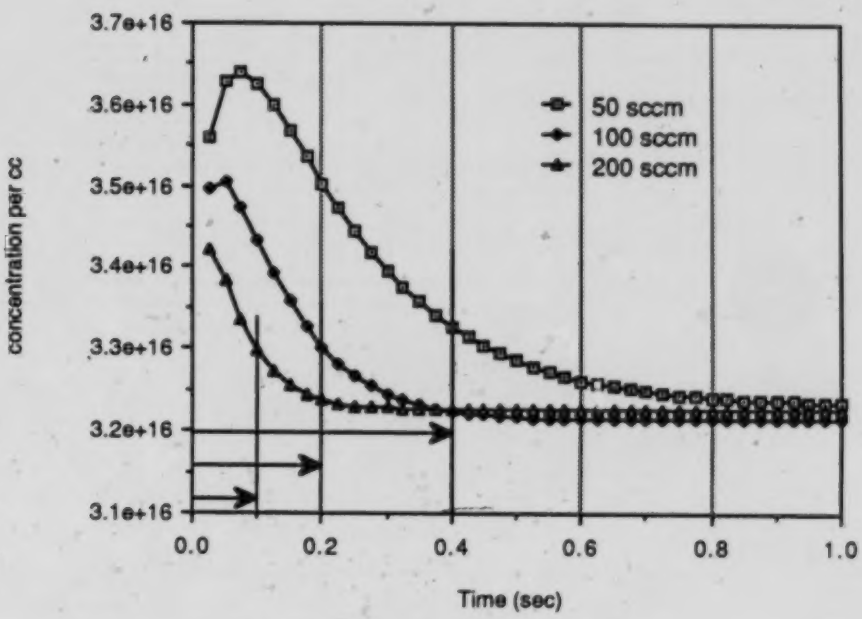

Fig. 5.2.2) Computed total concentration in a 50/50% CF_4/O_2 plasma as a function of time for various total gas flow rates. The initial and steady state pressure is 1.0 Torr, the power is 900 Watts and the plasma volume 259 cm^3. The arrows indicate the residence time corresponding to each flow rate.

This phenomenon was brought up by the simulation and there is no experimental evidence indicating that it really happens in the discharge. One might argue that the calculated difference in pumping speed without and

with plasma (100 and 132 sccm) necessary to maintain the initial total pressure should be seen by reading the Lam etcher's AC2 valve angle controlling the pumping in the reactor chamber. No difference was observed before and after the plasma was turned on. On the other hand, a slight difference in the angle can be seen when flowing 50/50 sccm (angle 33.4^{o}) or 82/50 sccm (angle 35^{o}) of CF_4/O_2 in the Lam etcher model 590 without plasma. Yet in the simulation, one assumes that the reactor volume is just the plasma volume, whereas in the Lam etcher, the plasma volume is much smaller than the total chamber volume. Therefore, in the etcher, the pressure increase occurring in the plasma and predicted by the simulation propagates throughout the chamber, attenuating the overall pressure increase. As a result, the adjustment of the outlet valve angle might be too small to be read. But this does not prove that the simulation is wrong in predicting lower argon concentrations between the electrodes when the plasma is on. Since in the machine, the plasma is contained within the narrow electrode gap, the local production of species occurring there may still influence the average argon content in the glow region.

According to Fig. 5.2.2, at 100 sccm total flow rate, the steady state is reached after about 0.4 sec. Mass spectrometric data of the CF_3^+ line indicate however that the amount of converted CF_4 increases constantly over an etch period of 3 minutes (Fig. 5.2.3). Although the signals have not been calibrated the decrease of the CF_3^+ line is correlated with the increase in the COF_2^+/SiF_2^+ and the SiF_3^+ lines. Therefore, the decreasing recombination of CF_n ($n \leq 3$) radicals into CF_4 corresponds to an increasing amount of SiF_4 and possibly COF_2.

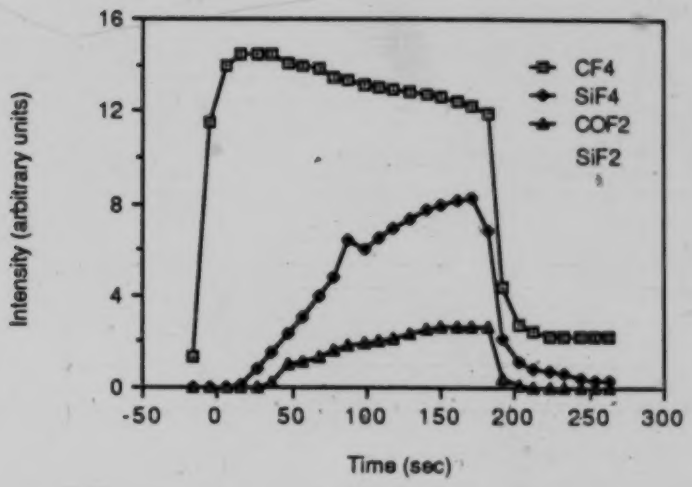

Fig. 5.2.3) Mass spectra signals of the 69 line (CF_3^+ parent to CF_4), the 66 line (COF_2^+ & SiF_2^+ parent to COF_2 & SiF_4) and the 85 line (SiF_3^+ parent to SiF_4) as a function of time during silicon etching (6 inch wafer) in a 87.5/50/5 sccm $CF_4/O_2/Ar$ plasma, at 1.4 Torr, 900 Watts, 0.8 cm gap. The power is turned on at time 0 and off after 180 sec. The signals are not calibrated.

5.2.4 Flow rates

Let us see how the pumping rate can be estimated when the process parameters are varied.

Since the Lam etcher feeds the input gases in the reactor through a perforated top electrode, it is assumed that the relevant reactor volume is the volume comprised between the two 8 inch electrodes rather than the total chamber volume. This is an approximation which seems reasonable since the electrode spacing is much smaller than the electrode radius. This volume is also assumed to be the plasma volume which means that the sheath thickness is neglected.

Under those assumptions, the feeding rate constant is given by :

$$k_f = 3.77 \cdot 10^{17} \cdot F/(gT) \quad [cm^{-3}sec^{-1}] \qquad (5.7)$$

where F, the total input flow rate, must be split proportionally to the individual input gas flow rates. F is expressed in sccm, g the gap in cm and T the temperature in degrees Kelvin. The increase in the total concentration is now given by :

$$(d[M]/dt)_{in} = k_f \qquad (5.8)$$

which is expressed as a zero order reaction for every input species in "chemk". Since the plasma creates lots of new species X_j in a priori unknown concentrations $[X_j]$ (this is what we are looking for !), we do not know what should be their net escape rates. But we know that they should escape proportionally to their concentrations, as given by :

$$(d[X_j]/dt)_{esc} = -q[M][X_j] \qquad (5.9)$$

where q is the second order pumping rate. Since everything that gets in must get out, we can write :

$$\Sigma_j(d[X_j]/dt)_{esc} = (d[M]/dt)_{out} = (d[M]/dt)_{in} = k_f = -q[M]\,\Sigma_j[X_j] = -q[M]^2 \qquad (5.10)$$

where $\Sigma_j[X_j] = [M]$ was used. This gives $q = -k_f/[M]^2$. For a parallel plate reactor, the pumping rate of each species to be introduced in "chemk" is :

$$k_{out} = 4.04 \cdot 10^{-21}\, F \cdot T/(gp^2) \quad [cm^3 sec^{-1}] \qquad (5.11)$$

where p is the total pressure in Torr. There is no need for the minus sign since "chemk" understands that the pumping is a product-free reaction of the second order (see appendix D).

This expression for the pumping rate indicates how it should be adapted to different conditions of pressure, gap, total flow rate and temperature. Yet it does not account for the increase in total concentration due to the chemical reactions. In particular, the pumping must be adapted to changing percentages of O_2 in the feed. Figure 5.2.4 shows the adjusted pumping speed

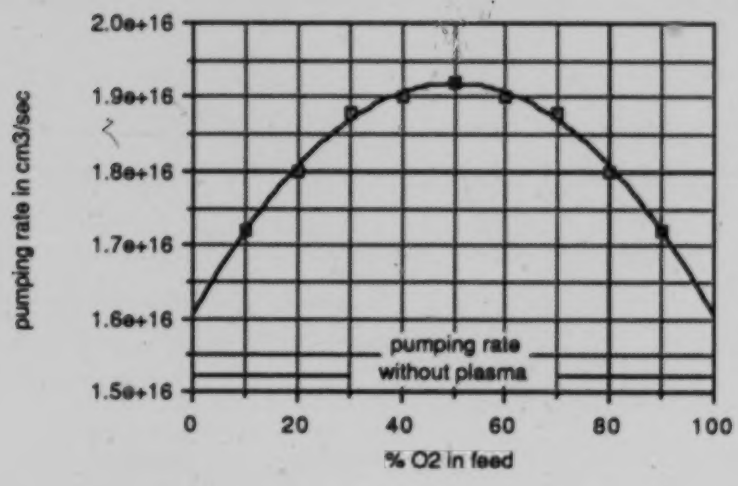

Fig. 5.2.4) Pumping rate required to maintain a constant total pressure of 1.0 Torr as a function of the percentage of O_2 in the CF_4/O_2 input mixture, with 100 sccm total feeding rate. The power is 900 Watts and the plasma volume 259 cm^3.

as a function of the O_2 content in the feed required to maintain a constant operating pressure.

Following the argument stating that, for a fixed input flow rate, increasing output flow rates lower the effective argon concentration in the discharge, one concludes that varying the O_2 content affects the calibration

of the emission intensities by actinometry. When the argon emission line intensity is corrected to a given concentration as it is done when the pressure is varied (remember that during the experiment the argon partial pressure follows the total pressure variations. The argon emission intensities are then normalized to a fixed absolute amount of argon), the argon concentration might not be exactly in the same percentage in the plasma as it is in the feed gas mixture. The computed fraction of argon, however, does not change with the pressure which means that, according to the simulation, the relative variations of the excitation efficiency shown previously still holds (Fig. 4.4.1). It is when both pressure and percentage of oxygen are changed simultaneously that the correction for the argon intensity might be somewhat inaccurate.

5.3 Computed and measured relative concentrations

All the upcoming calculated results are for steady state at 1.0 second after the plasma is "turned on". The measured intensities represent the peak value for as close as we could get to the true peak within the analyzer's resolution. It is assumed that the relative variations of the emission line area are correlated to the relative variations of the peak value (see appendix C).

Figure 5.3.1 shows computed concentrations of the most abundant species with a total flow of 100 sccm of CF_4 and O_2, at 900 Watts, 1.0 Torr and 259 cm^3 plasma volume. As discussed in [32], CF_2 is in this model the most abundant CF_n radical from CF_4 dissociation by electron impact. Free fluorine is the product with the highest concentration and it compares with that of CF_4 or O_2. The most abundant stable products are respectively COF_2, CO and CO_2.

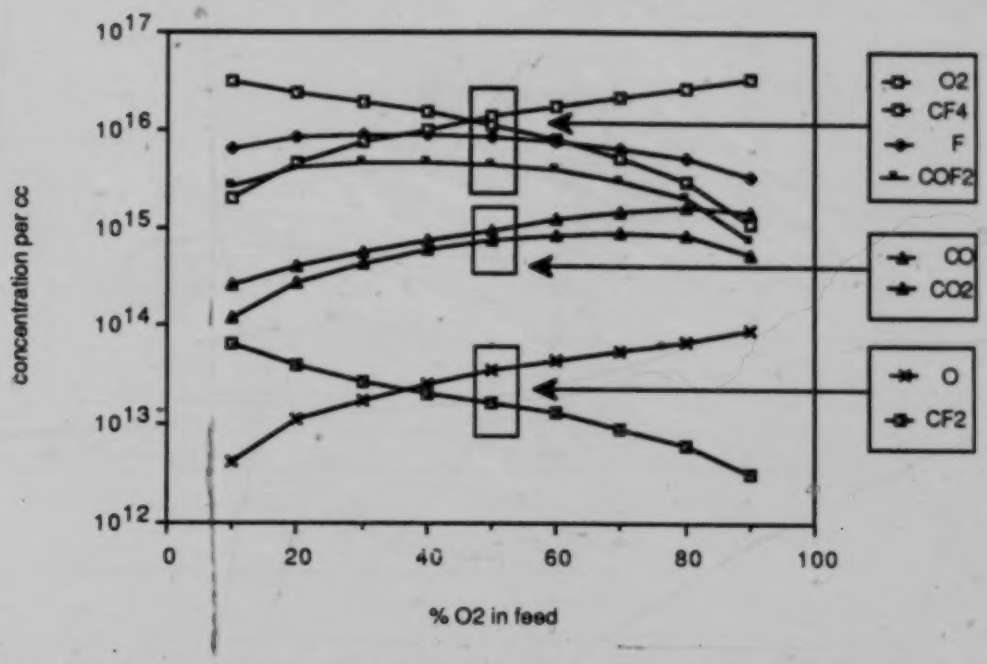

Fig. 5.3.1) Computed concentrations of some species as a function of the percentage of O_2 in the CF_4/O_2 input mixture, with 100 sccm total feeding rate. The pressure is 1.0 Torr, the power is 900 Watts and the plasma volume 259 cm^3.

In the following figures, the computed relative concentrations of fluorine and oxygen are compared to the spectroscopic measurements. Using the formula relating the spectrometer readings to the total concentration of an excited atom (section 4.3.2), the measured emission intensity ratio is related to the calculated concentration ratio as shown below for fluorine and argon :

$$(N_{703.7}/N_{750.4}) = (k_F/k_{Ar}) \cdot (C(750.4)/C(703.7)) [F]/[Ar] \qquad (5.12)$$

measured calculated

where $C(\mu)$ is the analyzer's sensitivity at frequency μ. Since the electron impact excitation rates k_F, k_O, k_{Ar}, are yet unknown, the curves can only be compared qualitatively. The conditions in Fig. 5.3.2 to 5.3.10 are : 50/50 sccm

CF_4/O_2 , 5 sccm Ar, 1.4 Torr, 900 Watts and 0.8 cm gap except for the parameter varied of course. The dotted squares represent the calculated concentration ratios corresponding to the left axis scale, while the black diamonds represent the measured emission intensity ratios corresponding to the right axis scale.

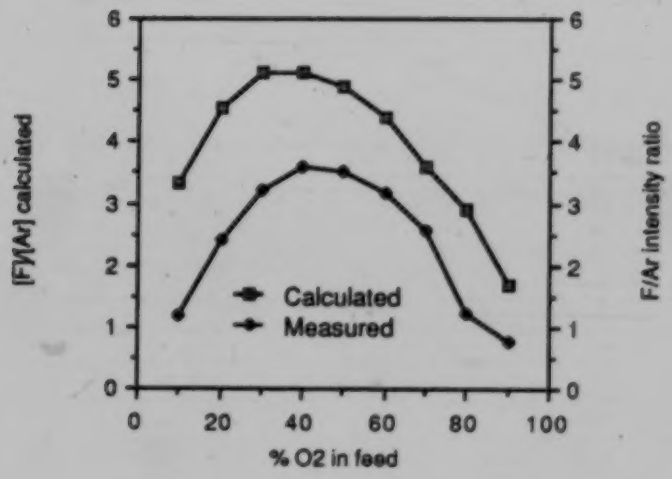

Fig. 5.3.2) Comparison of computed [F]/[Ar] concentration ratio with measured F(703.7nm)/Ar(750.4nm) emission intensities versus the O_2 content in the feed. The process parameters are : 100 sccm CF_4/O_2 input gas mixture with 5 sccm Ar, 1.4 Torr pressure, 900 Watts power, 259 cm^3 plasma volume corresponding to 0.8 cm electrode gap. The measurements are related to the calculation by the relationship : $F(703.7nm)/Ar(750.4nm) = (k_F/k_{Ar})[F]/[Ar]$ where k_F and k_{Ar} are respectively the F and Ar electron impact excitation rates.

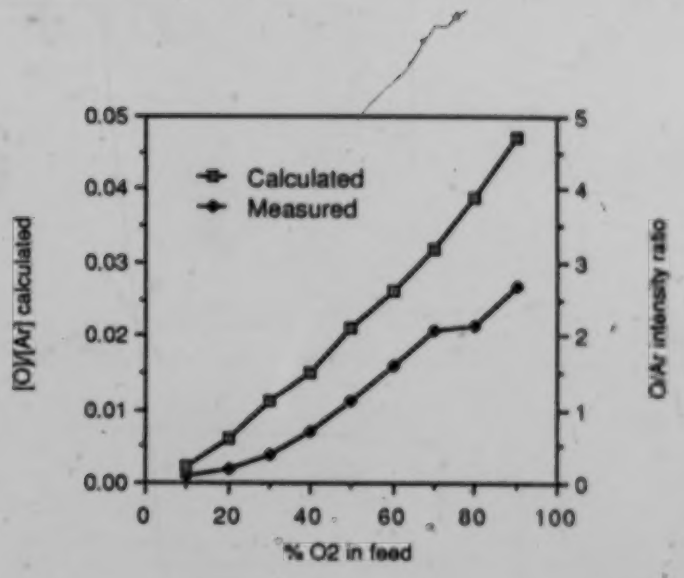

Fig. 5.3.3) Comparison of computed [O]/[Ar] concentration ratio with measured O(777.4nm)/Ar(750.4nm) emission intensities versus the O_2 content in the feed at 1.4 Torr, 900 Watts, 0.8 cm gap. The measurements are related to the calculation by the relationship: $O(777.4nm)/Ar(750.4nm) = (k_O/k_{Ar})[O]/[Ar]$, where k_O and k_{Ar} are respectively the O and Ar electron impact excitation rates.

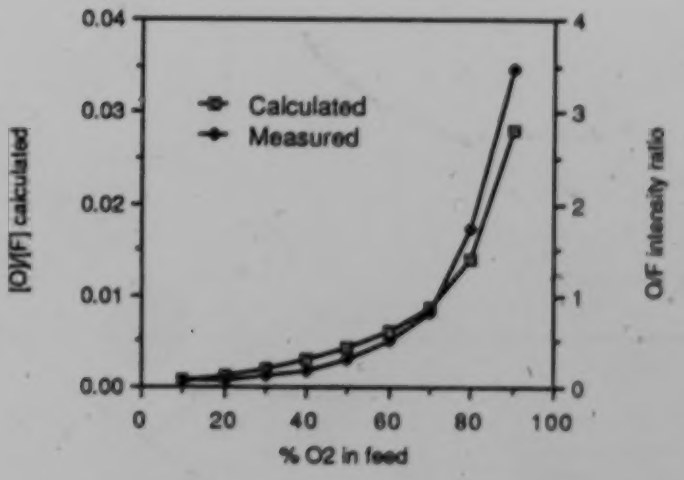

Fig. 5.3.4) Comparison of computed [O]/[F] concentration ratio with measured O(777.4nm)/F(703.7nm) emission intensities versus the O_2 content in the feed at 1.4 Torr, 900 Watts, 0.8 cm gap. The measurements are related to the calculation by the relationship : $O(777.4nm)/F(703.7nm) = (k_O/k_F)[O]/[F]$, where k_O and k_F are respectively the O and F electron impact excitation rates.

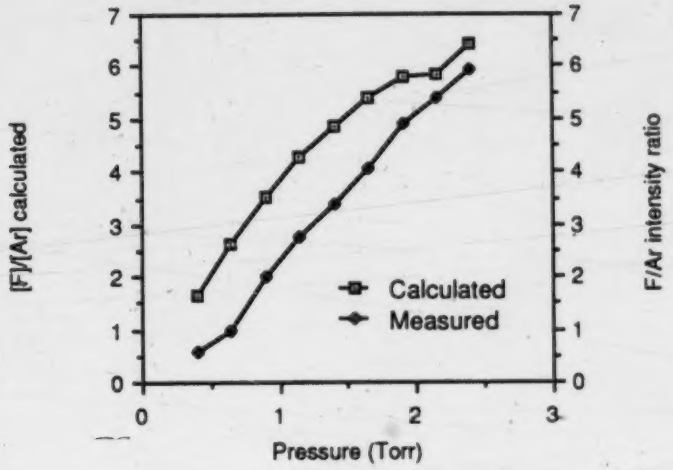

Fig. 5.3.5) Comparison of computed [F]/[Ar] concentration ratio with measured F(703.7nm)/Ar(750.4nm) emission intensities versus pressure in a 50/50 sccm CF_4/O_2 input gas mixture with 5 sccm Ar at 900 Watts,0.8 cm gap.

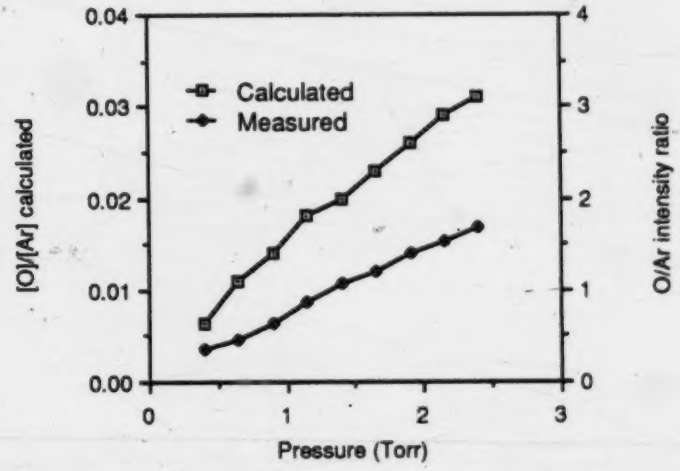

Fig. 5.3.6) Comparison of computed [O]/[Ar] concentration ratio with measured O(777.4nm)/Ar(750.4nm) emission intensities versus pressure in a 50/50 sccm CF_4/O_2 input gas mixture with 5 sccm Ar at 900 Watts,0.8 cm gap.

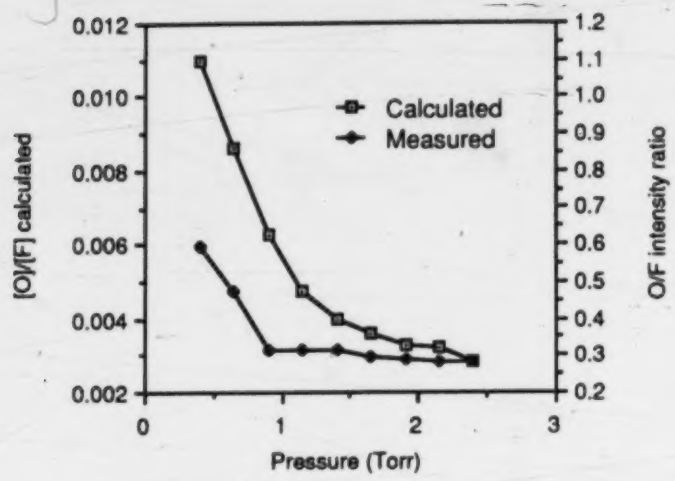

Fig. 5.3.7) Comparison of computed [O]/[F] concentration ratio with measured O(777.4nm)/F(703.7nm) emission intensities versus pressure in a 50/50 sccm CF_4/O_2 input gas mixture with 5 sccm Ar at 900 Watts,0.8 cm gap. The measurements are related to the calculation by the relationship : $O(777.4nm)/F(703.7nm) = (k_O/k_F)[O]/[F]$, where k_O and k_F are respectively the O and F electron impact excitation rates.

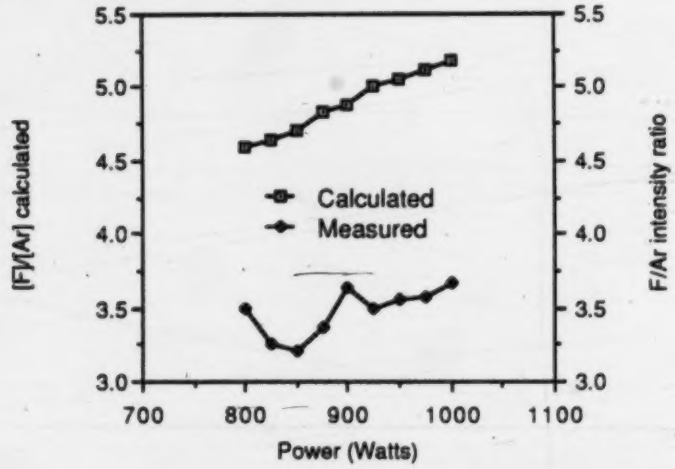

Fig. 5.3.8) Comparison of computed [F]/[Ar] concentration ratio with measured F(703.7nm)/Ar(750.4nm) emission intensities versus power in a 50/50 sccm CF_4/O_2 input gas mixture with 5 sccm Ar at 1.4 Torr,0.8 cm gap. The measurements are related to the calculation by the relationship : $F(703.7nm)/Ar(750.4nm) = (k_F/k_{Ar})[F]/[Ar]$ where k_F and k_{Ar} are respectively the F and Ar electron impact excitation rates.

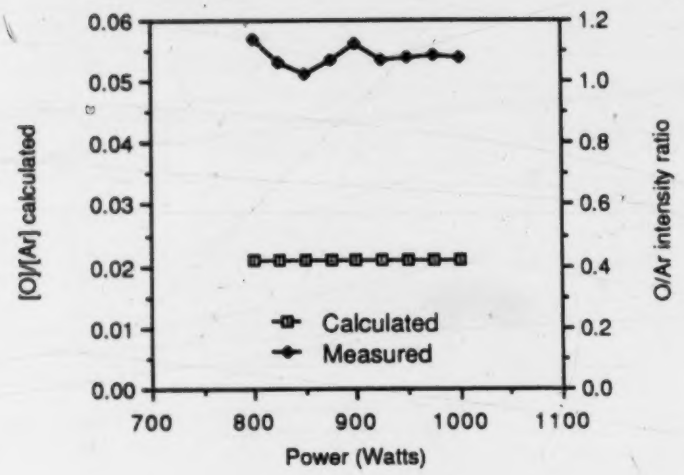

Fig. 5.3.9) Comparison of computed [O]/[Ar] concentration ratio with measured O(777.4nm)/Ar(750.4nm) emission intensities versus power in a 50/50 sccm CF_4/O_2 input gas mixture with 5 sccm Ar at 1.4 Torr,0.8 cm gap. The measurements are related to the calculation by the relationship: O(777.4nm)/Ar(750.4nm) = (k_O/k_{Ar})[O]/[Ar] where k_O and k_{Ar} are respectively the O and Ar electron impact excitation rates.

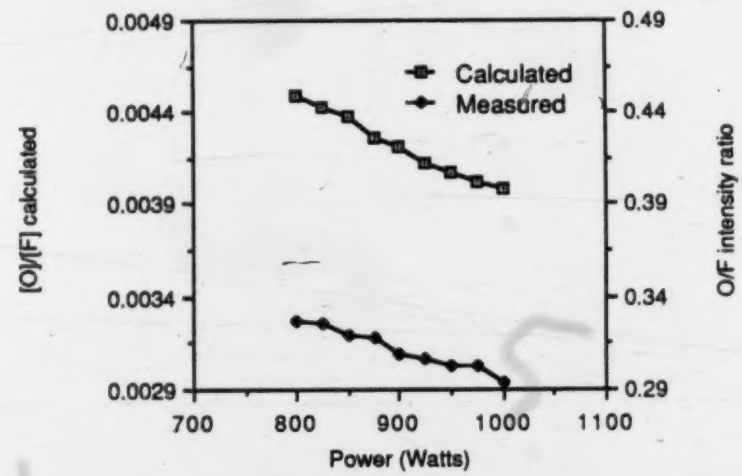

Fig. 5.3.10) Comparison of computed [O]/[F] concentration ratio with measured O(777.4nm)/F(703.7nm) emission intensities versus power in a 50/50 sccm CF_4/O_2 input gas mixture with 5 sccm Ar at 1.4 Torr,0.8 cm gap. The measurements are related to the calculation by the relationship : O(777.4nm)/F(703.7nm) = (k_O/k_F)[O]/[F] , where k_O and k_F are respectively the O and F electron impact excitation rates.

Since the largest concentration found in the plasma after that of CF_4 and O_2 is that of atomic fluorine, the pumping rate must be adapted accordingly to the fluorine concentration (Fig. 5.3.2) which explains the dependence of the pumping rate on the O_2 content in the feed shown in Fig. 5.2.4 .

The general trends of the dependence of free fluorine and oxygen concentrations on O_2 content in the feed, pressure and power are very well reproduced by the simulation over a wide range of the process parameter space.

At constant pressure and fraction of O_2 in the feed, the simulation yields the same results if the total flow to gap ratio F/g and the power density W/g are kept constant. F/g and W/g are the real model parameters for the total flow, the gap and the power. In this model, constant W/g and F/g values correspond respectively to fixed electrical (section 5.2.1) and flow (section 5.2.4) characteristics. Spectroscopic measurements were made keeping those ratios constant over a wide range of conditions. Figures 5.3.11 through 5.3.13 show the relative fluorine and oxygen concentrations with varying gaps. The corresponding total flow and power values are also indicated. The pressure was fixed at 1.4 Torr and CF_4, O_2 and Ar were mixed in the proportion 47.6/47.6/4.8%.

It can be seen that when the data are sorted in order of increasing gap, flow and power, the F/Ar and O/Ar intensity ratios increase while the O/F intensity ratio remain almost constant. Since the pressure is fixed, the supply of CF_4 and O_2 is constant. Figures 5.3.8 and 5.3.9, however, show that both [F] and [O] are pretty much independent of the power. Yet increasing power or flow rate make the dissociative reactions more predominant with respect to

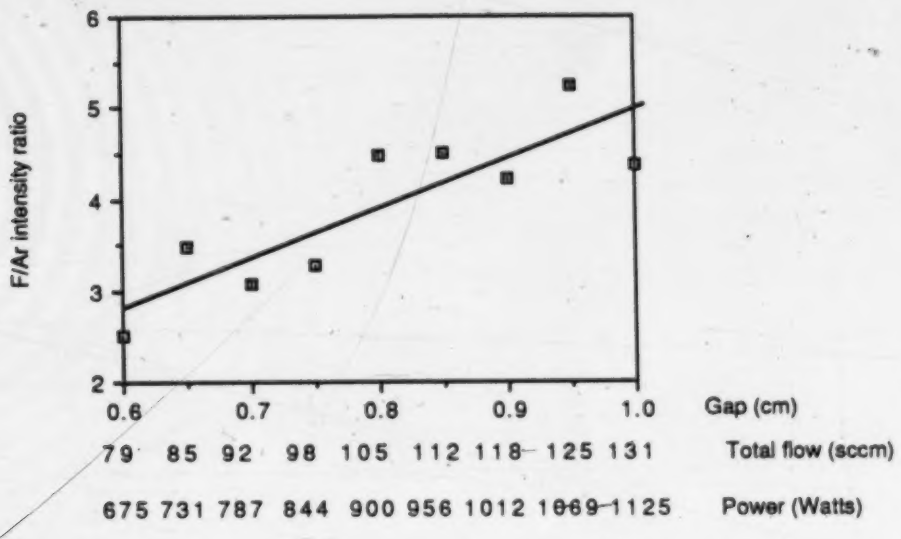

Fig. 5.3.11) Measured F/Ar intensity ratio keeping the total flow to gap ratio F/g and the power to gap ratio W/g constant. The pressure is 1.4 Torr, the proportion of $CF_4/O_2/Ar$ is 47.6/47.6/4.8 %. The solid line represents a least-squares fit to data. Under those conditions the calculated [F]/[Ar] concentration ratio would be constant.

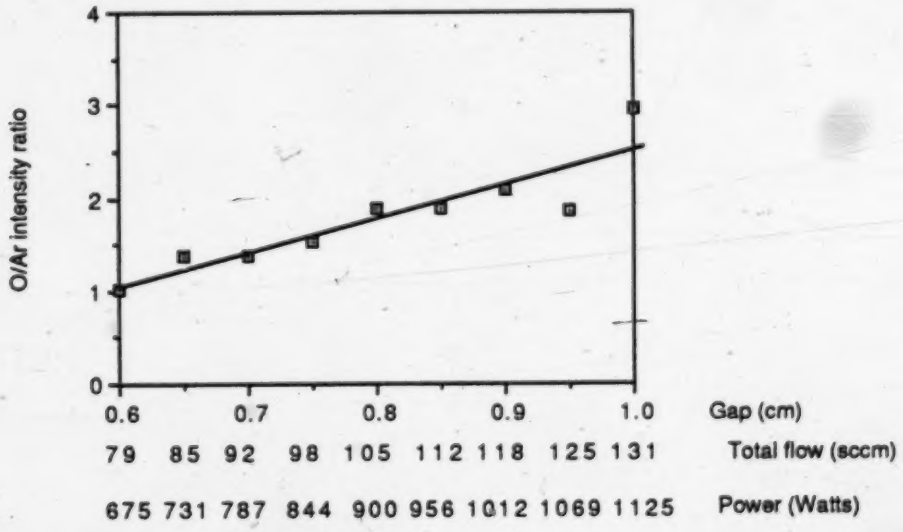

Fig. 5.3.12) Measured O/Ar intensity ratio keeping the total flow to gap ratio F/g and the power to gap ratio W/g constant. The pressure is 1.4 Torr, the proportion of $CF_4/O_2/Ar$ is 47.6/47.6/4.8 %. The solid line represents a least-squares fit to data. Under those conditions the calculated [O]/[Ar] concentration ratio would be constant.

the chemical reactions, therefore one expects the concentration of chemical-reactions-dependent products, such as F in O_2 containing CF_4 plasmas, to decrease. In a 50/50 % CF_4/O_2 plasma at 1.0 Torr, 900 Watts, 259 cm^3 plasma volume, the model indicates that the F concentration calculated for 50, 100 and 200 sccm total flow decreases with increasing flow rate ($8.207 \cdot 10^{15}$, $6.838 \cdot 10^{15}$, $5.625 \cdot 10^{15}$ cm^{-3} resp.), while the O concentration increases slightly ($2.547 \cdot 10^{13}$, $2.749 \cdot 10^{13}$, $2{,}935 \cdot 10^{13}$ cm^{-3} resp.). One concludes that the observed intensity increase in Fig. 5.3.11 and 5.3.12 is either due to unaccounted effects of varying gaps or due to an uncontrolled increase in Ar density.

Increasing power decreases the [O]/[F] concentration ratio (Fig. 5.3.10) while the simulation predicts an increase when the total flow alone increases. Both trends compensate each other (Fig. 5.3.13) and this ratio

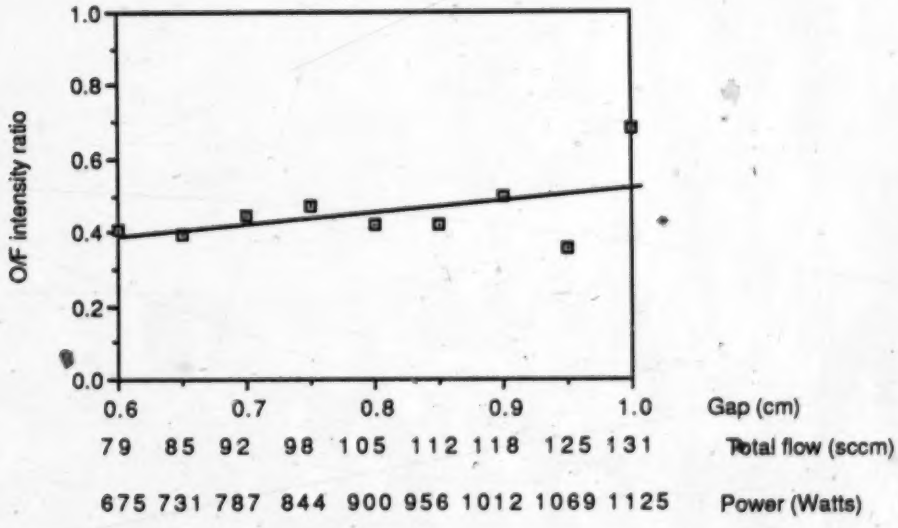

Fig. 5.3.13) Measured O/F intensity ratio keeping the total flow to gap ratio F/g and the power to gap ratio W/g constant. The pressure is 1.4 Torr, the proportion of $CF_4/O_2/Ar$ is 47.6/47.6/4.8 %. The solid line represents a least-squares fit to data. Under those conditions the calculated [O]/[F] concentration ratio would be constant.

remains pretty much constant in the "equiplasma".

The gas phase chemistry of the CF_4/O_2 plasma being well modeled by this simulation, we can now see how the etch rate of crystalline silicon correlates with the fluorine concentration when the O_2 content in the feed, the pressure and the power are varied.

5.4 Silicon etch rates

The volatile products of the reaction between F atoms and solid silicon have been identified as SiF_2 and SiF_4 [5,24]. SiF_n n>1 results from the adsorption of F or F_2 by SiF_{n-1}. SiF and SiF_3 are not believed to be gas phase products because they react very quickly with atomic fluorine. The overall stable product is SiF_4 which alone can be traced by the mass spectrometer. The reaction scheme introduced in the simulation for the removal of silicon is as described in [34], reactions with F_2 molecules according to [33] have been added too :

(Si) + F ---> SiF	limiting step		(5.13)
SiF + F ---> SiF_2	very fast	10^{-10} cm^3/sec	(5.14)
SiF_2 + F ---> SiF_3	very fast	"	(5.15)
SiF_3 + F ---> SiF_4	very fast	"	(5.16)
(Si) + F_2 ---> SiF + F	limiting step		(5.17)
SiF + F_2 ---> SiF_2 + F	very fast	10^{-10} cm^3/sec	(5.18)
SiF_2 + F_2 ---> SiF_3 + F	very fast	"	(5.19)
SiF_3 + F_2 ---> SiF_4 + F	very fast	"	(5.20)

The rates for reactions (5.18) to (5.20) are the same as those of reactions (5.14) to (5.16). Reactions (5.13) and (5.17) are the limiting steps in the production of SiF_4 so that their rates become the only etching parameter. The other reaction rates are made arbitrarily faster. Because of the nature of the simulation all the species are gas phase products. Reactions (5.13) and (5.17) express a net loss of fluorine and atomic silicon is not really included in the model. The etch rate E is simply related to the production of SiF_4 according to :

$$E = V/(A \cdot \rho) \cdot d[SiF_4]/dt \tag{5.21}$$

where V is the interelectrode volume, A the silicon exposed area and ρ the density of atoms in crystalline silicon ($5 \cdot 10^{22}$ cm^{-3}). According to reaction (5.13), the production of SiF_4 is related to the F concentration :

$$d[SiF_4]/dt = k_E[F] \tag{5.22}$$

where k_E is reaction (5.13) rate. k_E accounts for the supply of etchant to the surface, since diffusion processes are neglected, the flux of F atoms to the silicon surface is simply given by the impingement rate I_s.

$$I_s = p \cdot (2\pi m_F k_B T)^{-1/2} \tag{5.23}$$

where $p=[M] \cdot k_B T$ is the total pressure, [M] the total concentration, k_B the

Boltzmann constant, T the temperature (300 K) and m_F the fluorine atomic mass. It leads to :

$$k_E = I_s A \Theta / (4 \cdot [M] \cdot V) \qquad (5.24)$$

where Θ = 0.00168, is the probability for F to react on the silicon surface at room temperature (300 K) after Flamm *et al.* [41]. The impingement rate is divided by 4 because 4 fluorine atoms are needed to form SiF_4. Finally, we have :

$$k_E = (\Theta \cdot A/(4 \cdot V)) \cdot (k_B T/(2\pi m_F))^{1/2} \qquad (5.25)$$

At 300 K and with m_F = 19 atomic mass units, k_E = 3614 $\Theta \cdot A/V$ cm/sec, where A and V are expressed in cm. Reaction (5.17) rate $k_{E'}$ is given by $k_{E'} = k_E (2.0)^{-1/2}$ to account for the F_2 molecular mass.

In Fig. 5.4.1, computed etch rates are compared with silicon etch rates measured on 5 inch wafers corresponding to 126 cm^2 exposed area. Not only predicted etch rates are lower than actual etch rates for O_2 contents below 50% but also the peaks do not coincide. Equations (5.13) through (5.22) imply that the etch rate is roughly proportional to the F concentration because molecular fluorine, which in the model is found in lower concentrations than atomic fluorine, does not play a major role. It was found both experimentally and numerically that the maximum F concentration

corresponds to 40 to 50 % O_2 content (Fig. 5.3.2) while the maximum etch rate occurs at 20 to 30 % O_2 content. The same observation is made in [24] (and reference therein) and they concluded that a competition for active sites on the silicon surface between F and O atoms explains this discrepancy.

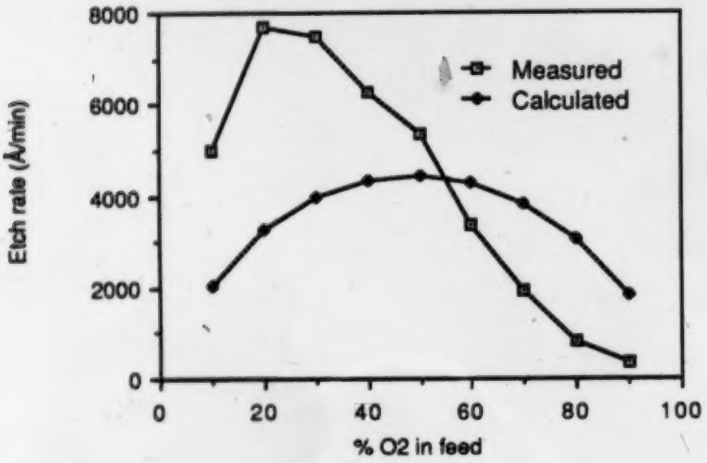

Fig. 5.4.1) Comparison of computed and measured silicon etch rates versus the O_2 content in a 100 sccm CF_4/O_2 input gas mixture with 5 sccm Ar at 900 Watts, 1.4 Torr, 0.8 cm gap. The silicon exposed area is 126 cm^2 (5 inch wafers).

Although the surface chemistry cannot be truly included in the model, a competitive process between F and O atoms can be simulated by slowing down the production of SiF_4 with increasing oxygen concentration. Since both reactions (5.13) and (5.14) are surface reactions [41], they will now compete for the production of SiF_2, which in the model quickly forms SiF_4, according to the following phenomenological reactions :

$$SiF + O \text{ -- } k_c \text{--> } F + O \qquad (5.26)$$

$$SiF_2 + O \text{ -- } k_c \text{--> } SiF + F + O \qquad (5.27)$$

Reactions (5.26) and (5.27) describe a competition between F and O atoms for the production of SiF_4 which is of the second order in the O concentration, therefore the competition is relatively more acute at high O concentrations than it is at low O concentrations.

A side effect of that competition is to lower the calculated etch rate which is already too slow. Reaction (5.13) rate has been adapted to account for the high observed etch rates by introducing an adjusting parameter ß in k_E :

$$k_E = I_s A \Theta \cdot ß/(4 \cdot [M] \cdot V) \qquad (5.28)$$

ß and reactions (5.26) and (5.27) rate k_c are now simulation parameters. ß controls the magnitude of the etch rate while k_c controls the position of the maximum etch rate. Figures 5.4.2 and 5.4.3 show comparisons between calculated etch rates with ß=8 and measured etch rates for 5 and 6 inch silicon wafers. $k_c = 3.0 \cdot 10^{-8}$ was used. Since reactions (5.14)-(5.16) are made arbitrarily faster than (5.13), the value of k_c itself does not bear any physical meaning. The etch rate dependence on the O_2 content in the feed is indeed well simulated when the competitive process for the production of SiF_4 is included in the model. It was assumed that the effective reaction rate k_E of F atoms with atomic silicon is 8 times larger than the one calculated in (5.24).

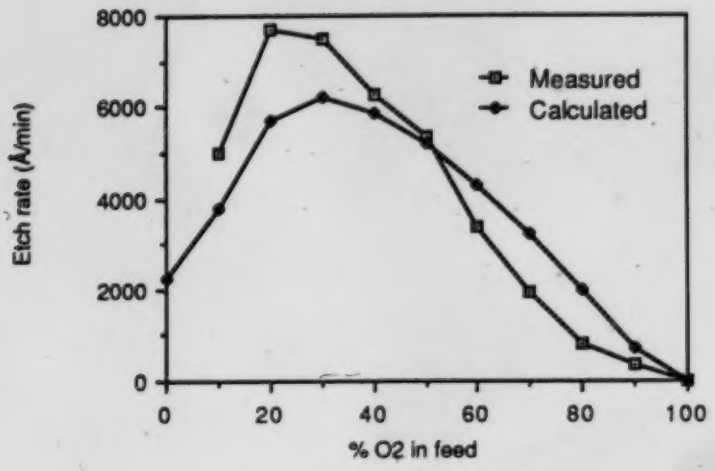

Fig. 5.4.2) Comparison of computed and measured silicon etch rates versus the O_2 content in a 100 sccm CF_4/O_2 input gas mixture with 5 sccm Ar at 900 Watts, 1.4 Torr, 0.8 cm gap. The silicon exposed area is 126 cm^2 (5 inch wafer). Competition between F and O atoms for the formation of SiF_4 is included and β=8.

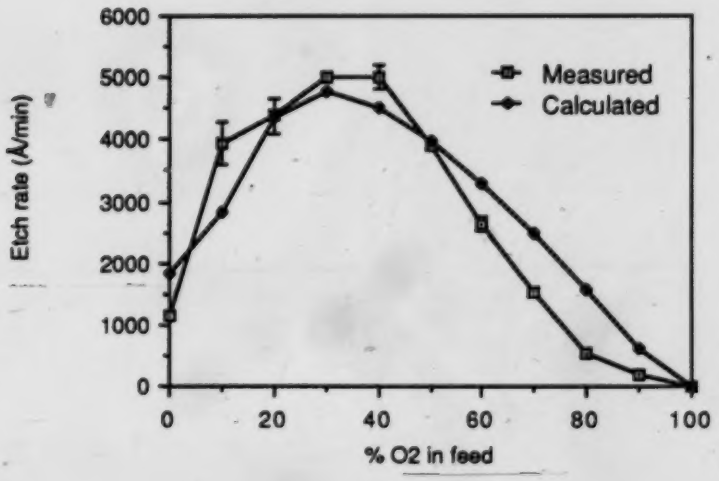

Fig. 5.4.3) Comparison of computed and measured silicon etch rates versus the O_2 content in a 100 sccm CF_4/O_2 input gas mixture with 5 sccm Ar at 900 Watts, 1.4 Torr, 0.8 cm gap. The silicon exposed area is 182 cm^2 (6 inch wafer). Competition between F and O atoms for the formation of SiF_4 is included and β=8.

Note that ß is not necessarily a correction factor for the fluorine reaction probabability with silicon alone (Θ = 0.00168). It may include other phenomena not, or only partially, accounted for in the model.

The purpose here is not to find what values of ß and k_c make the calculated etch rates fit at best the experimental values. Analyzing the impact of the competitive process for the production of SiF_4 on the gas phase chemistry is more interesting. In particular, under the conditions described in Fig. 5.4.2, the computed °F concentration appears as shown by the black diamonds in Fig. 5.4.4. It can be seen that, with silicon in the model, the

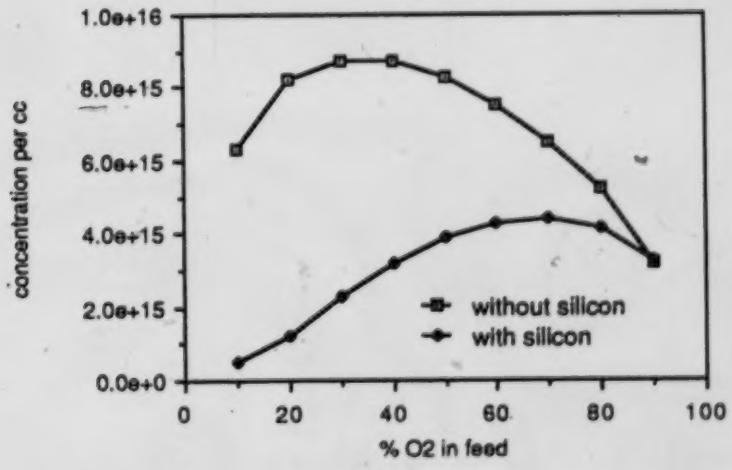

Fig. 5.4.4) Comparison of computed atomic fluorine concentrations with and without silicon in the system versus the O_2 content in a 100 sccm CF_4/O_2 input gas mixture with 5 sccm Ar at 900 Watts, 1.4 Torr, 259 cm^3 plasma volume. In the presence of silicon, the active exposed area is 126 cm^2 and competition between F and O atoms for the formation of SiF_4 is included along with ß=8.

consumption of F atoms lowers the fluorine concentration while the competitive process shifts the peak F concentration toward higher O_2

contents. This shift is in contradiction with experimental observations of the fluorine emission line intensity monitored with a wafer sitting in the reactor as illustrated in Fig. 5.4.5.

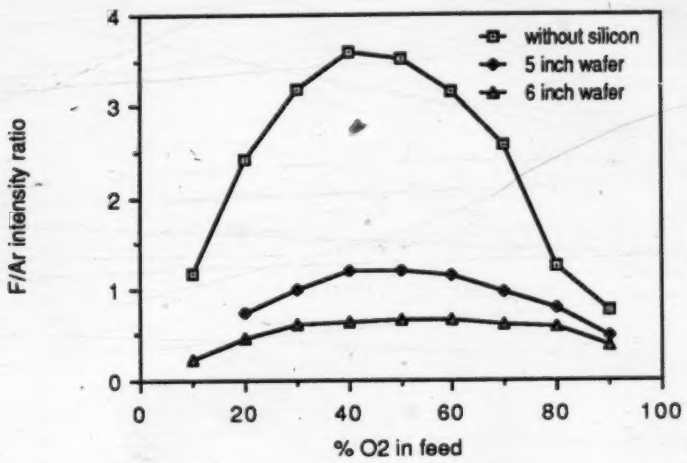

Fig. 5.4.5) Comparison of F(703.7nm)/Ar(750.4nm) emission intensities with and without silicon wafer in the system versus the O_2 content in a 100 sccm CF_4/O_2 input gas mixture with 5 sccm Ar at 900 Watts, 1.4 Torr, 0.8 cm gap. It can be seen that the relative concentration of fluorine with silicon present in the system does not correlate with that computed and shown in Fig. 5.4.4.

Although, as discussed in section 5.2.4, the spectroscopic diagnostic along with the actinometry provide only qualitative results, the position of the peak F/Ar intensity can be determined within ±10% of the O_2 percentage. The 30% O_2 content shift predicted by the simulation is therefore larger than the uncertainty.

With $\beta=8$ and the competition for production of SiF_2 as above, the computed etch rates are in excellent agreement with the measurements when the pressure is varied (Fig. 5.4.6). This result assesses the etch rate

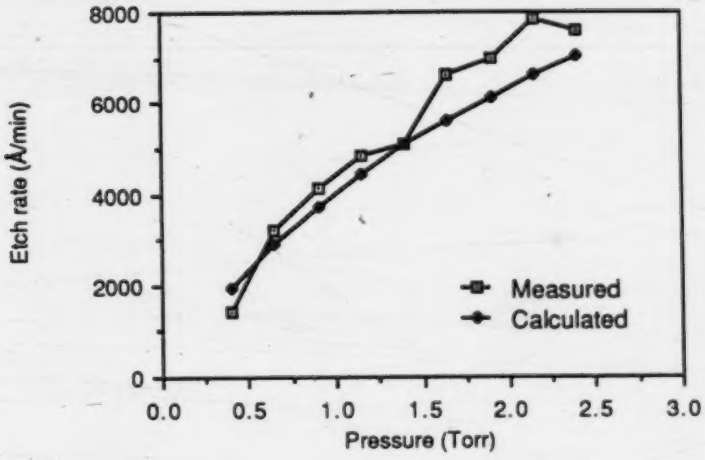

Fig. 5.4.6) Comparison of measured and calculated silicon etch rate versus pressure with 182 cm^2 load (6 inch wafer), in a 87.5/50/5 sccm $CF_4/O_2/Ar$ input gas mixture at 900 Watts, 0.8 cm gap. The simulation includes "competition for sites" between F and O atoms and ß=8.

proportionality to the fluorine concentration over a wide range of operating pressures. Since the fluorine concentration does not change much with the injected power (Fig. 5.3.8), one expects the etch rate to increase only a little with increasing power. This is confirmed in Fig. 5.4.7 which shows that, in spite of incidental plasma instabilities, the etch rate did not vary significantly over the range 800 to 975 Watts. The spread in etch rate between the lowest and the highest value is only 10% of their average value. Because of the narrow etch rate scale of Fig. 5.4.7 (3400 Å/min to only 4400 Å/min), model predictions appear worse than they actually are.

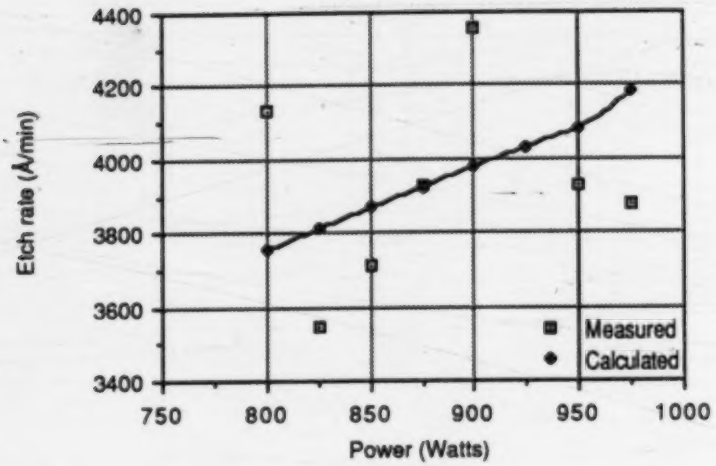

Fig. 5.4.7) Comparison of measured and calculated silicon etch rate versus power with 182 cm^2 load (6 inch wafer), in a 50/50/5 sccm $CF_4/O_2/Ar$ input gas mixture at 1.4 Torr, 0.8 cm gap. The simulation includes "competition for sites" between F and O atoms and δ=8.

The effect of the silicon exposed area on the etch rate is plotted in Fig. 5.4.8

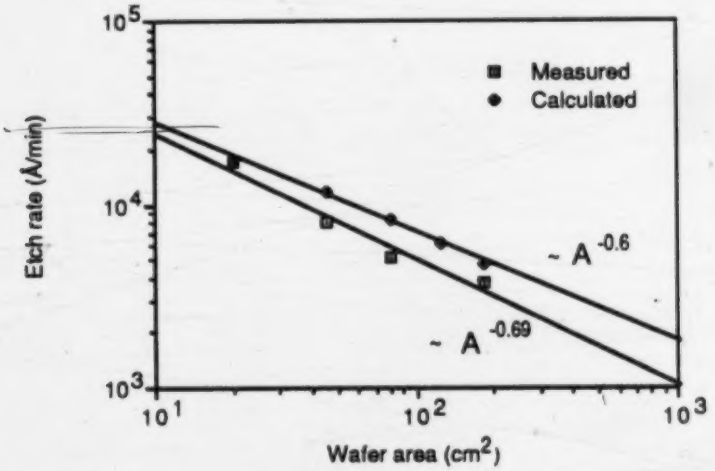

Fig. 5.4.8) Comparison of measured and calculated silicon etch rate versus silicon exposed area (load : 2,3,4,5,6 inch wafers), in a 70/30/5 sccm $CF_4/O_2/Ar$ input gas mixture at 900 Watts, 1.4 Torr, 0.8 cm gap. The simulation includes "competition for sites" between F and O atoms and δ=8. The solid lines represent logarithmic least-squares fits showing a $1/A^{0.69}$ dependence of the experimental etch rate on the silicon exposed area and a $1/A^{0.6}$ dependence for the computed etch rate.

for 2, 3, 4, 5 (not measured) and 6 inch wafers. One recognizes the loading effect described in [42] where the "pseudo-black-box" approach leads to an etch rate inversely proportional to the exposed area A. According to a least-squares fit to the experimental data of Fig. 5.4.8, the dependence is in $A^{-0.69}$ (statistical test $0 \leq R \leq 1$: R=0.98) and it agrees well with the simulation showing an $A^{-0.6}$ dependence (R=1.00).

5.5 Discussion

The radical gas phase chemistry of a CF_4/O_2 plasma etching silicon has been simulated. The model includes all of the etcher's process parameters which are in this case, the O_2 content in the feed gas, the pressure, the power and the gap (plasma volume). The reactions and their rates from [32] have not been changed except for the electron impact dissociation rates which have been made proportional to the power density. Those rates implicitly include the average electron density $\tilde{n}_e$.

The pressure dependence of the electron density is now discussed. If ΔE_j is the bond energy in the reaction : $X_j + e \xrightarrow{k_j} \text{products}$, by which X_j is dissociated, then the power W necessary for breaking the bonds should be at least :

$$W = V \cdot \sum_j \Delta E_j \cdot k_j \cdot \tilde{n}_e \cdot e^{-\Delta E_j / k_B T_e} \cdot [X_j] \qquad (5.29)$$

whereby $\tilde{n}_e$ has the same form as in [20] with $r_j = \Delta E_j \cdot k_j \cdot e^{-\Delta E_j / k_B T_e}$ the rate at which electrons loose energy to species X_j. The summation is taken on all the molecules undergoing electron impact dissociation. V is the plasma

volume, k_B the boltzmann constant and T_e the electron temperature. The electron density can be rewritten as follows :

$$\tilde{n}_e = (W/V)(\sum_j r_j[M]\cdot([X_j]/[M]))^{-1} \qquad (5.30)$$

where [M] is the total concentration related to the total pressure p by $p=k_B T\cdot[M]$. If the products of the r_j's by the fraction of species X_j that are not in the input gas mixture are much smaller than those for the species fed into the plasma, then, if X_j is in the feed gas, the ratio $[X_j]/[M]$ does not change as the total pressure alone changes. $\tilde{n}_e$ now writes :

$$\tilde{n}_e = (W/V)\,(\sum_j r_j f_j[M])^{-1} \qquad (5.31)$$

where the summation is restricted to those species fed into the plasma and undergoing direct electron impact dissociation. $f_j = [X_j]/[M]$ is therefore assumed pressure independent. One can also write :

$$\sum_j f_j \Delta E_j \cdot e^{-\Delta E_j/k_B T_e}\cdot k_j \tilde{n}_e = W/(V\cdot[M]) \qquad (5.32)$$

One remarks that the left hand side of that equation has a 1/p dependence similar to that of the argon discharge excitation efficiency $k_{Ar} n_e$ found experimentally (Fig. 4.4.1). It is expected that the average electron density increases with increasing pressure. Therefore the 1/p behavior observed in

Fig. 4.4.1 for the excitation efficiency and reported valid over an energy range of 8-20 ev [25], as well as the 1/p behavior assumed in equation (5.32) which involves energies from 2.2-6.1 ev (dissociation energies of CF_n n=1,4 [20]), is mainly the result of variations in the electron energy distribution. Since we do not know what is the electron density dependence on the pressure and since this dependence is clearly much weaker than the variations in the energy distribution, the electron density has been made pressure independent. This is to say that the rate r_j at which electrons loose energy by dissociative collisions is itself 1/p dependent which, considering equation (5.31), leaves a pressure independent electron density.

Regarding the electron impact dissociations present in the CF_4/O_2 reaction scheme (appendix D), the assumption stating that the products $r_j[X_j]/[M]$ can be neglected for those species not directly fed into the reactor can be discussed. According to the simulation, CF_n n=1,2,3, C_2F_4 and C_2F_6 radicals (reactions 1-4,10,11) are in much lower concentrations than CF_4. Atomic oxygen densities are also orders of magnitude lower than the O_2 concentration (reactions 17,18,19,26) as well as CF_3O_2 (reaction 34). The assumption seems therefore reasonable for those species and it might still hold for F_2 and CO_2 found in lower concentrations than the input gases too (reactions 35,37). COF_2 on the other hand is found in concentrations only slightly lower than those of CF_4 and O_2 (Fig. 5.3.1) and its fraction increases with increasing pressure. Hence, depending on the COF_2 dissociation rate value, the product $r_{COF2}[COF_2]/[M]$ might not be negligible with respect to

$r_{CF4}[CF_4]/[M]$ and $r_{O2}[O_2]/[M]$.

The feeding of CF_4, O_2 and Ar as well as the pumping of all the species present in the plasma have been included in the model. The dissociation of the input gas molecules results in the production of numerous species tending to increase the total pressure. This effect is balanced by increasing the pumping rate. Consequently, it lowers the argon concentration though it does not react in the plasma. This model indicates therefore that the argon concentration depends on the chemistry which might add some uncertainty to the calibration of the emission intensity of excited species by actinometry.

In the simulation, steady state concentrations are reached a short time after the plasma is "turned on" as opposed to mass spectrometric data indicating that steady state is not reached during the etching period. This might be due to wall effects and wafer surface chemistry not accounted for in the model. Changes in concentrations occurring over a time scale longer than the corresponding residence time of a packet of gas traveling in a tubular reactor, might also be due to flow vortices in the reactor chamber, acting as a reservoir.

Qualitatively speaking, the computed fluorine and oxygen concentrations values are in good agreement with the F/Ar, O/Ar, O/F emission intensity ratios when the O_2 content in the feed, the pressure and the power are varied.

A quantitative evaluation of the model can be made by comparing computed and measured crystalline silicon etch rates. The simplest theory of silicon etching, whereby the etch rate is proportional to the fluorine thermal impingement flux toward the wafer surface, fails to reproduce the measured etch rates, both quantitatively and qualitatively, as the O_2 content

in the feed is varied. The maximum experimental etch rate occurs at 20 to 30% of O_2 in the CF_4/O_2 gas mixture and the etching is about twice as fast as the maximum predicted etch rate occurring at 50% O_2. Etch rate data for 5 and 6 inch wafers can be reproduced by speeding the theoretical fluorine reaction rate on the surface by a factor $\beta=8$, and by introducing a competition between F and O atoms for the production of SiF and SiF_2 to simulate a competition for active sites on the surface as proposed in [24]. Yet, doing this, the resulting computed F concentration as a function of the $\%O_2$ contradicts the experimental F/Ar intensity ratio monitored with a wafer in the reactor. On the other hand, once the model has been adapted to a given gas composition, the computed etch rates, as pressure, power and wafer size are changed, agree very well with the experimental observations. Thus, once a suitable rate for the production of SiF_4, major silicon desorption product, with varying O_2 content has been found, the variations of the measured etch rate with changing pressure, power and load are found to be correlated to the variations of the fluorine concentration. This implies that, in this experiment, the process parameters affect independently the production of free fluorine which is confirmed by the statistical design of experiment presented in section 4.4.1 indicating that the F/Ar intensity ratio is insignificantly correlated to cross terms such as $(\%O_2)\cdot$(pressure), $(\%O_2)\cdot$(power), (pressure)·(power)...(Table II).

The disagreement between the observed etch rates and etch rates calculated when $\beta=1$ and without competition for sites, as the O_2 percentage is varied, may be due to changing electron energy distribution not accounted

for in the model [37]. The large ß value required to fit the experimental data would then account for enhanced diffusion of F atoms and ions [20]. It seems difficult to explain this discrepancy by a pure chemical argument alone. If indeed atomic silicon and SiF_n radicals (n=1,2,3) react solely with F atoms, then, since the overall stable silicon-containing product is SiF_4, the etch rate should be simply proportional to the fluorine consumption which is the difference in the fluorine concentration with and without wafer. The resulting fluorine concentration should then reach a maximum at high O_2 contents (Fig. 5.4.4). Fig. 5.4.5, however, indicates that the consumption of fluorine does not correlate with the etch rate (Fig. 5.4.2 & 5.4.3). Therefore, the only consistent "chemistry-only" explanation would be that SiF_n molecules (n=1,2,3) react with fluorine containing species to form SiF_{n+1}, of which there is no evidence.

Because COF_2, CO, CO_2 and SiF_4 are found in relatively large amounts in the simulation, the reactions involving those stable products are critical in determining the F concentration and experiments aiming to study their concentrations are still to be conducted. Such a study could be carried out using the reduced reaction scheme proposed in [32] and consisting of only 13 determining reactions. Simulated surface reactions with F_2 (5.17)-(5.20) could be dropped out because the reaction probability of molecular fluorine on silicon is much lower than that of atomic fluorine [43] and F_2 molecules are found in much lower concentrations than F atoms too.

6. CONCLUSIONS

Two different approaches to the modeling of plasma etching processes on a commercial plasma etcher have been investigated.

Since, at the present time, the physical and chemical modeling of glow discharges does not answer the questions raised by dry-etch process engineers, one has to rely on experiments to improve those processes.

For that purpose, a software package has been developed that provides the process engineer with a tool for computer-aided optimization and characterization of any process depending on several independent parameters. It is based on the empirical mathematical modeling method using the statistical design of experiments [4]. This method gives a maximum of information with a minimum of experiments which saves time when it is applied to production equipment. In this thesis, the usefulness of the statistical design of experiments using this software has been demonstrated for the optimization of contact etching in SiO_2. The software developed for this study is not restricted to plasma etching. It can be applied to the optimization of photolithography, thin film deposition and other microelectronic processing steps. The underlying method is increasingly used in the industry [11,14-19]. The software written in the course of this thesis is currently used at LSI Logic Corporation R&D department for plasma etching and resist process optimization. This package and its user-guide are available at the Alberta Microelectronic Centre (appendix A).

The statistical design of experiments is a black-box approach providing a direct link between the characteristics of a process and the process parameters of the equipment, but it does not give any insight about what happens during the etching and why it happens. In this respect, physical and/or chemical simulations are complementary to the empirical modeling.

The latter can serve as a data base to compare numerical simulation results with experimental data.

In [32], a reaction scheme for the CF_4/O_2 plasma has been developed that includes first order electron impact dissociations and gas phase radical chemistry. The authors conclude that the agreement of computed CO_2, CO, and COF_2 concentrations with experimental data from [33] is generally better than a factor of 2 under various plasma conditions. They also find that the F concentration is very well predicted. In [26], it is explained how to relate the emission line intensity of an excited species with its concentration in the ground state, allowing thus to measure the relative variations of F and O atoms with changing plasma conditions.

In this thesis, the reaction scheme of [32] has been completed with feeding and pumping parameters and the first order electron impact dissociation rates have been made proportional to the power density. This chemical kinetics, tubular reactor model reproduces very well the variations in atomic F and O concentrations measured in a commercial parallel plate single wafer etcher using the method described in [26], with changing O_2 content in the feed, pressure and power.

Silicon etch rates measured with changing pressure, power and load are well predicted by the model once it has been adapted to a given O_2 percentage. On the other hand, making the etch rate proportional to the fluorine impingement rate fails to explain the etch rate dependency on the O_2 percentage in the feed gas mixture. Adjusting the computed etch rates with experimental data by speeding up the production of SiF and by introducing a simulated competition between F and O atoms for active sites on

the surface as proposed in the literature [24], results in a fluorine concentration which contradicts the experimental observation. Measurements of the DC plate to plate self-bias indicate that it depends on the percentage of O_2 in the CF_4/O_2 mixture which suggests that the etch rate dependency on the chemistry might be due to changing plasma electrical properties.

The model can be developed further by modifying the chemical kinetics simulation program [40] in order to solve self-consistently the interaction of the plasma with the surface or/and the RF discharge. The ion chemistry and the ion enhanced diffusion toward the surface may also play an important role and should be treated as well.

Further experiments include probe measurements in the plasma which would be useful in determining the dependence of the electron density on the process parameters. Cross comparisons between spectroscopic analyses of excited species and a more detailed mass spectrometric study could also be carried out.

7. REFERENCES

[1] K. E. Peterson, 'Silicon as a Mechanical Material', *Proceedings of the IEEE*, **70**, pp. 420-457, May 1982.

[2] S. M. Sze, *VLSI Technology*, McGraw-Hill, New Jersey, 1983.

[3] T. Sugano, *Applications of Plasma Processes to VLSI Technology*, Wiley, New York, 1985.

[4] G. E. P. Box, W. G. Hunter, J. S. Hunter, *Statistics for Experimenters*, Wiley, New York, 1978.

[5] M. J. Vasile, F. A. Stevie, 'Reaction of atomic fluorine with silicon : The gas phase products', *J. Appl. Phys.*, **53**, pp. 3799-3805, May 1982.

[6] D. C. Hinson, 'Plasmas for Semiconductor Fabrication', *Microelectronic Manufacturing and Testing*, 'Part I: DC Discharges' : September 1986, 'Part II : RF & Magnetron Discharges' : October 1986.

[7] B. Chapman, *Glow Discharge Processes*, Wiley, New York, 1980.

[8] M. J. Kushner, 'A kinetic study of the plasma-etching process. II. Probe measurements of electron properties in an rf plasma-etching reactor', *J. Appl. Phys.*, **53**, pp. 2939-2946, April 1982.

[9] C. J. Mullins, 'Plasma Etchers: Design and Performance', *Microelectronic Manufacturing and Testing*, June 1986.

[10] P. R. Bevington, *Data Reduction and Error Analysis for the Physical Sciences*, McGraw-Hill, 1969.

[11] M. W. Jenkins, M. T. Mocella, K. D. Allen, H. H. Sawin, 'The Modeling of Plasma Etching Processes Using Response Surface Methodology', *Solid State Technology*, pp. 175-182, April 1986.

[12] A. L. Edwards, *Multiple Regression and the Analysis of Variance and Covariance*, Second Edition, Freeman, 1979.

[13] N. Draper, H. Smith, *Applied Regression Analysis, Second Edition*, Wiley, 1981.

[14] C. S. Roades, M. R. Chin, 'Characterization of an Al Plasma Etching System Using Factorial Experimental Designs', *Proceedings 3rd Int. IEEE VLSI Multilevel Interconnection Conf.*, pp. 219-224, June 9-10, 1986.

[15] M. J. walker, S. C. Quinlan, 'Analysis of a Metal Etch Plasma Process', *Proceedings 3rd Int. IEEE VLSI Multilevel Interconnection Conf.*, pp. 225-231, June 9-10, 1986.

[16] J. Poisson *et al.*, ' Via Contact Dry Etching Using a Plasma Low Resistance Photoresist', *Proceedings 3rd Int. IEEE VLSI Multilevel Interconnection Conf.*, pp. 308-316, June 9-10, 1986.

[17] P. E. Riley, 'Development of a Highly uniform Silicon Dioxide Etching Process Using The Response-Surface Methodology', *J. Electrochemical Soc. : Solid-State Science and Technology*, pp. 1971-1972, September 1986.

[18] M. Johnson, K. Lee, 'Optimization of a Photoresist Process Using Statistical Design of Experiments', *Solid State Technology*, pp. 281-284, September 1984.

[19] A. R. Alvarez, D. L. Young, B. L. Abdi, H. D. Weed, 'Application of Response Surface Designs to Coupled Process and Device Simulation', Stanford University Computer-Aided Design of IC Fabrication Processes, Conference hand-outs, August 28, 1986.

[20] M. J. Kushner, 'A kinetic study of the plasma-etching process. I. A model for the etching of Si and SiO_2 in C_nF_m/H_2 and C_nF_m/O_2 plasmas', *J. Appl. Phys.*, 53, April 1982.

[21] D. Manning, Alberta Microelectronic Centre, private communication on contact etching in SiO_2 films on the Lam AutoEtch 590.

[22] B. E. Cherrington, 'The Use of Electrostatic Probes for Plasma Diagnostics', *Plasma Chem. Plasma Process.*, **2**, pp. 113-140, 1982.

[23] P. Bletzinger, C. A. DeJoseph, 'Structure of RF Parallel-Plate Discharges', *IEEE Trans. on Plasma Science*, **PS-14**, pp. 124-131, April 1986.

[24] C. J. Mogab, A. C. Adams, D. L. Flamm, 'Plasma etching of Si and SiO_2-The effect of oxygen additions to CF_4 plasma', *J. Appl. Phys.*, **49**, pp. 3796-3803, July 1978.

[25] R. d'Agostino, F. Cramarossa, S. De Benedictis, G. Ferraro, 'Spectroscopic diagnostic of CF_4-O_2 plasmas during Si and SiO_2 etching processes', *J. Appl. Phys.*, **52**, pp. 1259-1265, March1981.

[26] J. W. Coburn, M. Chen, 'Optical emission spectroscopy of reactive plasmas: A method for correlating emission intensities to reactive particle density', *J. Appl. Phys.*, **51**, pp. 3134-3136, June 1980.

[27] J. W. Coburn, M. Chen, 'Dependence of F Atom density on Pressure and Flow Rate in CF_4 Glow Discharges as Determined by Emission Spectroscopy', *J. Vac. Sci. Technol.*, **18**,p. 353, 1981.

[28] M. J. Kushner, 'Monte-Carlo simulation of electron properties in rf parallel plate capacitively coupled discharges', *J. Appl. Phys.*, **54**, pp. 4958-4965, September 1983.

[29] D. B. Graves, K. F. Jensen, 'A Continuum Model of DC and RF Discharges', *IEEE Trans. on Plasma Science*, **PS-14**, pp. 78-91, April 1986.

[30] G. L. Rogoff, J. M. Kramer, R. B. Piejak, 'A Model for the Bulk Plasma in a RF Chlorine Discharge', *IEEE Trans. on Plasma Science*, **PS-14**, pp. 103-111, April 1986.

[31] D. Edelson, D. L. Flamm, 'Computer simulation of a CF_4 plasma etching silicon', *J. Appl. Phys.*, **56**, pp. 1522-1531, September 1984.

[32] I. C. Plumb, K. R. Ryan, 'A Model of the Chemical Processes Occuring in CF_4/O_2 Discharges Used in Plasma Etching', *Plasma Chem. Plasma Process.*, **6**, pp. 205-230, 1986.

[33] G. Smolinsky, D. L. Flamm, 'The plasma oxidation of CF_4 in a tubular-alumina fast-flow reactor', *J. Appl. Phys.*, **50**, pp. 4982-4987, July 1979.

[34] K. R. Ryan, I. C. Plumb, 'A Model for the Etching of Si in CF_4 Plasmas: Comparison with Experimental Measurements', *Plasma Chem. Plasma Process.*, **6**, pp. 231-246, 1986.

[35] M. Dalvie, K. F. Jensen, D. B. Graves, 'Modelling of Reactors For Plasma Processing. I. Silicon Etching by CF_4 in a Radial Flow Reactor', *Chem. Eng. Science*, **41**, pp. 653-660, 1986.

[36] K. S. Uhm, M. R. Kump, J. P. McVittie, R. W. Dutton, 'Kinetic Modeling of the Active Species in Dry Etching', Conf. hand-outs : Stanford University IC Lab., *Process Simulators for Silicon VLSI and High Speed GaAs Devices*, pp. 253-262, July 1986.

[37] H. M. Anderson, J. A. Merson, R. W. Light, 'A Kinetic Model for Plasma Etching Silicon in a SF_6/O_2 RF Discharge', *IEEE Trans. on Plasma Science*, **PS-14**, pp. 156-164, April 1986.

[38] L. E. Kline, 'Electron and Chemical Kinetics in the low-Pressure RF Discharge Etching of Silicon in SF_6', *IEEE Trans. on Plasma Science*, **PS-14**, pp. 145-155, April 1986.

[39] D. C. Schram, 'Physics of Plasmachemistry', *Europhysics News*, **18**, pp. 28-31, 1987.

[40] G. Z. Whitten, J. P. Meyer, *A Computer Modeling Scheme for Chemical Kinetics*, FORTRAN program "Chemk", Systems Applications Inc., San Raphael CA.

[41] D.L. Flamm, V. M. Donnelly, J. A. Mucha, 'The reaction of fluorine atoms with silicon', *J. Appl. Phys.*, **52**, pp. 3633-3639, May 1981.

[42] H. F. Winters, J. W. Coburn, E. Kay,'Plasma etching-A "pseudo-black-box" approach', *J. Appl. Phys.*, **48**, pp. 4973-4983, December 1977.

[43] M. Chen, V. J. Minkiewicz, K. Lee, 'Etching Silicon with Fluorine Gas', *J. Electrochemical Soc.*, **126**, pp. 1946-1948, 1979.

APPENDIX A, LSIFIT & MAPPING LISTINGS AND USER-GUIDE

```
      PROGRAM LSIFIT
C
C     V1.1 MACINTOSH
C
C           FROM : PHILIPPE SCHOENBORN
C           DATE : JAN. 25, 1987
C
C           ALGORITHM FROM "DATA REDUCTION AND ERROR ANALYSIS
C           FOR THE PHYSICAL SCIENCES", PH.R. BEVINGTON., FREEMAN 1979.
C
C     PERFORMS WEIGHTED NON-LINEAR LEAST SQUARES FIT ON DATA INPUT
C     FROM THE "ANAME" FILE USING THE FUNCTION FUNCTN.
C
C !!  INPUT DATA ARE NORMALIZED TO [-1,+1] RANGE AND THEN STANDARDIZED.
C
C     DATA FILE (ANAME) MUST APPEAR AS FOLLOWS :
C     NPAR
C     NDEP
C     NPTS
C     PARA(1)(*20 CHARACTERS)
C      :
C     PARA(NPAR)
C     RESP(1)(*20CHARACTERS)
C      :
C     RESP(NDEP)
C     X(1,1).....X(NPAR,1)   Y1(1,1)...Y(NDEP,1)                SIGMAY(1)
C      .          .           .          .                        .
C      .          .           .          .                        .
C     X(1,NPTS).....X(NPAR,NPTS) Y1(NPTS)..Y(NDEP,NPTS)      SIGMAY(NPTS)
C
C     PARAMETERS :
C     RP          :  RELATIVE PRECISION REQUIRED ON STD DEVIATION
C     NPAR        :  NUMBER OF INDEPENDENT PARAMETERS
C     NDEP        :  NUMBER OF DEPENDENT PARAMETERS
C     NPTS        :  NUMBER OF DATA POINTS
C     NOD         :  ORDER OF POLYNOMIAL
C     X           :  ARRAY OF DATA POINTS (INDEPENDENT VARIABLES)
C     Y           :  ARRAY OF DATA POINTS (DEPENDENT VARIABLES)
C     W           :  DATA POINT WEIGHT
C     MODE        :  SPECIFIES METHOD OF WEIGHTING :
C                    +1 (INSTRUMENTAL) W(I)=1/SIGMAY(I)**2
C                    0 (NO WEIGHTING) W(I)=1.0
C                    -1 (STATISTICAL)  W(I)=1/Y(I)
C
C     ********** NOTE
C     SUBROUTINE CURFIT IS ALLOWED TO PROCEED WITH NFREE=0 !!
C           SEE LINE 11 IN CURFIT
C
      DOUBLE PRECISION TEST,CHISQR,RP,CHISQRD
      DIMENSION X(28,100),Y(10,100),SIGMAY(100),ERROR(28,28),
     1  DELTAA(28),A(28),YFIT(100),SIGMAA(28),XMIN(28),XMAX(28),
```

```
      1  AVERAGE(38),EXPERROR(10),SIGMAX(28),AVEX(28),VARY(100)
         CHARACTER*16 ANAME
         CHARACTER*20 PARA(28),RESP(10)
         INTEGER DD,MM,YY
         ANAME=' '
         OPEN(UNIT=4,STATUS='UNKNOWN')
         OPEN(UNIT=2,STATUS='UNKNOWN',FILE='MAP.IN')
         WRITE(9,60)
         WRITE(4,60)
   60    FORMAT('- LSIFIT.FOR BEGIN')
         TYPE 65,ANAME
   65    FORMAT('- EXPERIMENT : ',A16)
         ACCEPT ANAME
         WRITE(4,65) ANAME
         CALL DATE(MM,DD,YY)
         WRITE(9,70) DD,MM,YY
         WRITE(4,70) DD,MM,YY
   70    FORMAT('- DATE 'I2.2,2('/',I2.2))
  100    TYPE 600
         WRITE(4,600)
  600    FORMAT('- INPUT FILENAME : ')
         ACCEPT ANAME
C
C        READING THE INPUT FILE
C
         OPEN(UNIT=3,STATUS='OLD',FILE=ANAME)
         READ(3,*)NPAR
         READ(3,*)NDEP
         READ(3,*)NPTS
C
C        WRITING IN MAP.IN
C
         WRITE(2,*) NPAR
         WRITE(2,*) ' '
         DO 605 J=1,NPAR
          READ(3,613) PARA(J)
          WRITE(9,609) J,PARA(J)
          WRITE(4,609) J,PARA(J)
  605     WRITE(2,613) PARA(J)
         DO 607 J=1,NDEP
          READ(3,613) RESP(J)
          WRITE(9,612) J,RESP(J)
  607     WRITE(4,612) J,RESP(J)
  609    FORMAT(' X(',I2,') <= ',A20)
  612    FORMAT(' Y(',I2,') <= ',A20)
  613    FORMAT(A20)
         TYPE *,(' X(',J,') ',J=1,NPAR)
         WRITE(9,*) (' Y(',I,') ',I=1,NDEP)
         TYPE (4,*) (' X(',J,') ',J=1,NPAR)
         WRITE(4,*) (' Y(',I,') ',I=1,NDEP)
C
         DO 110 I=1,NPTS
         READ(3,*)(X(J,I),J=1,NPAR),(Y(J,I),J=1,NDEP),SIGMAY(I)
```

```
      IF (SIGMAY(I).LE.0.0) SIGMAY(I)=1.0
      WRITE(9,*)(X(J,I),J=1,NPAR),(Y(J,I),J=1,NDEP),SIGMAY(I)
      WRITE(4,*)(X(J,I),J=1,NPAR),(Y(J,I),J=1,NDEP),SIGMAY(I)
110   CONTINUE
C             NORMALIZATION
      DO 105 J=1,NPAR
      XMIN(J)=1.E37
105   XMAX(J)=-1.E36
      DO 120 J=1,NPAR
      DO 120 I=1,NPTS
      XMIN(J)=MIN(X(J,I),XMIN(J))
120   XMAX(J)=MAX(X(J,I),XMAX(J))
      DO 130 J=1,NPAR
      DO 130 I=1,NPTS
130   X(J,I)=2.*(X(J,I)-XMIN(J))/(XMAX(J)-XMIN(J))-1.
      CLOSE(UNIT=3)
C       STANDARDIZATION
      PTS=NPTS
      DO 131 I=1,NPAR
       SIGMAX(I)=0.
131    AVEX(I)=0.
      DO 132 I=1,NPTS
       DO 132 J=1,NPAR
        AVEX(J)=AVEX(J)+X(J,I)/PTS
132     SIGMAX(J)=SIGMAX(J)+X(J,I)**2/PTS
      DO 133 J=1,NPAR
       SIGMAX(J)=(SIGMAX(J)-AVEX(J)**2)*PTS/(PTS-1.)
       DO 133 I=1,NPTS
        X(J,I)=(X(J,I)-AVEX(J))/SQRT(SIGMAX(J))
133     IF (ABS(X(J,I)).LT.1E-6) X(J,I)=0.
C     STATEMENT 133 PREVENTS OVERFLOW DUE TO (1E-6)**6=1E-36
      WRITE(4,137)
137   FORMAT(/'-  MINIMUM    MAXIMUM',5X,
     1  'VARIANCE   AVERAGE PARAMETER')
      DO 134 J=1,NPAR
      WRITE(4,136) XMIN(J),XMAX(J),SQRT(SIGMAX(J)),AVEX(J),J
134   WRITE(2,136) XMIN(J),XMAX(J),SQRT(SIGMAX(J)),AVEX(J),J
136   FORMAT(4(X,E10.3),X,I2)
      WRITE(2,*) ' '
C
C     DISPLAY CORRELATION MATRIX FROM DATA POINTS
C
      TYPE '- SUBROUTINE CORR IN PROGRESS...'
      CALL CORR(X,Y,NPTS,NT,NPAR,
     1  NDEP,AVERAGE,EXPERROR,NDF,NREPLICATE)
      WRITE(9,135)
135   FORMAT('TERMINATED.')
C
C     CHOOSE DEPENDENT PARAMETER
C
140   IF (NDEP.EQ.1) THEN
      ND=1
      GOTO 73
```

```
      END IF
      TYPE 9300
      WRITE(4,9300)
9300  FORMAT(/'- ENTER NUMBER OF DEPENDENT PARAMETER : ')
      ACCEPT ND
      WRITE(4,9310) ND
9310  FORMAT(I3)
      IF (ND.GT.NDEP) GOTO 140
73    TYPE 75
      WRITE(4,75)
75    FORMAT('- ENTER ORDER OF POLYNOMIAL : ')
      ACCEPT NOD
      WRITE(4,80) NOD
80    FORMAT(I3)
      IF (NOD.EQ.2) THEN
       NTERMS=1+2*NPAR+(NPAR-1)*NPAR/2
      ELSE
      IF (NOD.EQ.3) THEN
       IF (NPAR.GT.3) THEN
        WRITE(9,87)
87      FORMAT('- !! TOO MANY PARAMETERS FOR 3-RD ORDER FIT')
        GOTO 73
       ELSE
        NTERMS=1+3*(NPAR+(NPAR-1)*NPAR/2)
        IF (NPAR.EQ.3) NTERMS=NTERMS+1
       END IF
      ELSE
       IF (NOD.EQ.1) THEN
        NTERMS=1+NPAR
       ELSE
        IF (NOD.EQ.0) THEN
         TYPE '- ENTER NUMBER OF MODEL TERMS : '
         ACCEPT NTERMS
        ELSE
         WRITE(9,89)
89       FORMAT('- !! FIRST SECOND OR THIRD ORDER FIT ONLY')
         GOTO 73
        END IF
       END IF
      END IF
      END IF
      WRITE(9,72)
72    FORMAT('- ENTER WEIGHTING MODE :')
      TYPE '  (+1=INSTRUMENTAL,0=NO WEIGHTING,-1=STATISTICAL) '
      ACCEPT MODE
      IF (MODE) 730,740,750
730   WRITE(4,731)
731   FORMAT('- WEIGHTING MODE : STATISTICAL')
      GOTO 752
740   WRITE(4,741)
741   FORMAT('- WEIGHTING MODE : NO WEIGHTING')
      GOTO 752
750   WRITE(4,751)
```

```
751   FORMAT('- WEIGHTING MODE : INSTRUMENTAL')
752   NORD=1
      IF (MODE.EQ.0) THEN
      DO 760 I=1,NPTS
760    VARY(I)=1.
      ELSE
      DO 770 I=1,NPTS
770    VARY(I)=SIGMAY(I)
      END IF
C
C     FIRST GUESS ON COEFFICIENTS
C
      DO 9016 I=1,NTERMS
      A(I)=0.0
      SIGMAA(I)=0.0
9016  CONTINUE
      TYPE 9505
9505  FORMAT('- INPUT GUESSES ? (YES/NO) :')
9506  FORMAT('- INPUT GUESSES :')
      ACCEPT ANAME
      IF (ANAME.EQ.'YES') THEN
       WRITE(4,9506)
       DO 3304 I=1,NTERMS
        TYPE 3305,I
        WRITE(4,3305) I
        ACCEPT A(I)
        WRITE(9,3333) I,A(I)
3304    WRITE(4,3333) I,A(I)
      ELSE
       DO 3310 I=1,NTERMS
3310    A(I)=1.0
       WRITE(9,3340) A(1)
       WRITE(4,3340) A(1)
      END IF
3305  FORMAT('      A(',I2,') = ')
3333  FORMAT('      A(',I2,') = ',1PE11.3 )
3340  FORMAT('- ALL COEFFICIENTS SET TO ',1PE11.4)
      TYPE 9401
      WRITE(4,9401)
9401  FORMAT('- ENTER RELATIVE ACCURACY REQUIRED : ')
      ACCEPT RP
      WRITE(4,9402) RP
9402  FORMAT(1PE11.3)
      TYPE 9404
      WRITE(4,9404)
9404  FORMAT('- ENTER MAXIMUM NUMBER OF ITERATIONS : ')
      ACCEPT MAXIT
      WRITE(4,9406) MAXIT
9406  FORMAT(I10)
      CALL TIME(NSEC1)
      TEST=1.E10
      DO 216 I=1,NTERMS
      DELTAA(I)=A(I)/10.0
```

```
216   CONTINUE
      FLAMDA=0.001
C
C     ITERATION LOOP
C
      TYPE '- LEAST-SQUARES FIT IN PROGRESS...'
      DO 52 JJJ=1,MAXIT
       KJJ=JJJ
       CALL CURFIT(X,Y,SIGMAY,NPTS,NTERMS,MODE,A,DELTAA,
     1      SIGMAA,0.001,YFIT,CHISQR,ERROR,NPAR,NOD,ND)
       IF (CHISQR.EQ.0.0) THEN
       CHISQRD=1.
       ELSE
       CHISQRD=CHISQR
       END IF
       TEST=(TEST-CHISQR)/CHISQRD
       IF (TEST.LE.RP) GO TO 54
       TEST=CHISQR
52    CONTINUE
9301  FORMAT(' !! NO CONVERGENCE')
      WRITE(9,9301)
      WRITE(4,9301)
54    WRITE(9) 'TERMINATED.'
      WRITE(9,9099) KJJ
      WRITE(4,9099) KJJ
      CALL TIME(NSEC2)
      WRITE(9,9097) NSEC2-NSEC1
      WRITE(4,9097) NSEC2-NSEC1
      WRITE(9,9100)
      WRITE(4,9100)
      WRITE(9,9110)
      WRITE(4,9110)
9097  FORMAT('- ELAPSED TIME : ',I6,' SEC'/)
9099  FORMAT(/'-',I4,' ITERATIONS'/)
9100  FORMAT(/'- MODEL COEFFICIENTS',5X,'STD ERROR',8X,'F-RATIO')
9110  FORMAT(52('_')/)
      DO 8888 I=1,NTERMS
      WRITE(9,7777) A(I),I,SIGMAA(I)*SQRT(CHISQR),
     1 (A(I)/SIGMAA(I))**2/CHISQR
      WRITE(4,7777) A(I),I,SIGMAA(I)*SQRT(CHISQR),
     1 (A(I)/SIGMAA(I))**2/CHISQR
8888  CONTINUE
7777  FORMAT(E11.4,' = A(',I2,') +/- ',F9.6,10X,F6.1)
      WRITE(9,8889) CHISQR
      WRITE(4,8889) CHISQR
8889  FORMAT(/'- CHI SQUARE = ',1PE11.4)
      PAUSE
C
C     SEARCH FOR AN EXTREMUM IN WINDOW
C
      IF (NOD.EQ.2) CALL EXTREMUM(A,XMIN,XMAX,SIGMAX,AVEX,NPAR)
C
C     STATISTICAL ANALYSIS
```

```
C
      CALL STAT(X,A,Y,VARY,YFIT,NPAR,NPTS,NTERMS,NT,
     1 ND,AVERAGE,EXPERROR,NDF,NREPLICATE,NDEP)
      TYPE '- SAVE FIT IN MAP.IN (Y/N) ? '
      ACCEPT ANAME
      IF (ANAME.EQ.'Y') THEN
       WRITE(2,613) RESP(ND)
       DO 9600 I=1,NTERMS
9600   WRITE(2,7777) A(I),I,SIGMAA(I)*SQRT(CHISQR)
      END IF
      WRITE(9,9500)
9500  FORMAT(/'- ENTER "END" TO STOP')
      ACCEPT ANAME
      IF (ANAME.NE.'END') GOTO 140
      WRITE(9,1001)
      WRITE(4,1001)
1001  FORMAT(/'- END PROGRAM LSIFIT.')
      PAUSE
      STOP
      END
C
      SUBROUTINE CURFIT(X,Y,SIGMAY,NPTS,NTERMS,MODE,A,DELTAA,
     1          SIGMAA,FLAMDA,YFIT,CHISQR,ERROR,NPAR,NOD,ND)
      DOUBLE PRECISION ARRAY,CHISQR,CHISQ1,FCHISQ
      DIMENSION X(28,100),Y(10,100),SIGMAY(100),A(28),DELTAA(28),
     1         ERROR(28,28),SIGMAA(28),YFIT(100)
      DIMENSION WEIGHT(100),ALPHA(28,28),BETA(28),DERIV(28),
     1         ARRAY(28,28),B(28)
11    NFREE=NPTS-NTERMS
      IF (NFREE) 13,20,20
13    CHISQR=0.0
      GOTO 110
C
C     EVALUATE WEIGHTS
C
20    DO 30 I=1,NPTS
21    IF(MODE) 22,27,29
22    IF(Y(ND,I)) 25,27,23
23    WEIGHT(I)=1./Y(ND,I)
      GOTO 30
25    WEIGHT(I)=1./(-Y(ND,I))
      GOTO 30
27    WEIGHT(I)=1.0
      GOTO 30
29    WEIGHT(I)=1./SIGMAY(I)**2
30    CONTINUE
C
C     EVALUATE ALPHA AND BETA MATRICES
C
31    DO 34 J=1,NTERMS
      BETA(J)=0.0
      DO 34 K=1,J
34    ALPHA(J,K)=0.0
```

```
41    DO 50 I=1,NPTS
      CALL FDERIV(X,I,A,DELTAA,NTERMS,DERIV,NPAR,NOD)
      DO 46 J=1,NTERMS
      BETA(J)=BETA(J)+WEIGHT(I)*(Y(ND,I)-
     1      FUNCTN(X,I,A,NPAR,NOD))*DERIV(J)
      DO 466 K=1,J
      ALPHA(J,K)=ALPHA(J,K)+WEIGHT(I)*DERIV(J)*DERIV(K)
466   CONTINUE
46    CONTINUE
50    CONTINUE
51    DO 53 J=1,NTERMS
      DO 53 K=1,J
53    ALPHA(K,J)=ALPHA(J,K)
C
C     EVALUATE CHI SQUARE AT STARTING POINT
C
61    DO 62 I=1,NPTS
62    YFIT(I)=FUNCTN(X,I,A,NPAR,NOD)
63    CHISQ1=FCHISQ(Y,SIGMAY,NPTS,NFREE,MODE,YFIT,ND)
C
C     INVERT MODIFIED CURVATURE MATRIX TO FIND NEW PARAMETERS
C
71    DO 74 J=1,NTERMS
      DO 73 K=1,NTERMS
73    ARRAY(J,K)=ALPHA(J,K)/SQRT(ALPHA(J,J)*ALPHA(K,K))
74    ARRAY(J,J)=1.+FLAMDA
80    CALL MATINV(ARRAY,NTERMS,DET)
81    DO 84 J=1,NTERMS
      B(J)=A(J)
      DO 84 K=1,NTERMS
84    B(J)=B(J)+BETA(K)*ARRAY(J,K)/SQRT(ALPHA(J,J)*ALPHA(K,K))
C
C     IF CHI-SQUARE INCREASED, INCREASE FLAMDA AND TRY AGAIN
C
91    DO 92 I=1,NPTS
92    YFIT(I)=FUNCTN(X,I,B,NPAR,NOD)
93    CHISQR=FCHISQ(Y,SIGMAY,NPTS,NFREE,MODE,YFIT,ND)
      IF(CHISQ1-CHISQR) 95,101,101
95    FLAMDA=10.*FLAMDA
      GOTO 71
C
C     EVALUATE PARAMETERS AND UNCERTAINTIES
C
101   DO 103 J=1,NTERMS
      A(J)=B(J)
      DELTAA(J)=BETA(J)/FLAMDA/ALPHA(J,J)
103   SIGMAA(J)=SQRT(ARRAY(J,J)/ALPHA(J,J))
      FLAMDA=FLAMDA/10.
110   CONTINUE
      END
C
      FUNCTION FCHISQ(Y,SIGMAY,NPTS,NFREE,MODE,YFIT,ND)
      DOUBLE PRECISION CHISQ,WEIGHT,FCHISQ,FREE
```

```
      DIMENSION Y(10,100),SIGMAY(100),YFIT(100)
11    CHISQ=0.0
12    IF(NFREE) 13,13,20
13    FCHISQ=0.0
      GOTO 40
C
C     ACCUMULATE CHI-SQUARE
C
20    DO 30 I=1,NPTS
21    IF(MODE) 22,27,29
22    IF(Y(ND,I)) 25,27,23
23    WEIGHT=1./Y(ND,I)
      GOTO 30
25    WEIGHT=1./(-Y(ND,I))
      GOTO 30
27    WEIGHT=1.0
      GOTO 30
29    WEIGHT=1./SIGMAY(I)**2
30    CHISQ=CHISQ+WEIGHT*(Y(ND,I)-YFIT(I))**2
C
C     DIVIDE BY NUMBER OF DEGREES OF FREEDOM
C
31    FREE=NFREE
32    FCHISQ=CHISQ/FREE
40    CONTINUE
      END
C
      SUBROUTINE FDERIV(X,I,A,DELTAA,NTERMS,DERIV,NPAR,NOD)
C
C     COMPUTES DERIVATIVES CORRESPONDING TO FUNCTION FUNCTN
C
      DIMENSION X(28,100),A(28),DELTAA(28),DERIV(28)
      DO 10 M=1,NTERMS
      AJ=A(M)
      DELTA=DELTAA(M)
      A(M)=AJ+DELTA
      F1=FUNCTN(X,I,A,NPAR,NOD)
      A(M)=AJ-DELTA
      DERIV(M)=(F1-FUNCTN(X,I,A,NPAR,NOD))/(2.*DELTA)
      A(M)=AJ
10    CONTINUE
      END
C
      SUBROUTINE MATINV(ARRAY,NORDER,DET)
      DOUBLE PRECISION ARRAY,AMAX,SAVE
      DIMENSION ARRAY(28,28),IK(28),JK(28)
10    DET=1.0
11    DO 100 K=1,NORDER
C
C     FIND LARGEST ELEMENT ARRAY(I,J) IN REMAINDER OF MATRIX
C
      AMAX=0.0
21    DO 30 I=K,NORDER
```

```
      DO 30 J=K,NORDER
23    IF(DABS(AMAX)-DABS(ARRAY(I,J))) 24,24,30
24    AMAX=ARRAY(I,J)
      IK(K)=I
      JK(K)=J
30    CONTINUE
C
C     INTERCHANGE ROWS AND COLUMNS TO PUT AMAX IN ARRAY(K,K)
C
31    IF(AMAX) 41,32,41
32    DET=0.0
      GOTO 140
41    I=IK(K)
      IF(I-K) 21,51,43
43    DO 50 J=1,NORDER
      SAVE=ARRAY(K,J)
      ARRAY(K,J)=ARRAY(I,J)
50    ARRAY(I,J)=-SAVE
51    J=JK(K)
      IF(J-K) 21,61,53
53    DO 60 I=1,NORDER
      SAVE=ARRAY(I,K)
      ARRAY(I,K)=ARRAY(I,J)
60    ARRAY(I,J)=-SAVE
C
C     ACCUMULATES ELEMENTS OF INVERSE MATRIX
C
61    DO 70 I=1,NORDER
      IF(I-K) 63,70,63
63    ARRAY(I,K)=-ARRAY(I,K)/AMAX
70    CONTINUE
71    DO 80 I=1,NORDER
      DO 80 J=1,NORDER
      IF(I-K) 74,80,74
74    IF(J-K) 75,80,75
75    ARRAY(I,J)=ARRAY(I,J)+ARRAY(I,K)*ARRAY(K,J)
80    CONTINUE
81    DO 90 J=1,NORDER
      IF(J-K) 83,90,83
83    ARRAY(K,J)=ARRAY(K,J)/AMAX
90    CONTINUE
      ARRAY(K,K)=1./AMAX
100   DET=DET*AMAX
C
C     RESTORE ORDERING OF MATRIX
C
101   DO 130 L=1,NORDER
      K=NORDER-L+1
      J=IK(K)
      IF (J-K) 111,111,105
105   DO 110 I=1,NORDER
      SAVE=ARRAY(I,K)
      ARRAY(I,K)=-ARRAY(I,J)
```

```
110   ARRAY(I,J)=SAVE
111   I=JK(K)
      IF(I-K) 130,130,113
113   DO 120 J=1,NORDER
      SAVE=ARRAY(K,J)
      ARRAY(K,J)=-ARRAY(I,J)
120   ARRAY(I,J)=SAVE
130   CONTINUE
140   DET=DET
      END
C
      SUBROUTINE CORR(X,Y,NPTS,NT,NPAR,
     1 NDEP,AVERAGE,EXPERROR,NDF,NREPLICATE)
      DIMENSION X(28,100),SIGMAT(38),CMAT(38,38),
     1 AVERAGE(38),Y(10,100),T(38,100),EXPERROR(10)
      LOGICAL*4 COUNTED(100)
C
C     CALCULATE PURE ERROR
C
      DO 200 I=1,NDEP
200    EXPERROR(I)=0.
      NDF=0
      NREPLICATE=0
      DO 285 K=1,NPTS
285    COUNTED(K)=.FALSE.
      DO 280 I=1,NPTS-1
       DO 280 K=I+1,NPTS
       NREP=0
       DO 270 J=1,NPAR
270     IF (X(J,K).EQ.X(J,I)) NREP=NREP+1
       IF (NREP.EQ.NPAR) THEN
        DO 275 L=1,NDEP
275      EXPERROR(L)=EXPERROR(L)+(Y(L,I)-Y(L,K))**2/2.
        NDF=NDF+1
        IF (.NOT.COUNTED(K)) THEN
         NREPLICATE=NREPLICATE+1
         COUNTED(K)=.TRUE.
        END IF
       END IF
280   CONTINUE
C     ADJUSTED EXPERIMENTAL ERROR
      DO 290 I=1,NDEP
290   EXPERROR(I)=EXPERROR(I)*FLOAT(NREPLICATE)/FLOAT(NDF)
C             INITIALIZE
C     LESS THAN 4 INDEPENDENT PARAMETERS, CUBIC TERMS INCLUDED :
      IF (NPAR.LT.4) THEN
       NT=3*(NPAR+(NPAR-1)*NPAR/2)
C      EXACTLY 3 PARAMETERS :
       IF (NPAR.EQ.3) NT=NT+1
      ELSE
C     MORE THAN 3 PARAMETERS, ONLY QUADRATIC TERMS :
       NT=2*NPAR+(NPAR-1)*NPAR/2
      END IF
```

```
C     ADD RESPONSES
      NT=NT+NDEP
      PTS=FLOAT(NPTS)
      DO 10 I=1,NT
       SIGMAT(I)=0.
       AVERAGE(I)=0.
       DO 10 J=1,I
10     CMAT(I,J)=0.
C           DEFINE MATRIX OF TERMS
      CALL TERMS(X,Y,T,NPTS,NT,NDEP,NPAR)
C         CALCULATE AVERAGES AND AVERAGE OF SQR.
      DO 20 I=1,NPTS
       DO 20 J=1,NT
        AVERAGE(J)=AVERAGE(J)+T(J,I)/PTS
        SIGMAT(J)=SIGMAT(J)+T(J,I)**2/PTS
20     CONTINUE
C         CALCULATE VARIANCES AND CORRELATIONS
      DO 30 I=1,NT
       SIGMAT(I)=(SIGMAT(I)-AVERAGE(I)**2)*PTS/(PTS-1.)
       DO 30 K=1,NPTS
        DO 30 J=1,I
         CMAT(I,J)=CMAT(I,J)+(T(I,K)-AVERAGE(I))*
     1   (T(J,K)-AVERAGE(J))/SQRT(SIGMAT(I)*SIGMAT(J))/(PTS-1.)
30     CONTINUE
C           DIAGONALIZE CORRELATION MATRIX
      DO 40 I=1,NT
       DO 40 J=1,I
40      CMAT(I,J)=CMAT(I,J)/SQRT(CMAT(I,I)*CMAT(J,J))
C           DISPLAY CORRELATION MATRIX
      WRITE(4,43)
43    FORMAT(/'- CORRELATION MATRIX :'/)
      DO 60 I=1,NT
60     WRITE(4,110) (CMAT(I,J),J=1,I)
      TYPE(4,*) (' X',I,I=1,NPAR)
      DO 70 I=1,NPAR
70     TYPE(4,*) (I,**',J,J=I,NPAR)
      IF (NPAR.LT.4) THEN
       IF (NPAR.GE.1) TYPE(4,*) ' 1^3'
       IF (NPAR.GE.2) TYPE(4,*) '2*1^21*2^22^3'
       IF (NPAR.EQ.3) TYPE(4,*) '3*1^21*3^23*2^22*3^21*2*33^3'
      END IF
      TYPE(4,*) (' Y',I,I=1,NDEP)
      WRITE(4,*) ' '
110   FORMAT(38(X,F3.1))
      END
C
      SUBROUTINE STAT(X,A,Y,SIGMAY,YFIT,NPAR,NPTS,NTERMS,NT,
     1 ND,AVERAGE,EXPERROR,NDF,NREPLICATE,NDEP)
      DIMENSION X(28,100),A(28),AVERAGE(38),
     1 Y(10,100),YFIT(100),EXPERROR(10),SIGMAY(100)
C
C     VARIABLES :
C     SSTOT = (1/W(I)**2)Σ(Y(ND,I)-AVERAGE(Y))**2 =
```

```
C               (1/W(I)**2)(Σ(YFIT(I)-AVERAGE(Y))**2 +Σ(Y(ND,I)-YFIT(I))**2)
C              = SREGF + R2
C      SSREG= SSTOT-R2 = SREGF
C      RY2    = SSREG/SSTOT
C      RYY    = (1-(R2*(NPTS-1)/(SSTOT*(NPTS-NTERMS)) ADJUSTED R2
C      FRATIO = (RY2*(NPTS-NTERMS))/((1-RY2)*(NTERMS-1))  F-RATIO
C
       SSTOT=0.
       DO 10 I=1,NPTS
10      SSTOT=SSTOT+((Y(ND,I)-AVERAGE(NT-NDEP+ND))/SIGMAY(I))**2
       WRITE(9,9405)
       WRITE(4,9405)
       WRITE(9,9403)
       WRITE(9,9407)
       WRITE(4,9403)
       WRITE(4,9407)
9405   FORMAT(/53X,'RELATIVE')
9403   FORMAT('POINT #',4X,'DATA',9X,'RESIDUAL',9X,'FIT',9X,'RESIDUAL')
9407   FORMAT(62('_')/)
       R2=0.
       SREGF=0.
       DO 213 J=1,NPTS
       R=YFIT(J)-Y(ND,J)
       SREGF=SREGF+((YFIT(J)-AVERAGE(NT-NDEP+ND))/SIGMAY(J))**2
       R2=R2+(R/SIGMAY(J))**2
       WRITE(9,9330) J,Y(ND,J),R,YFIT(J),R/Y(ND,J)
       WRITE(4,9330) J,Y(ND,J),R,YFIT(J),R/Y(ND,J)
213    CONTINUE
9330   FORMAT(I3,4(5X,E10.3))
C      SUM OF SQUARE OF REGRESSIONS
       SSREG=SSTOT-R2
C      ADJUSTED R2
       RYY=1-R2*FLOAT(NPTS-1)/SSTOT/FLOAT(NPTS-NTERMS)
C      F-RATIO
       FRATIO=SSREG/R2*FLOAT(NPTS-NTERMS)/FLOAT(NTERMS-1)
       WRITE(9,9305)
       WRITE(4,9305)
9305   FORMAT(/'- LEAST-SQUARES REGRESSION ANALYSIS :'/)
       WRITE(9,9307)
       WRITE(4,9307)
9307   FORMAT(14X,'SUM OF',4X,'DEGREES OF',5X,'MEAN')
       WRITE(9,9309)
       WRITE(4,9309)
9309   FORMAT(4X,'SOURCE',4X,'SQUARES',5X,'FREEDOM',5X,
     1 'SQUARE',3X,'F-RATIO')
       WRITE(9,9313)
       WRITE(4,9313)
9313   FORMAT(53('_')/)
       WRITE(9,90) SSREG,NTERMS-1,SSREG/FLOAT(NTERMS-1),FRATIO
       WRITE(4,90) SSREG,NTERMS-1,SSREG/FLOAT(NTERMS-1),FRATIO
90     FORMAT('REGRESSION',2X,F9.4,7X,I2,5X,F9.4,3X,F7.1)
       WRITE(9,9311) R2,NPTS-NTERMS,R2/FLOAT(NPTS-NTERMS)
       WRITE(4,9311) R2,NPTS-NTERMS,R2/FLOAT(NPTS-NTERMS)
```

```
9311  FORMAT(' RESIDUAL ',2X,F9.4,7X,I2,5X,F9.4)
      WRITE(9,92) EXPERROR(ND),NREPLICATE,
     1  EXPERROR(ND)/FLOAT(NREPLICATE)
      WRITE(4,92) EXPERROR(ND),NREPLICATE,
     1  EXPERROR(ND)/FLOAT(NREPLICATE)
92    FORMAT('PURE ERROR',2X,F9.4,7X,I2,5X,F9.4)
      NFL=NPTS-NTERMS-NREPLICATE
      FITER=R2-EXPERROR(ND)
      RATIO=FITER/EXPERROR(ND)*FLOAT(NREPLICATE)/FLOAT(NFL)
      WRITE(9,94) FITER,NFL,FITER/FLOAT(NFL),RATIO
      WRITE(4,94) FITER,NFL,FITER/FLOAT(NFL),RATIO
94    FORMAT('LACK OF FIT',X,F9.4,7X,I2,5X,F9.4,3X,F7.1)
      WRITE(9,93) SSTOT,NPTS-1,SSTOT/FLOAT(NPTS-1)
      WRITE(4,93) SSTOT,NPTS-1,SSTOT/FLOAT(NPTS-1)
93    FORMAT('  TOTAL  ',2X,F9.4,7X,I2,5X,F9.4)
      WRITE(9,95) RYY
      WRITE(4,95) RYY
95    FORMAT(/'ADJUSTED R2 : ',F4.2)
      WRITE(9,100) SREGF,SREGF+R2
      WRITE(4,100) SREGF,SREGF+R2
100   FORMAT('CALCULATED REGRESSION = ',F9.4,' AND TOTAL = ',F9.4)
      END
C
      SUBROUTINE EXTREMUM(A,XMIN,XMAX,SIGMAX,AVEX,NPAR)
      DOUBLE PRECISION XMAT,SAVEMAT
      DIMENSION A(28),XMIN(28),XMAX(28),XMAT(28,28),
     1 SAVEMAT(28,28),EX(28),SIGMAX(28),AVEX(28)
      DO 10 I=1,NPAR
       DO 10 J=1,NPAR
        IF (J.EQ.I) THEN
         N=1+2*J+(J-1)*J/2
         XMAT(I,J)=2.*A(N)
        ELSE
         N=(J+1)*J/2+I+1
         XMAT(I,J)=A(N)
        END IF
10    CONTINUE
      DO 20 I=1,NPAR
       DO 20 J=1,NPAR
20     SAVEMAT(I,J)=XMAT(I,J)
      CALL MATINV(SAVEMAT,NPAR,DMAT)
      DO 40 I=1,NPAR
       DO 30 J=1,NPAR
        DO 30 K=1,NPAR
         IF (J.EQ.I) THEN
          N=1+J*(J+1)/2
          SAVEMAT(J,K)=-A(N)
         ELSE
          SAVEMAT(J,K)=XMAT(J,K)
         END IF
30     CONTINUE
       CALL MATINV(SAVEMAT,NPAR,DET)
40     EX(I)=((DET/DMAT*SQRT(SIGMAX(I))+AVEX(I)+1.)/2.)*
```

```
     1   (XMAX(I)-XMIN(I))+XMIN(I)
         DO 50 I=1,NPAR
          IF ((EX(I).LT.XMIN(I)).OR.(EX(I).GT.XMAX(I))) THEN
           TYPE 60
           WRITE(4,60)
           GOTO 100
          END IF
    50    CONTINUE
    60    FORMAT(/'- EXTREMUM IS NOT IN WINDOW.')
         WRITE(9,70)
         WRITE(4,70)
    70    FORMAT('- EXTREMUM IS AT :')
         DO 80 I=1,NPAR
         WRITE(9,90) I,EX(I)
         WRITE(4,90) I,EX(I)
    80    CONTINUE
    90    FORMAT(5X,'X(',I2,') = ',1PE11.4)
    100   CONTINUE
         END
    C
         SUBROUTINE TERMS(X,Y,T,NPTS,NT,NDEP,NPAR)
         DIMENSION X(28,100),Y(10,100),T(38,100)
    C    LINEAR AND QUADRATIC TERMS :
         DO 12 I=1,NPTS
         NI=NPAR
         DO 12 J=1,NPAR
          T(J,I)=X(J,I)
          DO 11 K=J,NPAR
    11     T(NI+K-J+1,I)=X(J,I)*X(K,I)
    12    NI=NI+NPAR-J+1
    C     CUBIC TERMS WHEN LESS THAN 4 PARAMETERS :
          IF (NPAR.LT.4) THEN
           NI=2*NPAR+(NPAR-1)*NPAR/2
           DO 13 I=1,NPTS
            T(NI+1,I)=X(1,I)**3
            IF (NPAR.GT.1) THEN
             T(NI+2,I)=X(2,I)*X(1,I)**2
             T(NI+3,I)=X(1,I)*X(2,I)**2
             T(NI+4,I)=X(2,I)**3
             IF (NPAR.EQ.3) THEN
              T(NI+5,I)=X(3,I)*X(1,I)**2
              T(NI+6,I)=X(1,I)*X(3,I)**2
              T(NI+7,I)=X(3,I)*X(2,I)**2
              T(NI+8,I)=X(2,I)*X(3,I)**2
              T(NI+9,I)=X(1,I)*X(2,I)*X(3,I)
              T(NI+10,I)=X(3,I)**3
             END IF
            END IF
    13      CONTINUE
           END IF
           DO 15 I=1,NPTS
           DO 15 J=1,NDEP
    15      T(NT-NDEP+J,I)=Y(J,I)
```

```
      END
C
      FUNCTION FUNCTN(X,I,A,NPAR,NOD)
      DIMENSION X(28,100),A(28)
      IF (NOD.EQ.3) THEN
       FU=A(1)+A(2)*X(1,I)+A(3)*X(1,I)**2+
     1 A(4)*X(1,I)**3+
     1 A(5)*X(2,I)+A(6)*X(1,I)*X(2,I)+A(7)*X(2,I)**2+
     1 A(8)*X(2,I)*X(1,I)**2+A(9)*X(1,I)*X(2,I)**2+
     1 A(10)*X(2,I)**3+A(11)*X(3,I)+A(12)*X(1,I)*X(3,I)+
     1 A(13)*X(2,I)*X(3,I)+A(14)*X(3,I)**2+A(15)*X(3,I)*
     1 X(1,I)**2+A(16)*X(1,I)*X(3,I)**2+A(17)*X(3,I)*
     1 X(2,I)**2+A(18)*X(2,I)*X(3,I)**2+
     1 A(19)*X(1,I)*X(2,I)*X(3,I)+A(20)*X(3,I)**3
      ELSE
       IF (NOD.EQ.2) THEN
        FU=A(1)
        DO 10 K=1,NPAR
        DO 10 L=1,K+1
        IF (L.EQ.1) THEN
         XC=1.
        ELSE
         XC=X(L-1,I)
        END IF
        N=(K+1)*K/2+L
10      FU=FU+A(N)*X(K,I)*XC
       ELSE
        IF (NOD.EQ.1) THEN
         FU=A(1)
         DO 20 K=2,NPAR
20        FU=FU+A(K)*X(K,I)
        ELSE
          FU=A(1)+A(2)*X(1,I)+A(3)*X(1,I)**2+A(4)*X(2,I)+
     1  A(5)*X(1,I)*X(2,I)+A(6)*X(2,I)**2+A(7)*X(3,I)+
     1  A(8)*X(1,I)*X(3,I)+A(9)*X(2,I)*X(3,I)+A(10)*X(3,I)**2+
     1  A(11)*X(4,I)+A(12)*X(1,I)*X(4,I)+A(13)*X(2,I)*X(4,I)+
     1  A(14)*X(3,I)*X(4,I)+A(15)*X(4,I)**2+A(16)*X(5,I)+
     1  A(17)*X(1,I)*X(5,I)+A(18)*X(2,I)*X(5,I)+A(19)*X(3,I)*X(5,I)+
     1  A(20)*X(4,I)*X(5,I)+A(21)*X(5,I)**2
         END IF
        END IF
       END IF
       FUNCTN=FU
       END
```

```
      PROGRAM MAPPING
C
C     ************************************************
C     *                                              *
C     *       APPLICATION :                          *
C     *       2D MAP OF FUNCTION POLY                *
C     *       DEVELOPED AT :                         *
C     *       LSI LOGIC, SANTA CLARA CA, 22/10/1986  *
C     *       BY :                                   *
C     *       PHILIPPE SCHOENBORN                    *
C     *       FROM :                                 *
C     *       DEPARTMENT OF ELECTRICAL ENGINEERING   *
C     *          THE UNIVERSITY OF ALBERTA           *
C     *          EDMONTON, ALBERTA, CANADA           *
C     *                                              *
C     ************************************************
C
C     MODEL COEFFICIENTS ARE FOR STANDARDIZED NORMALIZED
C     INDEPENDENT PARAMETERS AS OUTPUT BY FORTRAN PROGRAM LSIFIT.FOR
C
C     INPUT FILE MUST APPEAR AS IN THE FOLLOWING EXAMPLE :
C        INPUT EXAMPLE                  COMMENTS
C
C     ------------------------------------------------------------
C     3                              NPAR
C     20                             NUMBER OF MODEL COEFFICIENTS
C     Power (KWatt)
C     Pressure (Torr)                PARAMETER DESCRIPTION
C     Helium flow (%)
C     0.8   1.0   0.12   0.2        FIRST PARAMETER RANGE, STD DEV., AVERAGE
C     1.0   3.0   0.03   0.13       SECOND PAR. RANGE ...ETC
C     0.0   0.5   0.056  0.6
C     2                              NDEP
C     Etch rate (µm/min)
C     -1.2345E+01                    COEFFICIENTS FROM LSIFIT...
C        .
C        .
C     Uniformity (%)
C      0.567801
C        .
C
      DIMENSION A(10,38),R(20,4)
      LOGICAL*4 QUIT,EFF
      CHARACTER*16 ANAME
      CHARACTER TEXT(20)*20
      QUIT=.FALSE.
      EFF=.FALSE.
      TYPE 1
1     FORMAT('- ENTER INPUT FILE NAME : ')
      ACCEPT ANAME
      open(unit=3,status='old',file=ANAME)
      READ(3,*) NPAR
      READ(3,*) NTERMS
      DO 2 I=1,NPAR
```

```
2       READ(3,10) TEXT(I)
        DO 3 I=1,NPAR
3       READ(3,*) R(I,1),R(I,2),R(I,3),R(I,4)
        READ(3,*) NDEP
        DO 5 I=1,NDEP
        READ(3,10) TEXT(NPAR+I)
        DO 5 K=1,NTERMS
        read(3,*) A(I,K)
5       continue
7       CALL PLOT2(A,NPAR,R,QUIT,EFF,TEXT,NDEP)
        IF(EFF) GOTO 7
10      FORMAT(A20)
        STOP
        END
C
        SUBROUTINE PLOT2(A,NPAR,R,QUIT,EFF,TEXT,NDEP)
        INCLUDE toolbx.par
        DIMENSION A(10,38),XX(20),R(20,4)
        CHARACTER TEXT(20)*20
        INTEGER H,V
        INTEGER*2 RECT(4),CADRE(4),MOUSELOC(2),BOARD(4),
     1        COUNTER(4),LABRECT(4),HCNT(4),DHCNT(4),
     1          VERT(4),HOR(4),NEWMAP(4),UPON(4),LEVELS(4),
     1          NIVEAU(4),HORIZ(4),NIVEL(4),MORE(4),SHADOW(4),
     1          ERASE(4),LOW(4),STANDARD(4),HIGH(4)
        LOGICAL*4 BUTTONFLAG,UP,LEV,INCADRE,MOREMAP,SHADE,
     1        BASSE,NORMALE,HAUTE,CLEAR
C
C       INITIALIZATION
C
        DATA RECT /0,0,342,512/
        DATA HCNT /3,322,16,350/
        DATA DHCNT /3,410,16,489/
        CALL TOOLBX(SETRECT,NEWMAP,4,4,57,18)
        CALL TOOLBX(SETRECT,UPON,59,4,105,18)
        CALL TOOLBX(SETRECT,LEVELS,107,4,154,18)
        CALL TOOLBX(SETRECT,MORE,156,4,191,18)
        CALL TOOLBX(SETRECT,SHADOW,193,4,232,18)
        CALL TOOLBX(SETRECT,ERASE,234,4,298,18)
        CALL TOOLBX(SETRECT,NIVEAU,30,8,80,16)
        CALL TOOLBX(SETRECT,HORIZ,100,8,150,16)
        CALL TOOLBX(SETRECT,LOW,101,6,135,18)
        CALL TOOLBX(SETRECT,STANDARD,136,6,201,18)
        CALL TOOLBX(SETRECT,HIGH,203,6,242,18)
        BOARD(1)=2
        BOARD(2)=2
        BOARD(3)=20
        BOARD(4)=300
        COUNTER(1)=2
        COUNTER(2)=302
        COUNTER(3)=20
        COUNTER(4)=490
        CALL toolbx(ERASERECT,RECT)
```

```
C
C       DRAW BOARD AND COUNTER
C
        CALL TOOLBX(FRAMERECT,BOARD)
        BOARD(1)=3
        BOARD(2)=3
        BOARD(3)=19
        BOARD(4)=299
        CALL TOOLBX(FRAMERECT,COUNTER)
        COUNTER(1)=3
        COUNTER(2)=303
        COUNTER(3)=19
        COUNTER(4)=489
C
C       DEFINE WINDOW
C
2       H=20
        V=16
        CALL TOOLBX(ERASERECT,BOARD)
        CALL TOOLBX(ERASERECT,COUNTER)
        CALL TOOLBX(MOVETO,H,V)
        TYPE 4
4       FORMAT('- DEFINE GRAPH SIZE')
        H=310
        CALL TOOLBX(MOVETO,H,V)
        TYPE 11
11      FORMAT('H=',5X,'V=')
        H=323
        V=365
3       BUTTONFLAG=toolbx(BUTTON)
        IF (.NOT.BUTTONFLAG) GOTO 3
        CALL toolbx(GETMOUSE,MOUSELOC)
        NSY=INT(MOUSELOC(1))
        NSX=INT(MOUSELOC(2))
        CADRE(1)=MOUSELOC(1)
        CADRE(2)=MOUSELOC(2)
        CADRE(3)=MOUSELOC(1)
        CADRE(4)=MOUSELOC(2)
        WHILE (BUTTONFLAG)
        CALL toolbx(GETMOUSE,MOUSELOC)
        CALL toolbx(ERASERECT,CADRE)
        CALL TOOLBX(MOVETO,V,16)
        TYPE 33,ABS(INT(MOUSELOC(1)-CADRE(1)))
        CALL TOOLBX(MOVETO,H,16)
        CALL TOOLBX(CLIPRECT,HCNT)
        TYPE 33,ABS(MOUSELOC(2)-CADRE(2))
        CALL TOOLBX(CLIPRECT,RECT)
        IF (MOUSELOC(1)<CADRE(1)) THEN
        CADRE(3)=CADRE(1)
        CADRE(1)=MOUSELOC(1)
        NSY=INT(MOUSELOC(1))
        ELSE
        CADRE(3)=MOUSELOC(1)
```

```
      END IF
      IF (MOUSELOC(2)<CADRE(2)) THEN
      CADRE(4)=CADRE(2)
      CADRE(2)=MOUSELOC(2)
      NSX=INT(MOUSELOC(2))
      ELSE
      CADRE(4)=MOUSELOC(2)
      END IF
      NWY=INT(CADRE(3))
      NWX=INT(CADRE(4))
      CALL toolbx(FRAMERECT,CADRE)
      BUTTONFLAG=toolbx(BUTTON)
      REPEAT
33    FORMAT(1I3)
      CALL TOOLBX(ERASERECT,BOARD)
      CADRE(1)=CADRE(1)+1
      CADRE(2)=CADRE(2)+1
      CADRE(3)=CADRE(3)-1
      CADRE(4)=CADRE(4)-1
      NWP=NSX-NWX
      NSX=MIN0(NSX,NWX)
      NWX=ABS(NWP)
      NWP=NSY-NWY
      NSY=MAX0(NSY,NWY)
      NWY=ABS(NWP)
      WX=FLOAT(NWX)
      WY=FLOAT(NWY)
C
C     DEFINE LABEL RECTANGLES
C
      VERT(1)=NSY-NWY-10
      VERT(2)=NSX-44
      VERT(3)=NSY
      VERT(4)=NSX-4
      HOR(1)=NSY
      HOR(2)=NSX-8
      HOR(3)=NSY+12
      HOR(4)=NSX+NWX-11
C
C     DEFINE PARAMETERS AND PARAMETERS RANGE
C
      CALL TOOLBX(MOVETO,20,16)
      TYPE 555
555   FORMAT('- ENTER PARAMETER"S NUMBER')
      H=NSX+NWX+10
      V=NSY
      CALL toolbx(MOVETO,H,V)
      TYPE 5
5     FORMAT('X')
      ACCEPT J
      H=NSX+NWX-120
      CALL TOOLBX(MOVETO,H,NSY+25)
      TYPE 21,TEXT(J)
```

```
      H=NSX
      V=NSY-NWY-2
      CALL toolbx(MOVETO,H,V)
      TYPE 7
7     FORMAT('X')
      ACCEPT I
      CALL TOOLBX(MOVETO,NSX+18,NSY-NWY-2)
      TYPE 21,TEXT(I)
      CALL TOOLBX(ERASERECT,BOARD)
      CALL TOOLBX(MOVETO,20,16)
      TYPE 9
9     FORMAT('- ENTER VALUE OF FIXED PARAMETER')
      NLINE=25
      H=NSX+10
      DO 20 K=1,NPAR
      IF(K.EQ.I .OR. K.EQ.J) GOTO 20
      NLINE=NLINE+10
      CALL TOOLBX(MOVETO,H,NSY+NLINE)
      TYPE 10,K
10    FORMAT(' X',I1,'=')
      ACCEPT XX(K)
      CALL TOOLBX(MOVETO,NSX+66,NSY+NLINE)
      TYPE 21,TEXT(K)
      XX(K)=(2.*(XX(K)-R(K,1))/(R(K,2)-R(K,1))-1.-R(K,4))/R(K,3)
20    CONTINUE
21    FORMAT(A20)
      CALL TOOLBX(ERASERECT,BOARD)
4     CALL TOOLBX(MOVETO,20,16)
      TYPE 27
27    FORMAT('- ENTER HORIZ. LEFT BOUNDARY')
      H=NSX-10
      V=NSY+12
      CALL toolbx(MOVETO,H,V)
      ACCEPT XXMIN
      CALL TOOLBX(ERASERECT,BOARD)
      CALL TOOLBX(MOVETO,20,16)
      TYPE 31
31    FORMAT('- ENTER HORIZ. RIGHT BOUNDARY')
35    H=NSX+NWX-10
      V=NSY+12
      CALL toolbx(MOVETO,H,V)
      ACCEPT XXMAX
      IF(XXMAX.LT.XXMIN) GOTO 35
      CALL TOOLBX(ERASERECT,BOARD)
      CALL TOOLBX(MOVETO,20,16)
      TYPE 41
41    FORMAT('- ENTER VERT. BOTTOM BOUNDARY')
      H=NSX-30
      V=NSY
      CALL toolbx(MOVETO,H,V)
      CALL TOOLBX(CLIPRECT,VERT)
      ACCEPT XYMIN
      CALL TOOLBX(CLIPRECT,RECT)
```

```
      CALL TOOLBX(ERASERECT,BOARD)
      CALL TOOLBX(MOVETO,20,16)
      TYPE 51
51    FORMAT('- ENTER VERT. TOP BOUNDARY')
55    H=NSX-30
      V=NSY-NWY
      CALL toolbx(MOVETO,H,V)
      CALL TOOLBX(CLIPRECT,VERT)
      ACCEPT XYMAX
      CALL TOOLBX(CLIPRECT,RECT)
      IF(XYMAX.LT.XYMIN) GOTO 55
C
C     DEFINE LABELING
C
      CALL TOOLBX(ERASERECT,BOARD)
      CALL TOOLBX(MOVETO,20,16)
      TYPE 22
22    FORMAT('- DEFINE HORIZONTAL LABELING')
23    BUTTONFLAG=toolbx(BUTTON)
      IF (.NOT.BUTTONFLAG) GOTO 23
      H=395
      V=16
      CALL TOOLBX(MOVETO,H,V)
      TYPE 231
231   FORMAT('DH=')
      H=416
      LABRECT(1)=NSY
      LABRECT(2)=NSX
      LABRECT(3)=NSY+4
      LABRECT(4)=NSX+NWX
      WHILE (BUTTONFLAG)
      CALL TOOLBX(ERASERECT,LABRECT)
      CALL toolbx(GETMOUSE,MOUSELOC)
      IF ((INT(MOUSELOC(2)).LT.(NSX+NWX)) .AND.
     1    (INT(MOUSELOC(2)).GT.NSX)) THEN
       CALL TOOLBX(MOVETO,INT(MOUSELOC(2)),NSY)
       CALL TOOLBX(LINETO,INT(MOUSELOC(2)),NSY+3)
       CALL TOOLBX(MOVETO,H,V)
       STEP=FLOAT((INT(MOUSELOC(2))-NSX))
       STEP=STEP*(XXMAX-XXMIN)/WX
       CALL TOOLBX(CLIPRECT,DHCNT)
       TYPE 222,STEP
       CALL TOOLBX(CLIPRECT,RECT)
      ELSE
       GOTO 23
      END IF
      BUTTONFLAG=toolbx(BUTTON)
      REPEAT
222   FORMAT(F7.4)
      NSTEP=NINT(STEP/(XXMAX-XXMIN)*WX)
      H=NSX
      CALL TOOLBX(CLIPRECT,HOR)
      DO 111 S=(XXMIN+STEP),(XXMAX-STEP+.1*STEP),STEP
```

```
      H=H+NSTEP
      CALL TOOLBX(MOVETO,H,NSY)
      CALL TOOLBX(LINETO,H,NSY+3)
      CALL TOOLBX(MOVETO,H-20,NSY+12)
111   TYPE 333,S
      CALL TOOLBX(CLIPRECT,RECT)
333   FORMAT(F6.2)
      CALL TOOLBX(ERASERECT,BOARD)
      CALL TOOLBX(MOVETO,20,16)
      TYPE 221
221   FORMAT('- DEFINE VERTICAL LABELING')
233   BUTTONFLAG=toolbx(BUTTON)
      IF (.NOT.BUTTONFLAG) GOTO 233
      H=395
      V=16
      CALL TOOLBX(MOVETO,H,V)
      TYPE 234
234   FORMAT('DV=')
      CALL TOOLBX(ERASERECT,DHCNT)
      H=416
      LABRECT(1)=NSY-NWY
      LABRECT(2)=NSX-4
      LABRECT(3)=NSY
      LABRECT(4)=NSX
      WHILE (BUTTONFLAG)
      CALL TOOLBX(ERASERECT,LABRECT)
      CALL toolbx(GETMOUSE,MOUSELOC)
      IF ((INT(MOUSELOC(1)).LT.NSY) .AND.
     1    (INT(MOUSELOC(1)).GT.(NSY-NWY))) THEN
       CALL TOOLBX(MOVETO,NSX,INT(MOUSELOC(1)))
       CALL TOOLBX(LINETO,NSX-3,INT(MOUSELOC(1)))
       CALL TOOLBX(MOVETO,H,V)
       STEP=FLOAT((NSY-INT(MOUSELOC(1))))
       STEP=STEP*(XYMAX-XYMIN)/WY
       CALL TOOLBX(CLIPRECT,DHCNT)
       TYPE 222,STEP
       CALL TOOLBX(CLIPRECT,RECT)
      ELSE
       GOTO 233
      END IF
      BUTTONFLAG=toolbx(BUTTON)
      REPEAT
      NSTEP=NINT(STEP/(XYMAX-XYMIN)*WY)
      V=NSY
      DO 112 S=(XYMIN+STEP),(XYMAX-STEP+.1*STEP),STEP
      V=V-NSTEP
      CALL TOOLBX(MOVETO,NSX,V)
      CALL TOOLBX(LINETO,NSX-3,V)
      CALL TOOLBX(CLIPRECT,VERT)
      CALL TOOLBX(MOVETO,NSX-44,V+3)
      TYPE 333,S
      CALL TOOLBX(CLIPRECT,RECT)
112   CONTINUE
```

```
C
C       SELECT DEPENDENT PARAMETER
C
113     CALL SELECT(BOARD,COUNTER,ND,NDEP,NPAR,TEXT)
C
C       NORMALIZING AND STANDARDIZING
C
        HMINOR=((2.*(XXMIN-R(J,1))/(R(J,2)-R(J,1))-1.)-R(J,4))/R(J,3)
        HMAXOR=((2.*(XXMAX-R(J,1))/(R(J,2)-R(J,1))-1.)-R(J,4))/R(J,3)
        VMINOR=((2.*(XYMIN-R(I,1))/(R(I,2)-R(I,1))-1.)-R(I,4))/R(I,3)
        VMAXOR=((2.*(XYMAX-R(I,1))/(R(I,2)-R(I,1))-1.)-R(I,4))/R(I,3)
        DELH=(HMAXOR-HMINOR)/WX
        DELV=(VMAXOR-VMINOR)/WY
C
C       CHOOSE RESOLUTION
C
        CALL TOOLBX(ERASERECT,BOARD)
        CALL TOOLBX(ERASERECT,COUNTER)
        CALL TOOLBX(MOVETO,20,16)
        TYPE 1050
1050    FORMAT('RESOLUTION :',3X,'LOW',3X,'STANDARD',3X,'HIGH')
        CALL TOOLBX(FRAMERECT,LOW)
        CALL TOOLBX(FRAMERECT,STANDARD)
        CALL TOOLBX(FRAMERECT,HIGH)
        BASSE=.FALSE.
        NORMALE=.FALSE.
        HAUTE=.FALSE.
        BUTTONFLAG=.FALSE.
        WHILE (.NOT.((BASSE.OR.NORMALE.OR.HAUTE)
     1       .AND.BUTTONFLAG))
        CALL TOOLBX(GETMOUSE,MOUSELOC)
        BUTTONFLAG=TOOLBX(BUTTON)
        BASSE=TOOLBX(PTINRECT,MOUSELOC,LOW)
        NORMALE=TOOLBX(PTINRECT,MOUSELOC,STANDARD)
        HAUTE=TOOLBX(PTINRECT,MOUSELOC,HIGH)
        REPEAT
        IF (BASSE) NSTEPH=3
        IF (NORMALE) NSTEPH=2
        IF (HAUTE) NSTEPH=1
1100    BUTTONFLAG=TOOLBX(BUTTON)
        IF (BUTTONFLAG) GOTO 1100
        NSTEPV=NSTEPH
C
C       DRAWING...
C
        CALL DRAWING(BOARD,COUNTER,CADRE,RECT,
     1  NPAR,ND,TEXT,XX,A,HMINOR,VMINOR,DELH,DELV,
     1  NWX,NWY,NSX,NSY,NSTEPH,NSTEPV,I,J)
C
1150    CALL TOOLBX(ERASERECT,COUNTER)
        CALL TOOLBX(ERASERECT,BOARD)
        CALL TOOLBX(MOVETO,10,16)
C
```

```
C       GOODIES
C
        CALL TOOLBX(CLIPRECT,BOARD)
        TYPE 1200
1200    FORMAT('NEW MAP',2X,'ADD ON',2X,'LEVELS',2X,
     1  'MORE',2X,'SHADE',4X,'CLEAR')
        CALL TOOLBX(FRAMERECT,NEWMAP)
        CALL TOOLBX(FRAMERECT,UPON)
        CALL TOOLBX(FRAMERECT,LEVELS)
        CALL TOOLBX(FRAMERECT,MORE)
        CALL TOOLBX(FRAMERECT,SHADOW)
        CALL TOOLBX(FRAMERECT,ERASE)
        CALL TOOLBX(CLIPRECT,RECT)
        CALL TOOLBX(MOVETO,320,16)
        TYPE 1210
1210    FORMAT(9X,'QUIT')
        EFF=.FALSE.
        UP=.FALSE.
        LEV=.FALSE.
        SHADE=.FALSE.
        CLEAR=.FALSE.
        QUIT=.FALSE.
        MOREMAP=.FALSE.
        BUTTONFLAG=.FALSE.
        WHILE (.NOT.((QUIT.OR.EFF).OR.(UP.OR.LEV.OR.
     1  MOREMAP.OR.SHADE.OR.CLEAR)))
        UP=BUTTONFLAG.AND.TOOLBX(PTINRECT,MOUSELOC,UPON)
        LEV=BUTTONFLAG.AND.TOOLBX(PTINRECT,MOUSELOC,LEVELS)
        QUIT=BUTTONFLAG.AND.TOOLBX(PTINRECT,MOUSELOC,COUNTER)
        EFF=BUTTONFLAG.AND.TOOLBX(PTINRECT,MOUSELOC,NEWMAP)
        MOREMAP=BUTTONFLAG.AND.TOOLBX(PTINRECT,MOUSELOC,MORE)
        SHADE=BUTTONFLAG.AND.TOOLBX(PTINRECT,MOUSELOC,SHADOW)
        CLEAR=BUTTONFLAG.AND.TOOLBX(PTINRECT,MOUSELOC,ERASE)
        CALL TOOLBX(GETMOUSE,MOUSELOC)
        BUTTONFLAG=TOOLBX(BUTTON)
        REPEAT
1300    BUTTONFLAG=TOOLBX(BUTTON)
        IF (BUTTONFLAG) GOTO 1300
        IF (EFF.OR.QUIT) GO TO 2000
        IF (MOREMAP) GOTO 2
        IF (UP) GOTO 113
        IF (SHADE) THEN
        CALL SELECT(BOARD,COUNTER,ND,NDEP,NPAR,TEXT)
        CALL OMBRE(HMINOR,VMINOR,NSX,NSY,
     1  CADRE,RECT,DELH,DELV,NWX,NWY,A,ND,NPAR,
     1  TEXT,J,I,XX,BOARD,COUNTER,HAUT)
        GOTO 1150
        END IF
        IF (CLEAR) THEN
         CALL TOOLBX(ERASERECT,CADRE)
         GOTO 1150
        END IF
C
```

```
C       TYPE LEVELS
C
        IF (LEV) THEN
        CALL SELECT(BOARD,COUNTER,ND,NDEP,NPAR,TEXT)
        CALL TOOLBX(ERASERECT,COUNTER)
        CALL TOOLBX(MOVETO,320,16)
        TYPE 1210
        CALL TOOLBX(ERASERECT,BOARD)
        CALL TOOLBX(CLIPRECT,BOARD)
        CALL TOOLBX(MOVETO,20,16)
        TYPE 1400,J,I
1400    FORMAT('Y=',8X,'X',I1,'=',10X,'X',I1,'=')
        CALL TOOLBX(CLIPRECT,RECT)
1402    BUTTONFLAG=TOOLBX(BUTTON)
        IF (BUTTONFLAG) GOTO 1402
1403    CALL TOOLBX(GETMOUSE,MOUSELOC)
        BUTTONFLAG=TOOLBX(BUTTON)
        INCADRE=TOOLBX(PTINRECT,MOUSELOC,CADRE)
        QUIT=TOOLBX(PTINRECT,MOUSELOC,COUNTER)
        IF (.NOT.((BUTTONFLAG.AND.INCADRE).OR.QUIT)) GOTO 1403
C
        WHILE (BUTTONFLAG.AND.(INCADRE.OR.QUIT))
        XX(J)=FLOAT(INT(MOUSELOC(2))-NSX)
        XX(J)=HMINOR+XX(J)*(HMAXOR-HMINOR)/WX
        XX(I)=FLOAT(NSY-INT(MOUSELOC(1)))
        XX(I)=VMINOR+XX(I)*(VMAXOR-VMINOR)/WY
        Y=POLY(XX,A,ND)
        CALL TOOLBX(MOVETO,NIVEAU(1),16)
        CALL TOOLBX(CLIPRECT,NIVEAU)
        TYPE 1500,Y
        CALL TOOLBX(MOVETO,HORIZ(1),16)
        CALL TOOLBX(CLIPRECT,HORIZ)
        TYPE 1500,((XX(J)*R(J,3)+R(J,4)+1.)/2.*(R(J,2)-R(J,1))+R(J,1))
        CALL TOOLBX(MOVETO,195,16)
        CALL TOOLBX(CLIPRECT,BOARD)
        TYPE 1500,((XX(I)*R(I,3)+R(I,4)+1.)/2.*(R(I,2)-R(I,1))+R(I,1))
        CALL TOOLBX(CLIPRECT,RECT)
        CALL TOOLBX(GETMOUSE,MOUSELOC)
        BUTTONFLAG=TOOLBX(BUTTON)
        INCADRE=TOOLBX(PTINRECT,MOUSELOC,CADRE)
        QUIT=TOOLBX(PTINRECT,MOUSELOC,COUNTER)
        REPEAT
C
        IF (QUIT.AND.TOOLBX(BUTTON)) THEN
        CALL TOOLBX(ERASERECT,BOARD)
        CALL TOOLBX(MOVETO,20,16)
        TYPE 1180
1180    FORMAT('HIT CR OR CNTR-SHIFT-4/3')
        CALL TOOLBX(ERASERECT,COUNTER)
        CALL TOOLBX(MOVETO,320,16)
        CALL TOOLBX(CLIPRECT,COUNTER)
        TYPE 1450,TEXT(NPAR+ND)
        CALL TOOLBX(CLIPRECT,RECT)
```

```
1450  FORMAT(A20)
      PAUSE
      GOTO 1150
      ELSE
      IF (INCADRE) THEN
       H=INT(MOUSELOC(2)-7)
       V=INT(MOUSELOC(1))
       CALL TOOLBX(MOVETO,H,V)
       NIVEL(1)=MAX(V-8,NSY-NWY+1)
       NIVEL(2)=MAX(H-7,NSX+1)
       NIVEL(3)=MIN(V,NSY)
       NIVEL(4)=MIN(H+24,NSX+NWX-1)
       CALL TOOLBX(CLIPRECT,NIVEL)
       IF (Y.LT.0) THEN
       CALL TOOLBX(MOVETO,H-7,V)
       TYPE '-'
       END IF
       CALL TOOLBX(MOVETO,H,V)
       IF (ABS(Y).LT.9.995) THEN
       TYPE 1501,ABS(Y)
       ELSE
       TYPE 1502,ABS(Y)
       END IF
       IF (ABS(Y).LT.0.995) THEN
       CALL TOOLBX(MOVETO,H,V)
       NIVEL(4)=H+5
       CALL TOOLBX(CLIPRECT,NIVEL)
       TYPE '0'
       END IF
       CALL TOOLBX(CLIPRECT,RECT)
      END IF
      END IF
1500  FORMAT(F8.4)
1501  FORMAT(F4.2)
1502  FORMAT(F4.1)
      GOTO 1403
      END IF
C
C     END TYPE LEVELS
C
2000  CONTINUE
      END
C
C     DRAWING...
C
      SUBROUTINE DRAWING(BOARD,COUNTER,CADRE,RECT,
     1  NPAR,ND,TEXT,XX,A,HMINOR,VMINOR,DELH,DELV,
     1  NWX,NWY,NSX,NSY,NSTEPH,NSTEPV,I,J)
      INCLUDE TOOLBX.PAR
      DIMENSION A(10,38),XX(20),W(350,250)
      CHARACTER TEXT(20)*20
      INTEGER*2 BOARD(4),COUNTER(4),CADRE(4),RECT(4),
     1  MOUSELOC(2)
```

```
      INTEGER H,V
      LOGICAL*4 BUTTONFLAG
      CALL TOOLBX(ERASERECT,BOARD)
      CALL TOOLBX(ERASERECT,COUNTER)
      CALL TOOLBX(MOVETO,320,16)
      TYPE 1210
1210  FORMAT(9X,'QUIT')
      CST=100./FLOAT(NWX+NSTEPV)
      CALL TOOLBX(MOVETO,20,16)
      TYPE 'REMAINING...'
      DO 110 H=1,NWX+NSTEPH,NSTEPH
       XH=H; XX(J)=HMINOR+XH*DELH
       DO 100 V=1,NWY+NSTEPV,NSTEPV
        XV=V; XX(I)=VMINOR+XV*DELV
100     W(H,V)=POLY(XX,A,ND)
       CALL TOOLBX(MOVETO,100,16)
       TYPE 120,INT(100.-XH*CST)
       CALL TOOLBX(GETMOUSE,MOUSELOC)
       IF (TOOLBX(BUTTON).AND.TOOLBX(PTINRECT,MOUSELOC,
     1   COUNTER)) THEN
950           BUTTONFLAG=TOOLBX(BUTTON)
       IF (BUTTONFLAG) GOTO 950
       GOTO 1150
      END IF
110   CONTINUE
120   FORMAT(I3,'%')
130   CALL TOOLBX(ERASERECT,BOARD)
      CALL TOOLBX(ERASERECT,COUNTER)
      H=20
      V=16
      CALL TOOLBX(MOVETO,H,V)
      TYPE 1
1     FORMAT('DY=')
      ACCEPT YINC
      CALL TOOLBX(ERASERECT,BOARD)
      CALL TOOLBX(MOVETO,20,16)
      TYPE 21,TEXT(NPAR+ND)
21    FORMAT(A20)
      YINC=ABS(YINC)
      CALL TOOLBX(CLIPRECT,CADRE)
      DO 1000 H=1+NSTEPH,NWX,NSTEPH
       DO 900 V=1+NSTEPV,NWY,NSTEPV
        DELTAYV=ABS((W(H,V+NSTEPV)-W(H,V-NSTEPV))/4.)
        DELTAYH=ABS((W(H+NSTEPH,V)-W(H-NSTEPH,V))/4.)
        UMOD=ABS(MOD(W(H,V),YINC))
        UMOD=MIN(UMOD,YINC-UMOD)
        IF ((UMOD.LE.DELTAYV).OR.(UMOD.LE.DELTAYH)) THEN
         NH=NSX+H
         NV=NSY-V
         CALL TOOLBX(MOVETO,NH,NV)
         CALL TOOLBX(LINETO,NH,NV)
        END IF
900    CONTINUE
```

```
1000  CONTINUE
      CALL TOOLBX(CLIPRECT,RECT)
      CALL TOOLBX(ERASERECT,BOARD)
      CALL TOOLBX(MOVETO,20,16)
      TYPE '- WHERE PRINT LEGEND'
1110  BUTTONFLAG=TOOLBX(BUTTON)
      IF (.NOT.BUTTONFLAG) GOTO 1110
      CALL TOOLBX(GETMOUSE,MOUSELOC)
      H=MOUSELOC(2) ; V=MOUSELOC(1)
      CALL TOOLBX(MOVETO,H,V)
      TYPE 1130,TEXT(NPAR+ND)
1130  FORMAT(A20)
1150  CALL TOOLBX(CLIPRECT,RECT)
      END
C
C     SELECT DEPENDENT PARAMETER
C
      SUBROUTINE SELECT(BOARD,COUNTER,ND,NDEP,NPAR,TEXT)
      INCLUDE TOOLBX.PAR
      INTEGER*2 BOARD(4),COUNTER(4),MOUSELOC(2)
      CHARACTER TEXT(20)*20
      LOGICAL*4 INCADRE,OK,BUTTONFLAG
      CALL TOOLBX(ERASERECT,BOARD)
      CALL TOOLBX(ERASERECT,COUNTER)
      CALL TOOLBX(MOVETO,320,16)
      TYPE '       OK'
      CALL TOOLBX(MOVETO,20,16)
      ND=1
      TYPE 21,TEXT(NPAR+ND)
      OK=.FALSE.
      BUTTONFLAG=.FALSE.
21    FORMAT(A20)
      WHILE (.NOT.OK)
       CALL TOOLBX(GETMOUSE,MOUSELOC)
       INCADRE=TOOLBX(PTINRECT,MOUSELOC,BOARD)
       IF (BUTTONFLAG.AND.INCADRE) THEN
        CALL TOOLBX(ERASERECT,BOARD)
        ND=ND+1
        IF (ND.GT.NDEP) ND=1
        CALL TOOLBX(MOVETO,20,16)
        TYPE 21,TEXT(NPAR+ND)
800     BUTTONFLAG=TOOLBX(BUTTON)
        IF (BUTTONFLAG) GOTO 800
       END IF
       BUTTONFLAG=TOOLBX(BUTTON)
       OK=BUTTONFLAG.AND.TOOLBX(PTINRECT,MOUSELOC,COUNTER)
      REPEAT
      END
C
C     SHADE SELECTED AREA
C
      SUBROUTINE OMBRE(HMINOR,VMINOR,NSX,NSY,
     1  CADRE,RECT,DELH,DELV,NWX,NWY,A,ND,NPAR,
```

```
      1   TEXT,J,I,XX,BOARD,COUNTER,HIRES)
          INCLUDE TOOLBX.PAR
          DIMENSION A(10,38),XX(20)
          CHARACTER TEXT(20)*20
          INTEGER H,V
          INTEGER*2 BOARD(4),CADRE(4),RECT(4),MOUSELOC(2)
          LOGICAL*4 HIRES
          IF (HIRES) THEN
           NSTEP=1
          ELSE
           NSTEP=2
          END IF
          CALL TOOLBX(ERASERECT,BOARD)
          CALL TOOLBX(ERASERECT,COUNTER)
          CALL TOOLBX(MOVETO,20,16)
          TYPE 10,TEXT(NPAR+ND)
     10   FORMAT(A20,' < ')
          ACCEPT YSUP
          CALL TOOLBX(ERASERECT,BOARD)
          CALL TOOLBX(MOVETO,20,16)
          TYPE 20,TEXT(NPAR+ND)
     20   FORMAT(A20,' > ')
          ACCEPT YINF
          CALL TOOLBX(ERASERECT,BOARD)
          CALL TOOLBX(CLIPRECT,BOARD)
          CALL TOOLBX(MOVETO,20,16)
          TYPE 30,YINF,TEXT(NPAR+ND),YSUP
     30   FORMAT(F6.2,' < ',A20,'< ',F6.2)
          CALL TOOLBX(CLIPRECT,CADRE)
          CALL TOOLBX(PENMODE,10)
          DO 100 H=1,NWX,NSTEP
           XH=FLOAT(H)
           XX(J)=HMINOR+XH*DELH
           DO 80 V=1,NWY,NSTEP
            XV=FLOAT(V)
            XX(I)=VMINOR+XV*DELV
            Y=POLY(XX,A,ND)
            IF ((Y.LT.YSUP).AND.(Y.GT.YINF)) THEN
             NH=NSX+H
             NV=NSY-V
             CALL TOOLBX(MOVETO,NH,NV)
             CALL TOOLBX(LINETO,NH,NV)
            END IF
     80     CONTINUE
     100    CONTINUE
          CALL TOOLBX(PENMODE,8)
          CALL TOOLBX(CLIPRECT,RECT)
          CALL TOOLBX(ERASERECT,BOARD)
          CALL TOOLBX(MOVETO,20,16)
          TYPE '- WHERE PRINT LEGEND'
     1110 BUTTONFLAG=TOOLBX(BUTTON)
          IF (.NOT.BUTTONFLAG) GOTO 1110
          CALL TOOLBX(GETMOUSE,MOUSELOC)
```

```
      H=MOUSELOC(2) ; V=MOUSELOC(1)
      CALL TOOLBX(MOVETO,H,V)
      TYPE 1130,YINF,TEXT(NPAR+ND),YSUP
1130  FORMAT(F6.2,' < ',A20,'< ',F6.2)
      END
C
      FUNCTION POLY(X,A,ND)
      DIMENSION A(10,38),X(20)
C
C     THIRD ORDER POLYNOMIAL
C     ONE, TWO, THREE PARAMETERS
C
C     FU=A(ND,1)+A(ND,2)*X(1)+A(ND,3)*X(1)**2+
C    1 A(ND,4)*X(1)**3+
C    1 A(ND,5)*X(2)+A(ND,6)*X(1)*X(2)+A(ND,7)*X(2)**2+
C    1 A(ND,8)*X(2)*X(1)**2+A(ND,9)*X(1)*X(2)**2+
C    1 A(ND,10)*X(2)**3+A(ND,11)*X(3)+A(ND,12)*X(1)*X(3)+
C    1 A(ND,13)*X(2)*X(3)+A(ND,14)*X(3)**2+A(ND,15)*X(3)*
C    1 X(1)**2+A(ND,16)*X(1)*X(3)**2+A(ND,17)*X(3)*
C    1 X(2)**2+A(ND,18)*X(2)*X(3)**2+
C    1 A(ND,19)*X(1)*X(2)*X(3)+A(ND,20)*X(3)**3
C
C     SECOND ORDER POLYNOMIAL
C
C     ONE,TWO,THREE,FOUR,FIVE,SIX PARAMETERS
C
      FU=A(ND,1)+A(ND,2)*X(1)+A(ND,3)*X(1)**2
     1 +A(ND,4)*X(2)+
     1 A(ND,5)*X(1)*X(2)+A(ND,6)*X(2)**2+A(ND,7)*X(3)+
     1 A(ND,8)*X(1)*X(3)+A(ND,9)*X(2)*X(3)+A(ND,10)*X(3)**2
C    1 +A(ND,11)*X(4)+A(ND,12)*X(1)*X(4)+A(ND,13)*X(2)*X(4)+
C    1 A(ND,14)*X(3)*X(4)+A(ND,15)*X(4)**2
C    1 +A(ND,16)*X(5)+A(ND,17)*X(1)*X(5)+A(ND,18)*X(2)*X(5)+
C    1 A(ND,19)*X(3)*X(5)+A(ND,20)*X(4)*X(5)+A(ND,21)*X(5)**2
C    1 +A(ND,22)*X(6)+A(ND,23)*X(1)*X(6)+A(ND,24)*X(2)*X(6)
C    1 +A(ND,25)*X(3)*X(6)+A(ND,26)*X(4)*X(6)
C    1 +A(ND,27)*X(5)*X(6)+A(ND,28)*X(6)**2
      POLY=FU
      END
```

From : Philippe Schoenborn
The University of Alberta
Edmonton, Alberta, Canada

LSI LOGIC CORP. Santa Clara, CA, Oct. 7, 1986

User-guide for process analysis using the Response Surface Methodology : Application to plasma etching with the LAM 590

Abstract

The characterization of plasma etching processes using the Response Surface Methodology (RSM) is described step by step from the formatting of input data to the output of results. Fortran programs LSIFIT for fitting of designed experimental observations and MAPPING for displaying contour plots of response surfaces are described. Both programs run on Macintosh 512K. LSIFIT needs only minor modifications to run on any computer that supports fortran. The purpose of this work is to provide the process engineer with a tool that allows optimization and characterization of any processes involving several independent process parameters which can be varied continuously and which have a continuous effect on all observed responses. It is explained how to get a minimal mathematical model for the process under consideration (usually a polynomial). Criteria for the validity of the model are proposed. Once a suitable model has been obtained for a particular process, recharacterization of this process, if necessary, will require only minimum effort and time. Demonstration of the use of RSM is made with regard to plasma etching with a LAM 590. The present document, however, does not deal with the physics or the chemistry of such processes.

Contents :

	page #
1) Introduction	2
2) Statistics	2
i) Mathematical model	2
ii) Experimental error	3
iii) Parameter range	3
iv) Least-squares fit	4
v) Weighted least-squares fit	5
vi) Residuals	6
vii) Input data transformations	7
3) Design of experiments	8
A) Second order polynomial	8
i) 2 independent parameters	8
ii) 3 independent parameters	9
iii) 4 independent parameters	10
iv) 5 independent parameters	12
v) 6 independent parameters	14
B) Third order polynomial	16
i) 2 independent parameters	16
ii) 3 independent parameters	17
4) Experimental procedure	19
i) Synthesis	19
ii) Experiment	19
iii) Processing of data	
LSIFIT USER GUIDE	19
a) Input file	19
b) Response formatting	20
c) Running LSIFIT	20
d) LSIFIT output files	23
e) Correlation matrix	24
f) Customized model function	24
g) Dimensions of vectors and matrices	25
h) CPU times	25
j) Formats	25
iv) Contour plots, MAPPING USER GUIDE	25
a) Introduction	25
b) MAPPING input file	26
c) Model function	26
d) Tricks	26
e) Dimension statements	26
f) Running MAPPING	28
g) Printing results	29
h) Saving results	29
j) Useful features	29
5) SIMPLEX, an optimization technique	29
6) Remarks	31
7) Quick reference manual	34
8) Reference example	35
9) References	39

1) Introduction

Let us consider plasma etching of silicon dioxide (SiO_2) in a CF_4-He plasma using the LAM 590. The process parameters are : power, pressure, helium flow rate, freon 14 flow rate, electrode spacing and temperature. Since the chamber temperature is not a parameter that can be accurately controlled and as it is believed that its impact on the process is weak, it is eliminated of our model. The total flow of freon and helium is deliberately fixed at 200 sccm while the gap is held at 0.35 cm. This leaves us with three independent parameters : power, pressure, percentage of helium.

Two responses are investigated, SiO_2 etch rate and uniformity of etch. Let us say that the uniformity should be ±5% or less and the etch rate as high as possible. What configurations of power, pressure and He flow meet those specifications ?

If one has absolutely no idea about where to start in the parameter space (three-dimensional in this example) one can use an optimization technique such as SIMPLEX. This method will be shortly described later. Provided the target is well defined, as we did above, SIMPLEX guides the experimenter toward the goal, no matter where he starts almost. If the experimenter decides after all to change slightly his target, he has to continue the search. Often a process is known but if for some reason a response drifts out of specification it can be very long to tweak the process blindly until a suitable response is obtained. In both cases it is desirable to know how a response is affected by the change of one parameter or more. When no physical model exists the only way to get this information is to rely on experiments.

2) Statistics

i) Mathematical model

The experimental characterization of physical or chemical processes requires however some precaution. We want to get a response function as real as possible but requiring a minimum of experiments otherwise it would have the same inconveniences as a SIMPLEX or a random search. A least-squares fit with a polynomial function can solve our problem. For instance :

etch rate :

$$y_1 = a_1 + a_2X_1 + a_3X_1^2 + a_4X_2 + a_5X_1X_2 + a_6X_2^2 + a_7X_3 + a_8X_1X_3 + a_9X_2X_3 + a_{10}X_3^2$$

$$y_1 = a_1 + \Sigma a_jT_j \qquad j=2,\ldots,10$$

uniformity :

$$y_2 = b_1 + b_2X_1 + b_3X_1^2 + b_4X_2 + b_5X_1X_2 + b_6X_2^2 + b_7X_3 + b_8X_1X_3 + b_9X_2X_3 + b_{10}X_3^2$$

$$y_2 = b_1 + \Sigma b_jT_j \qquad j=2,\ldots,10$$

where y_1 the etch rate and y_2 the uniformity are functions of power X_1, pressure X_2 and helium percentage X_3. Model terms T_j are combinations of independent parameters. The model coefficients $a_1,\ldots,a_{10}$ and $b_1,\ldots,b_{10}$ must now be determined. Since there are 10 coefficients in this model we need at least 10 experimental points Y_{1i}, Y_{2i} $i=1,\ldots,10$ corresponding to 10 different combinations of X_{1i}, X_{2i}, X_{3i}. LSIFIT calculates the a's and b's such that $\Sigma(y-Y_i)^2$ is minimum. The X_{ji} $j=1,2,3$; $i=1,\ldots,10$ MUST be chosen adequately. In other words the experiment must be designed in order to minimize intercorrelations between X_1, X_2, X_3. The intercorrelation (also called simply correlation or covariance) :

$r_{jk}=\Sigma(T_{ji}-A_j)(T_{ki}-A_k)/(V_jV_k)^{1/2}$ measures the amount - comprised between -1 and +1- by which two model terms T_j, T_k are dependent to each other. A_j and V_j denote respectively the average and variance of model term T_j. When two terms are perfectly correlated ($r_{jk}=\pm1$) their effect on the response cannot be distinguished. Furthermore, a n^{th} order polynomial requires dependent parameters having at least n+1 levels.

There are many kinds of design that meet those conditions. The Box-Behnken design is one of them [1]. In our example it could be as follows :

Run #	X_1	X_2	X_3
+	950 W	2.5 T	37.5 %
0	900	2.0	25
-	850	1.5	12.5
1	+	+	0
2	+	-	0
3	-	+	0
4	-	-	0
5	+	0	+
6	+	0	-
7	-	0	+
8	-	0	-
9	0	+	+
10	0	+	-
11	0	-	+
12	0	-	-
13	0	0	0

+ denotes the upper level, - the lower level and 0 the intermediate level. + and - are at equal distance from the intermediate level.

ii) Experimental error

Sources of errors occur everywhere. In our example uncertainty is associated with film thickness measurement which itself splits into two parts. The intrinsic inaccuracy of the Nanospec contributes for one part. The etch rate is basically the difference between the film thickness before and after etching. When unpatterned wafers are used those measurements may not be done exactly at the same place which accounts for the second part. The etcher itself controls the parameters within some uncertainty. Last but not least, process repeatability is not perfect. To be consistent one would like to account for all those sources of errors in a simple and experimental manner. This is achieved by replicating several times the central point (X_1=900 W, X_2=2.0 Torr, X_3=25%). The experimental error associated to response Y_k is calculated according to :

$$E_k = \Sigma(Y_{ki}-Y_{kj})^2/(2m)$$

where i,j i≠j are all pairs of replicates and m is their number.

iii) Parameter range

The range over which a parameter is varied must be determined so that the response at + or - levels is different from the response at the center point by far more than the experimental error. 10 times more is a reasonable figure. On the other hand, the larger the range the higher must be the order of the polynomial. A trade-off must be found depending on

your specific goal. Measuring the response for four values of the most important parameter, if known, may help determine a suitable order of polynomial. If the curvature of the response seems monotonic (concave or convex only) go for a second order polynomial, if the curvature seems to have an inflection point (concave to convex) a third order fit is required.

iv) Least-squares fit

It is not the purpose of this document to expose the theory of least-squares fitting. If you wish to know more about that please refer to reference [2] from which LSIFIT's algorithm has been taken.

As mentioned earlier, a model with p terms requires at least p experiments. Practically p experimental points would yield a perfect but usually unrealistic fit. The experimenter must collect at least p+1 points not counting replicated points. The central point should be replicated at least twice. LSIFIT calculates the model coefficients in such a way as to minimize the square of the residuals between the observed response Y_i and its fitted function y_i.

The value to minimize is referred to as chi-square : X^2.

$$X^2 = \sum (y_i - Y_i)^2 \quad i=1,\ldots,n$$

where n is the number of experiments. X^2 is a function of all model coefficients in a p-dimensional space. One can write : $\sum (Y_i - Y)^2 = \sum (y_i - Y)^2 + \sum (Y_i - y_i)^2 \quad i=1,\ldots,n$

where $Y = \Sigma Y_i/n$ is the average of Y. The quantity on the left hand side of this equation is obviously determined by the experiment. Summation on the left of the right hand side is called the regression sum of squares S_{reg} and the remaining sum is just the residual sum of squares X^2. Thus, minimizing X^2 increases S_{reg} at the same time. A useful figure to evaluate the validity of the fit is to take the ratio between those two quantities $F=(S_{reg}/X^2)\cdot(n-p)/(p-1)$ where p is the number of model coefficients and n the number of experimental observations. This ratio is referred to as the F-ratio because it is the ratio of two variances obeying a normal law. The larger the F-ratio the better the fit. The F-ratio follows the Fisher-Snedecor distribution $f(\mu_n,\mu_d,L)$ tabulated in most statistical texts. The f law is a function of the number of degree of freedom of the numerator - S_{reg} with p-1 degree of freedom - and of the denominator - X^2 with n-p degree of freedom (d.f.) - it is also a function of the probability L that $S_{reg}/(p-1) > X^2/(n-p)$ is statistically true. One says that F has a level of confidence L if $F>f(p-1,n-p,L)$. Typically one fixes the level of confidence at 90%, 95%, 99% or more. If $F<f(p-1,n-p,L)$ the model is insufficient and either the number of model terms or the number of experiments must be increased. A F-ratio showing statistical significance does not necessarily mean that the fit is good though. Reference [3] gives another criterion for judging the quality of the fit. The critical F-ratio, they say, is :

$$F_0 = (1+g_0^2)\cdot f(\delta_0,n-p,L) \qquad \delta_0=(p-1)\cdot(1+g_0^2)^2/(1+2g_0^2)$$

where g_0=2,3,4,... is chosen by the experimenter. In all cases $F_0>4\cdot1$ should be satisfied.

The residual sum of squares splits into pure error E, as discussed above, and lack of fit. As said earlier, LSIFIT calculates E for all pairs of replicated points but the program displays

the adjusted error sum of squares E_r corresponding to n_r degrees of freedom where n_r is the number of replicated points -not counting the original say- $E_r = E \cdot m \cdot n_r$. Thus $(n-p)=n_r+n_l$, where n_l is the number of d.f. associated with the lack of fit $L = X^2 - E_r$. The F-ratio of lack of fit to pure error $F_r = L \cdot n_r/(E_r \cdot n_l)$ indicates to what extent pure error participates in the residual sum of squares. $F_r > f(n_l, n_r, L)$ must be satisfied.

The adjusted R^2 is defined as : $R^2 = 1 - X^2(p-1)/((S_{reg}+X^2)(n-p))$. R^2 takes values between 0 and 1. A perfect fit has an adjusted R^2 value of 1.0 in which case the model accounts for all variations in the data. LSIFIT displays R^2 with only two decimals. A value of 1.00 may occur. It has been observed that an $R^2 > 0.95$ indicates a good fit in terms of predicted responses. Assuming that the critical F-ratio must satisfy (at worse) :

$$F = 4 \cdot f(p-1, n-p, L) = S_{reg}/X^2 \cdot (n-p)/(p-1)$$

one gets :

$S_{reg} = 4 \cdot f(p-1) \cdot X^2/(n-p)$, introducing S_{reg} in $R^2=0.95$ and assuming $(n-p)/(p-1)=20$ yields f=50. To insure a good fit in terms of predictions, a minimum figure for the critical F-ratio is then f=50, no matter what fit.

Since the number of data points exceeds the number of model coefficients, getting a perfect fit is very unlikely. Practically there is always some lack of fit.

To each model coefficient can be associated a standard error which is derived from the last increment on the coefficient. The square of the ratio of a coefficient to its standard error is just the F-ratio associated to this model term with 1 and (p-1) degrees of freedom. This F-ratio is often referred to as "partial" F-ratio or decremental F-ratio.

$$F_{d,i} = (a_i/\Delta a_i)^2 > f(p-1,1,L) \qquad i=2,\ldots,p$$

The partial F-ratio can be expressed as :

$$F_{d,i} = (p-1) \cdot (X_i^2 - X^2)/X^2 \qquad i=2,\ldots,p$$

where X_i^2 is the residual sum of squares that would be obtained if the i^{th} model terms was dropped out. The partial F-ratio gives therefore the statistical importance of each model terms. A partial F-ratio below its critical value may indicate a lack of data points. Otherwise model terms with small F-ratios can be dropped out of the model thus reducing the number of experiments needed for further characterizations of the process under consideration.

LSIFIT proceeds by successive iteration of the least-squares fit subroutine named CURFIT [2], until the relative variation of X^2 becomes smaller than a value chosen by the user. When the required relative accuracy on X^2 is too small, the coefficients standard errors go to zero and the partial F-ratios are undefined. In that case, a larger relative accuracy value must be used.

v) Weighted least-squares fit

LSIFIT can perform weighted least-squares fits. That is the response to be fitted can be assigned a statistical weight. Every data point has its own weight. Briefly said, a data point having a high weighting value will be seen by CURFIT as more significant than a data point with a small weighting value. As a result one expects smaller residuals on data points with large weights.

The true statistical meaning of weighting is somehow more profound than the picturesque description given here. For example, if successive measurements of the response for a specific set of operating conditions yield a Gaussian distribution, the peak value will be fitted with a weight of $1/S_d^2$ where S_d is the standard deviation. In LSIFIT this weighting mode is referred to as instrumental. If the experiment consists of counting the number of times a certain event occur within a time interval, the response y_i will probably obey a Poisson distribution. Under the assumption that the shape of the individual poisson distributions can be approximated by Gaussian distributions with $S_d^2 = y_i$, LSIFIT assigns the mean observation y_i a weight $1/y_i^2$. This weighting mode is referred to as statistical.

Let us now see how weighting data can be useful in characterizing plasma etching processes. The etch rate is usually the average of 5 -4" wafers- or 9 -5" wafers- actual etch rates measured at different locations on the wafer. Multiple points measurements are made in order to derive the uniformity of etch defined as :
U = (Maximum etch rate - Minimum etch rate)/(Maximum etch rate + Minimum etch rate).
Since the etch rate must be within a specified uniformity, we would like to get good predictions on the etch rates where the uniformity is low. For instance, it is not necessary predicting an average etch rate of 4000 Å/min while the "observed" average etch rate is 4100 Å/min, which leaves us a residual of 100 Å/min, if the minimum and maximum measured etch rates are 2000 Å/min and 5000 Å/min. We would prefer the program to concentrate its efforts on predicting well regions with low uniformity of etch.

It is achieved by assigning the average etch rate an instrumental weight $1/S_d^2$, where S_d is the standard deviation of etch rates on the wafer. Note that THIS PROCEDURE IS NOT MATHEMATICALLY JUSTIFIED since etch rates are obviously NOT "gaussianly" distributed around their average value. The only justification is that it does just what one expects it to do as shown by comparisons between instrumentally weighted and non weighted etch rate fits.

vi) Residuals

Residuals $(y_i - Y_i)$ should be plotted versus Y_i . Residuals should be evenly scattered with respect to the zero axis. An insufficient number of model terms may lead to unevenly distributed residuals. Residuals should also be evenly distributed along the Y axis to make sure that observed responses cover evenly the range over which the responses vary.

LSIFIT also gives the relative residuals $(y_i - Y_i)/Y_i$ which indicate the true accuracy of the fit. With regard to plasma etching, etch-rate fits which relative residuals would all be smaller than the corresponding uniformities would be judged as excellent and representative. However, a relative residual greater than the corresponding uniformity does not always indicate that the data point is badly fitted.

The final decision is left to the experimenter who decides what a fair fit is depending on the circumstances. Under operating conditions that do not etch, for example, one might get an average etch rate of -20 Å/min, 2% uniformity and predict 40 Å/min. The relative residual is -3.0 (300% versus 2%) but practically speaking the prediction would still be correct. Now if the same absolute residual 60 Å/min was obtained for an observed 6000 Å/min ± 5% repeatedly measured under other conditions (6060 Å/min predicted say), the relative residual would only be 1% < 5% .

Let us say that n observed etch rates y_i have uniformities u_i i=1,...,n . Defining {y} as the set of data points which relative residuals are smaller than their corresponding uniformity u_i and {u} the set of data points which uniformities are smaller than a critical value u, one can write :

$\{y\}_i = 1$ if $|y_i - Y_i| < u_i$ otherwise $\{y\}_i = 0$

$\{u\}_i = 1$ if $u_i < u$ otherwise $\{u\}_i = 0$ for all $i = 1,...,n$

one can define :

$$g_u = (\sum ((1-\{y\}_i) \cdot \{u\}_i))/(\sum (\{y\}_i \cdot \{u\}_i)) \qquad G = (\sum (1-\{y\}_i))/(\sum \{u\}_i)$$

where the summation is made for i=1,...,n. Ideally g_u and G should be zero. Denoting N the symbolic operator that returns the number of elements of a set of data points, and using logic statements one can also write :

$$g_u = N(\{u\} \text{ AND NOT}\{y\}) / N(\{u\} \text{ AND } \{y\}) \qquad G = N(\text{NOT}\{y\})/N(\{y\})$$

To calculate g_u, firstly eliminate all data points which uniformity is greater than u. Then take the ratio of the number of all remaining data points which relative residual is greater than their uniformity to the number of points which relative residual is smaller than their uniformity. To calculate G perform the same calculation but keeping all data points regardless of their uniformity. g_u and G are therefore the ratios of the number of bad estimations to the number of good estimations. g_u and G ratios of a reasonably good, yet not excellent fit, may be greatly improved using a weighted fit.

vii) Input data transformations

LSIFIT automatically normalizes and standardizes the input coordinates X_{ki}. These transformations are made in order to save computer time. Firstly, the X_k 's are normalized to the range [-1,+1] :

$$x_{ki} = 2.0 \cdot (X_{ki} - \min(X_{ki}, i=1,...,n))/(\max(X_{ki}, i=1,...,n) - \min(X_{ki}, i=1,...,n)) - 1.0$$

then calculating A_k and V_k average and variance of parameter x_k , the x_k's are standardized :

$$X_{.ki} = (x_{ki} - A_k)/V_k^{1/2} \qquad i=1,...,n$$

A designed experiment has $A_k = 0.0$ k=1,...,NPAR. Where NPAR is the number of independent parameters. The A_k's and V_k's are the transformation coefficients.

3) Design of experiments

Designs currently found in textbooks are given for second order polynomials with 2,3,4,5 and 6 independent parameters as well as for third order polynomials with 2 and 3 parameters. Unless otherwise specified, averages and variances are those of normalized and standardized parameters.

A) Second order polynomial (quadratic model)

i) 2 independent parameters X_1, X_2

response function : $y = a_1+a_2X_1+a_3X_1^2+a_4X_2+a_5X_1X_2+a_6X_2^2$

number of model coefficients : 6

design : fully factored 3-levels

Run #	X_1	X_2
Average	0.0	
Variance	0.774597	
1	+	+
2	+	-
3	-	+
4	-	-
5	+	0
6	0	+
7	-	0
8	0	-
9	0	0
10	0	0
11	0	0

correlation matrix :

	X_1	X_1^2	X_2	X_1X_2	X_2^2
X_1	1.00				
X_1^2	.00	1.00			
X_2	.00	.00	1.00		
X_1X_2	.00	.00	.00	1.00	
X_2^2	.00	.27	.00	.00	1.00

ii) 3 independent parameters X_1, X_2, X_3

response function :

$$y = a_1 + a_2X_1 + a_3X_1^2 + a_4X_2 + a_5X_1X_2 + a_6X_2^2 + a_7X_3 + a_8X_1X_3 + a_9X_2X_3 + a_{10}X_3^2$$

number of model coefficients : 10

design : Box-Behnken 3-levels

Run #	X_1	X_2	X_3
	Average		0.0
	Variance		0.755929
1	+	+	0
2	+	-	0
3	-	+	0
4	-	-	0
5	+	0	+
6	+	0	-
7	-	0	+
8	-	0	-
9	0	+	+
10	0	+	-
11	0	-	+
12	0	-	-
13	0	0	0
14	0	0	0
15	0	0	0

FCC design 3-levels

Run #	X_1	X_2	X_3
		0.0	
		0.790569	
1	+	+	+
2	+	-	+
3	+	+	-
4	+	-	-
5	-	+	+
6	-	-	+
7	-	+	-
8	-	-	-
9	0	0	+
10	0	0	-
11	-	0	0
12	+	0	0
13	0	-	0
14	0	+	0
15	0	0	0
16	0	0	0
17	0	0	0

correlation matrix :

Box-Behnken

X_1	1.00								
X_1^2	0.00	1.00							
X_2	.00	.00	1.00						
X_1X_2	.00	.00	.00	1.00					
X_2^2	.00	-.07	.00	.00	1.00				
X_3	.00	.00	.00	.00	.00	1.00			
X_1X_3	.00	.00	.00	.00	.00	.00	1.00		
X_2X_3	.00	.00	.00	.00	.00	.00	.00	1.00	
X_3^2	.00	-.07	.00	.00	-.07	.00	.00	.00	1.
	X_1	X_1^2	X_2	X_1X_2	X_2^2	X_3	X_1X_3	X_2X_3	X_3^2

FCC

	1.00								
	.00	1.00							
	.00	.00	1.00						
	.00	.00	0.00	1.00					
	.00	.51	.00	.00	1.00				
	.00	.00	.00	.00	.00	1.00			
	.00	.00	.00	.00	.00	0.00	1.00		
	.00	.00	.00	.00	.00	.00	.00	1.00	
	.00	.51	.00	.00	.51	.00	.00	.00	1.
	X_1	X_1^2	X_2	X_1X_2	X_2^2	X_3	X_1X_3	X_2X_3	X_3^2

warning : intercorrelations between X_1^2, X_2^2 and X_3^2 in FCC design are significant at more than 97.5% level of confidence according to the t-test (values in bold characters).

iii) 4 independent parameters X_1, X_2, X_3, X_4

response function :

$$y = a_1 + a_2X_1 + a_3X_1^2 + a_4X_2 + a_5X_1X_2 + a_6X_2^2 + a_7X_3 + a_8X_1X_3 + a_9X_2X_3 + a_{10}X_3^2 + a_{11}X_4 + a_{12}X_1X_4 + a_{13}X_2X_4 + a_{14}X_3X_4 + a_{15}X_4^2$$

number of model coefficients : 15

design : 3-levels fractional factorial

Run #	X_1	X_2	X_3	X_4
Average		0.0		
Variance		0.816496		
1	+	+	+	0
2	+	-	+	0
3	-	-	-	0
4	-	+	-	0
5	+	+	0	+
6	+	-	0	+
7	-	-	0	-
8	-	+	0	-
9	+	0	+	+
10	+	0	-	+
11	-	0	-	-
12	-	0	+	-
13	0	+	+	+
14	0	+	-	+
15	0	-	-	-
16	0	-	+	-
17	0	0	0	0
18	0	0	0	0
19	0	0	0	0

correlation matrix :

X_1	1.0													
X_1^2	.0	1.0												
X_2	.0	.0	1.0											
X_1X_2	.0	.0	.0	1.0										
X_2^2	.0	.1	.0	.0	1.0									
X_3	.3	.0	.0	.0	.0	1.0								
X_1X_3	.0	.3	.0	.0	.3	.0	1.0							
X_2X_3	.0	.0	.0	.5	.0	.0	.0	1.0						
X_3^2	.0	.1	.0	.0	.1	.0	.3	.0	1.0					
X_4	.7	.0	.3	.0	.0	.0	.0	.0	.0	1.0				
X_1X_4	.0	.7	.0	.0	-.2	.0	-.3	.0	-.2	.0	1.0			
X_2X_4	.0	-.4	.0	.5	.3	.0	-.1	.0	.3	.0	-.3	1.0		
X_3X_4	.0	.0	.0	.0	.0	.0	.5	.5	.0	.0	.0	.0	1.0	
X_4^2	.0	.1	.0	.0	.1	.0	-.4	.0	.1	.0	.7	.3	.0	1.0
	X_1		X_2		X_2^2		X_1X_3		X_3^2		X_1X_4		X_3X_4	
		X_1^2		X_1X_2		X_3		X_2X_3		X_4		X_2X_4		X_4^2

warning : correlations greater or equal to 0.4 are significant at 95% level of confidence or more according to the t-test (values in bold characters).

iv) 5 independent parameters X_1, X_2, X_3, X_4, X_5

response function :

$$y = a_1 + a_2X_1 + a_3X_1^2 + a_4X_2 + a_5X_1X_2 + a_6X_2^2 + a_7X_3 + a_8X_1X_3 + a_9X_2X_3 + a_{10}X_3^2 + a_{11}X_4 + a_{12}X_1X_4 + a_{13}X_2X_4 + a_{14}X_3X_4 + a_{15}X_4^2 + a_{16}X_5 + a_{17}X_1X_5 + a_{18}X_2X_5 + a_{19}X_3X_5 + a_{20}X_4X_5 + a_{21}X_5^2$$

number of model coefficients : 21
design : 3-levels fractional factorial

Run #	X_1	X_2	X_3	X_4	X_5
Average	0.0				
Variance	0.787839				
1	-	-	-	-	-
2	+	0	0	-	-
3	0	+	+	-	-
4	+	0	-	0	-
5	0	+	0	0	-
6	-	-	+	0	-
7	0	+	-	+	-
8	-	-	0	+	-
9	+	0	+	+	-
10	0	0	-	-	0
11	-	+	0	-	0
12	+	-	+	-	0
13	-	+	-	0	0
14	+	0	0	0	0
15	0	-	+	0	0
16	+	-	-	+	0
17	0	0	0	+	0
18	-	+	+	+	0
19	+	+	-	-	+
20	0	-	0	-	+
21	-	0	+	-	+
22	0	-	-	0	+
23	-	0	0	0	+
24	+	+	+	0	+
25	-	0	-	+	+
26	+	+	0	+	+
27	0	-	+	+	+
28	0	0	0	0	0
29	0	0	0	0	0
30	0	0	0	0	0

correlation matrix :

X_1	1.00																			
X_1^2	.00	1.00																		
X_2	.06	.09	1.00																	
X_1X_2	.07	.05	-.07	1.00																
X_2^2	-.09	.03	.00	.05	1.00															
X_3	.00	.00	-.06	.00	.09	1.00														
X_1X_3	.00	.00	.00	.00	.00	.00	1.00													
X_2X_3	.00	.06	.07	.00	-.04	-.07	.00	1.00												
X_3^2	.00	.17	-.09	-.07	.31	.00	.00	-.04	1.00											
X_4	.00	.00	.00	.00	.00	.00	.00	.00	0.00	1.00										
X_1X_4	.00	.00	.00	.00	.00	.00	.00	.24	.00	.00	1.00									
X_2X_4	.00	.00	.00	.00	.00	.00	.25	.00	.00	.00	.00	1.00								
X_3X_4	.00	.00	.00	.26	.00	.00	.00	.00	.00	.00	.00	.00	1.00							
X_4^2	.00	.17	.00	-.07	.17	.00	.00	.06	.17	.00	.00	.00	.00	1.00						
X_5	.00	.00	.00	.00	.00	.00	.00	.00	.00	.00	.00	.00	.00	.00	1.00					
X_1X_5	.00	.00	.00	.52	.65	.00	.00	.00	.00	.00	.00	.00	.25	.00	.00	1.00				
X_2X_5	.00	.65	.00	.52	.00	.00	.00	.00	.00	.00	.00	.00	.25	.00	.00	.50	1.00			
X_3X_5	.00	.00	.00	.00	.00	.00	.00	.00	.00	.00	.25	.25	.00	.00	.00	.00	.00	1.00		
X_4X_5	.00	.00	.00	.00	.00	.00	.25	.24	.00	.00	.00	.00	.00	.00	.00	.00	.00	.00	1.00	
X_5^2	.00	.17	.00	.61	.17	.00	.00	.06	.17	0.00	.00	.00	.00	.17	0.00	.00	.00	.00	0.00	1.00

X_1 X_2 X_2^2 X_1X_3 X_3^2 X_1X_4 X_3X_4 X_5 X_2X_5 X_4X_5
X_1^2 X_1X_2 X_3 X_2X_3 X_4 X_2X_4 X_4^2 X_1X_5 X_3X_5 X_5^2

warning : correlations greater or equal to 0.25 are significant at 90% level of confidence or more according to the t-test (values in bold characters).

v) 6 independent parameters X_1, X_2, X_3, X_4, X_5, X_6

response function :

$$y = a_1 + a_2X_1 + a_3X_1^2 + a_4X_2 + a_5X_1X_2 + a_6X_2^2 + a_7X_3 + a_8X_1X_3 + a_9X_2X_3 + a_{10}X_3^2 + a_{11}X_4 + a_{12}X_1X_4 + a_{13}X_2X_4 + a_{14}X_3X_4 + a_{15}X_4^2 + a_{16}X_5 + a_{17}X_1X_5 + a_{18}X_2X_5 + a_{19}X_3X_5 + a_{20}X_4X_5 + a_{21}X_5^2 + a_{22}X_6 + a_{23}X_1X_6 + a_{24}X_2X_6 + a_{25}X_3X_6 + a_{26}X_4X_6 + a_{27}X_5X_6 + a_{28}X_6^2$$

number of model coefficients : 28

design : 3-levels fractional factorial design

Run #	X_1	X_2	X_3	X_4	X_5	X_6
Average	0.0					
Variance	0.686	0.594	0.686	0.686	0.686	0.767
1	+	+	0	+	0	0
2	+	-	0	-	0	0
3	-	+	0	-	0	0
4	-	-	0	+	0	0
5	0	+	+	0	+	0
6	0	+	-	0	-	0
7	0	-	+	0	-	0
8	0	-	-	0	+	0
9	0	0	+	+	0	+
10	0	0	+	-	0	-
11	0	0	-	+	0	-
12	0	0	-	-	0	+
13	+	0	0	+	+	0
14	+	0	0	-	-	0
15	-	0	0	+	-	0
16	-	0	0	-	+	0
17	0	+	0	0	+	+
18	0	+	0	0	-	-
19	0	-	0	0	+	-
20	0	-	0	0	-	+
21	+	0	+	0	0	+
22	+	0	-	0	0	-
23	-	0	+	0	0	-
24	-	0	-	0	0	+
25	0	0	+	0	+	+
26	0	0	+	0	-	-
27	0	0	-	0	+	-
28	0	0	-	0	-	+
29	+	0	0	+	0	+
30	+	0	0	-	0	-
31	-	0	0	+	0	-
32	-	0	0	-	0	+
33	0	0	0	0	0	0
34	0	0	0	0	0	0
35	0	0	0	0	0	0

correlation matrix :

X_1	1.0																					
X_1^2	.0	1.0																				
X_2	.0	.0	1.0																			
X_1X_2	.0	.0	.0	1.0																		
X_2^2	.0	-.2	.0	.0	1.0																	
X_3	.0	.0	.0	.0	.0	1.0																
X_1X_3	.0	.0	.0	.0	.0	.0	1.0															
X_2X_3	.0	.0	.0	.0	.0	.0	.0	1.0														
X_3^2	.0	-.4	.0	.0	-.2	.0	.0	.0	1.0													
X_4	.0	.0	.0	.5	.0	.0	.0	.0	.0	1.0												
X_1X_4	.0	.0	.3	.0	.0	.0	.0	.0	.0	.0	1.0											
X_2X_4	.5	.0	.0	.0	.0	.0	.0	.0	.0	.0	.0	1.0										
X_3X_4	.0	.0	.0	.0	.0	.0	.0	.0	.0	.0	.0	.0	1.0									
X_4^2	.0	.5	.0	.0	-.2	.0	.0	.0	-.4	.0	.0	.0	.0	1.0								
X_5	.0	.0	.0	.0	.0	.0	.0	.5	.0	.0	.3	.0	.0	.0	1.0							
X_1X_5	.0	.0	.0	.0	.0	.0	.0	.0	.0	.5	.0	.0	.0	.0	.0	1.0						
X_2X_5	.0	.0	.0	.0	.0	.4	.0	.0	.0	.0	.0	.0	.0	.0	.0	.0	1.0					
X_3X_5	.0	.0	.4	.0	.0	.0	.0	.0	.0	.0	.0	.0	.0	.0	.0	.0	.0	1.0				
X_4X_5	.5	.0	.0	.0	.0	.0	.0	.0	.0	.0	.0	.0	.0	.0	.0	.0	.0	.0	1.0			
X_5^2	.0	-.4	.0	.0	.3	.0	.0	.0	.1	.0	.0	.0	.0	-.4	.0	.0	.0	.0	.0	1.0		
X_6	.0	.0	.0	.0	.0	.0	.4	.0	.0	.0	.3	.0	.4	.0	.0	.0	.3	.3	.0	.0	1.0	
X_1X_6	.0	.0	.0	.0	.0	.4	.0	.0	.0	.4	.0	.0	.0	.0	.0	.0	.0	.0	.0	.0	.0	1.0
X_2X_6	.0	.0	.0	.0	.0	.0	.0	.0	.0	.0	.0	.0	.0	.0	.5	.0	.0	.0	.0	.0	.0	.0	1.0
X_3X_6	.3	.0	.0	.0	.0	.0	.0	.0	.0	.3	.0	.0	.0	.0	.3	.0	.0	.0	.0	.0	.0	.0	1.0
X_4X_6	.4	.0	.0	.0	.0	.4	.0	.0	.0	.0	.0	.0	.0	.0	.0	.0	.0	.0	.0	.0	.0	.0	1.0
X_5X_6	.0	.0	.4	.0	.0	.4	.0	.0	.0	.0	.0	.0	.0	.0	.0	.0	.0	.0	.0	.0	.0	.0	.0	1.0
X_6^2	.0	-.1	.0	.0	-.3	.0	.0	.0	.3	.0	.0	.0	.0	-.1	.0	.0	.0	.0	.0	-.1	.0	.0	.0	.0	.0	1.0

X_1	X_2	X_2^2	X_1X_3	X_3^2	X_1X_4	X_3X_4	X_5	X_2X_5	X_4X_5	X_6	X_2X_6	X_4X_6	X_6^2									
X_1^2	X_1X_2	X_3	X_2X_3	X_4	X_2X_4	X_4^2	X_1X_5	X_3X_5	X_5^2	X_1X_6	X_3X_6	X_5X_6										

warning : correlations greater or equal to 0.3 are significant at 90% level of confidence or more according to the t-test (values in bold characters).

B) Third order polynomial (cubic model)

i) 2 independent parameters X_1, X_2

response function :

$$y = a_1+a_2X_1+a_3X_1^2+a_4X_1^3+a_5X_2+a_6X_1X_2+a_7X_2^2+a_8X_2X_1^2+a_9X_1X_2^2+a_{10}X_2^3$$

number of model coefficients : 10

design : 5-levels fractional factorial, "p" denotes the intermediate level between levels 0 and + while "m" is the intermediate level between levels 0 and -.

Run #	X_1	X_2
Average	0.0	
Variance	0.707107	
1	p	p
2	p	m
3	m	p
4	m	m
5	+	0
6	-	0
7	0	+
8	0	-
9	+	+
10	+	-
11	-	+
12	-	-
13	0	0
14	0	0
15	0	0

correlation matrix :

X_1	1.00								
X_1^2	.00	1.00							
X_1^3	.96	.00	1.00						
X_2	.00	.00	.00	1.00					
X_1X_2	.00	.00	.00	.00	1.00				
X_2^2	.00	.33	.00	.00	.00	1.00			
$X_2X_1^2$	.00	.00	.00	.80	.00	.00	1.00		
$X_1X_2^2$	.80	.00	.82	.00	.00	.00	.00	1.00	
X_2^3	.00	.00	.00	.96	.00	.00	.82	.00	1.00
	X_1	X_1^2	X_1^3	X_2	X_1X_2	X_2^2	$X_2X_1^2$	$X_1X_2^2$	X_2^3

warning : correlations greater or equal to 0.80 are significant at 99.995% level of confidence or more according to the t-test (values in bold characters).

ii) 3 independent parameters X_1, X_2, X_3

response function :

$$y = a_1 + a_2X_1 + a_3X_1^2 + a_4X_1^3 + a_5X_2 + a_6X_1X_2 + a_7X_2^2 + a_8X_2X_1^2 + a_9X_1X_2^2 + a_{10}X_2^3 + a_{11}X_3 + a_{12}X_1X_3 + a_{13}X_2X_3 + a_{14}X_3^2 + a_{15}X_3X_1^2 + a_{16}X_1X_3^2 + a_{17}X_3X_2^2 + a_{18}X_2X_3^2 + a_{19}X_1X_2X_3 + a_{20}X_3^3$$

number of model coefficients : 20

design : 5-levels nested FCC external cube with +,- levels and Box-Behnken internal cube with p,m levels. As before +,- and p,m are equally spaced from the center point.

Run #	X_1	X_2	X_3
Average	0.0		
Variance	0.654654		
1	p	p	0
2	p	m	0
3	m	p	0
4	m	m	0
5	p	0	p
6	p	0	m
7	m	0	p
8	m	0	m
9	0	p	p
10	0	p	m
11	0	m	p
12	0	m	m

Run #	X_1	X_2	X_3
13	+	+	+
14	+	-	+
15	+	+	-
16	+	-	-
17	-	+	+
18	-	-	+
19	-	+	-
20	-	-	-
21	0	0	+
22	0	0	-
23	-	0	0
24	+	0	0
25	0	-	0
26	0	+	0
27	0	0	0
28	0	0	0
29	0	0	0

correlation matrix :

X_1	1.00																		
X_1^2	0.00	1.00																	
X_1^3	.95	0.00	1.00																
X_2	0.00	0.00	0.00	1.00															
X_1X_2	0.00	0.00	0.00	0.00	1.00														
X_2^2	0.00	.59	0.00	0.00	0.00	1.00													
$X_2X_1^2$	0.00	0.00	0.00	.84	0.00	0.00	1.00												
$X_1X_2^2$	.84	0.00	.89	0.00	0.00	0.00	0.00	1.00											
X_2^3	0.00	0.00	0.00	.95	0.00	0.00	.89	0.00	1.00										
X_3	0.00	0.00	0.00	0.00	0.00	0.00	0.00	0.00	0.00	1.00									
X_1X_3	0.00	0.00	0.00	0.00	0.00	0.00	0.00	0.00	0.00	0.00	1.00								
X_2X_3	0.00	0.00	0.00	0.00	0.00	0.00	0.00	0.00	0.00	0.00	0.00	1.00							
X_3^2	0.00	.59	0.00	0.00	0.00	.59	0.00	0.00	0.00	0.00	0.00	0.00	1.00						
$X_3X_1^2$	0.00	0.00	0.00	0.00	0.00	0.00	0.00	0.00	0.00	.84	0.00	0.00	0.00	1.00					
$X_1X_3^2$	.84	0.00	.89	0.00	0.00	0.00	0.00	.99	0.00	0.00	0.00	0.00	0.00	0.00	1.00				
$X_3X_2^2$	0.00	0.00	0.00	0.00	0.00	0.00	0.00	0.00	0.00	.84	0.00	0.00	0.00	.99	0.00	1.00			
$X_2X_3^2$	0.00	0.00	0.00	.84	0.00	0.00	.99	0.00	.89	0.00	0.00	0.00	0.00	0.00	0.00	0.00	1.00		
$X_1X_2X_3$	0.00	0.00	0.00	0.00	0.00	0.00	0.00	0.00	0.00	0.00	0.00	0.00	0.00	0.00	0.00	0.00	0.00	1.00	
X_3^3	0.00	0.00	0.00	0.00	0.00	0.00	0.00	0.00	0.00	.95	0.00	0.00	0.00	.89	0.00	.89	0.00	0.00	1.00

X_1 X_1^3 X_1X_2 $X_2X_1^2$ X_2^3 X_1X_3 X_3^2 $X_1X_3^2$ $X_2X_3^2$ X_3^3
X_1^2 X_2 X_2^2 $X_1X_2^2$ X_3 X_2X_3 $X_3X_1^2$ $X_3X_2^2$ $X_1X_2X_3$

warning : correlations greater or equal to 0.59 are significant at 99.995% level of confidence or more according to the t-test (values in bold characters).

4) Experimental procedure

i) Synthesis

To begin with, determine your objectives. Previous observations or analyses of other kinds should tell you what process parameters are to be kept in your model. The choice of those parameters may also depend on the type of responses you are studying. Once all process parameters and responses have been selected, determine the region of your parameter space to be modeled. Let us now assume that the center point has been determined. If you know what parameter has the most important impact on the response, you may want to measure the response(s) for 4 values of this parameter, fixing the others at their standard value (center value). Then proceed as described in the second paragraph under heading ' iii) Parameter range'. As far as major trends in the response(s) are concerned, you can widen a parameter's range beyond the limit where precise predictions are required. In the latter case, a quadratic fit on a reduced region might be more suitable than a cubic fit which tends sometimes to bend the surface into a S-shape.

ii) Experiment

The process parameters, their range, the response(s) and the model are now determined. Choose the corresponding design as given in the preceding paragraph. Convert the design's levels into the parameter actual values (units used on your equipment) and write the flow of your experiment.

Example :

Lam#A July 18, 1986

Oxide etching, blank 5" p-type (100) wafers

Total flow [CF_4] + [He] = 200 sccm

Gap = 0.35 cm

temperature 20.0 ^{o}C

Etching time 1.0 min unless otherwise specified

Wafer #	Power (Watt)	Pressure (Torr)	He flow (sccm)	CF_4 flow (sccm)	comments
1	800	1.0	100	100	
2	800	1.0	(50)	(150)	
3	(900)	1.0	50	150	30 SEC !
:	:	:	:	:	
	etc...				

Values that change from one run to another are in brackets. All inputs are clearly displayed. Even though the total flow is fixed, both [CF_4] and [He] flows are given.

iii) Processing of data : <u>LSIFIT USER-GUIDE</u>

a) Input file :

The experiment being done, it is time to fit the collected data. First of all an input data file that LSIFIT will read during its execution must be created. Illustrating The input file format with our example of plasma etching, it might appear as follows. On the first line appears the number of independent parameters, 3 in our case, then on the second line write the number of dependent parameters or responses, 2 for us, on the third line write the number of experimental runs, 15 for a Box-Behnken design. Next, type in the parameter's and response's descriptors in no more than 20 characters. On each of the following lines declare for each run the corresponding value of the independent parameters followed by the response

values. The last number to appear on a data point line is the weight associated to that measurement. A weight value must be specified even when not applicable. The first three numbers must be integers. Data points must be real numbers. Example :

LSIFIT input file

```
3
2
15
Power (Kwatts)
Pressure (Torr)
Fraction of helium
Etch rate (µm/min)
Uniformity/100
.9      2.      .25     .5408       .07256      .02201
.9      2.      .25     .5401       .08098      .02661
.9      2.      .25     .5410       .1109       .04112
.8      1.      .25     .0775       1.025       .08338
.8      2.      0.      .4158       .1104       .03652
.8      2.      .5      .6217       .02487      .009939
.8      3.      .25     .2377       .0442       .007563
.9      1.      0.      .6556       .05051      .02455
.9      1.      .5      .0020       1.141       .0028
.9      3.      0.      .1640       .1225       .01416
.9      3.      .5      .4455       .05748      .02048
1.      1.      .25     .1681       1.00        .1219
1.      2.      0.      .4139       .07617      .02331
1.      2.      .5      .7010       .03087      .01134
1.      3.      .25     .2369       .2405       .00387
```

b) Reponse formatting :

In order to save computer time responses should be expressed in units such that their magnitude is less than 100. Also, MAPPING displays only response values which magnitudes are below 99.95 .

c) Running LSIFIT :

At the beginning of a run, your screen appears as shown below (user's entries are displayed in bold characters for the sake of clarity) :

```
- LSIFIT.FOR BEGIN
- EXPERIMENT :                LAM#A  OXIDE
```

The run can be identified by a 16 characters character string. This entry does not affect the fit and can be skipped by hitting the carriage return at the first place. Next entry is the input file name which is partly displayed on your screen too. All numbers are read using the star (*) format :

```
- DATE  15/10/86
- INPUT FILENAME : LAM.SCC
X( 1) <= Power (Kwatts)
X( 2) <= Pressure (Torr)
```

X(3) <= Fraction of helium
Y(1) <= Etch rate (μm/min)
Y(2) <= Uniformity/100

X(1)	X(2)	X(3)	Y(1)	Y(2)	
.9000	2.0000	.2500	.5408	.0726	.0220
.9000	2.0000	.2500	.5401	.0810	.0266
.9000	2.0000	.2500	.5410	.1109	.0411
.8000	1.0000	.2500	.0775	1.0250	.0834
.8000	2.0000	.0000	.4158	.1104	.0365
.8000	2.0000	.5000	.6217	.0249	.0099
.8000	3.0000	.2500	.2377	.0442	.0076
.9000	1.0000	.0000	.6556	.0505	.0245
.9000	1.0000	.5000	.0020	1.1410	.0028
.9000	3.0000	.0000	.1640	.1225	.0142
.9000	3.0000	.5000	.4455	.0575	.0205
1.0000	1.0000	.2500	.1681	1.0000	.1219
1.0000	2.0000	.0000	.4139	.0762	.0233
1.0000	2.0000	.5000	.7010	.0309	.0113
1.0000	3.0000	.2500	.2369	.2405	.0039

- SUBROUTINE CORR IN PROGRESS... TERMINATED

The correlation matrix is not displayed on the screen. It will be explained in subsection e). Then if there are more than one response the identification number of the response to be fitted must be specified (number 1 corresponds to the first response in the data file etc)

- ENTER NUMBER OF DEPENDENT PARAMETER : 1

In this example the etch rate will be fitted. Now enter the order of the polynomial (options are 0,1,2,3) . A linear fit is of the 1^{st} order, a quadratic fit is of the 2^{nd} order while a cubic fit is of the 3^{rd} order. Polynomial functions of the 1^{st} and 2^{nd} order are automatically generated by the program for any number of independent parameters. 3^{rd} order polynomial functions for 2 and 3 parameters are also handled by the program. Any other functions can be defined using option 0. To use option 0 the customized function must be coded in FUNCTION FUNCTN of the source code as it will be explained later. If option 0 is selected LSIFIT requires the number of model coefficients.

- ENTER ORDER OF POLYNOMIAL : 2

Next, three weighting modes are proposed (options 1,0,-1). For explanations refer to section 2)v).

- ENTER WEIGHTING MODE :
(+1=INSTRUMENTAL, 0=NO WEIGHTING, -1=STATISTICAL) 0

Next option (Y,N) allows you to assign the model coefficients a first guess value by entering Y. If you choose this option you will then have to enter each model coefficient value. Therefore your normal entry will be N. In that case LSIFIT assigns all model coefficients a value of 1.0 .

- INPUT GUESSES ? (YES/NO) : N
- ALL COEFFICIENTS SET TO 1.0000E+00
- ENTER RELATIVE ACCURACY REQUIRED : 1.E-5

When the relative variation of chi-square becomes smaller than the relative accuracy, least-squares fit iterations are terminated. 10^{-5} is a typical value. For more information refer to the end of section 2)iv). The iteration loop will be terminated if the number of iterations exceeds a user-specified limit no matter what the chi-square value.

- ENTER MAXIMUM NUMBER OF ITERATIONS : 20

- LEAST-SQUARES FIT IN PROGRESS . . . TERMINATED
- 3 ITERATIONS

- ELAPSED TIME : 13 SEC

- MODEL COEFFICIENTS	STD ERROR	F-RATIO
.540633 = A(1) +/-	.082644	42.8
.015799 = A(2) +/-	.038371	.2
-.039788 = A(3) +/-	.042638	.9
.017093 = A(4) +/-	.038371	.2
-.013057 = A(5) +/-	.041021	.1
-.166259 = A(6) +/-	.042638	15.2
.011424 = A(7) +/-	.038371	.1
.011600 = A(8) +/-	.041021	.1
.133586 = A(9) +/-	.041021	10.6
.038341 = A(10) +/-	.042638	.8

- CHI SQUARE = 2.0633E-02

In the case of a second order fit, the program will search for an extremum in the selected response function and within the window. Since a quadratic function can only have either a maximum or a minimum, it is easy to see on the maps whether one has one or the other. This feature is especially useful when one has more than 3 parameters (in which case only quadratic functions are used). If there is an extremum, the coordinates of that point will be displayed, otherwise it will say :

- EXTREMUM IS NOT IN WINDOW

	DATA	RESIDUAL	FIT	RELATIVE RESIDUAL
1	.5408	-.0002	.5406	-.0003
2	.5401	.0005	.5406	.0010
3	.5410	-.0004	.5406	-.0007
4	.0775	.0362	.1137	.4669
5	.4158	.1066	.5224	.2563
6	.6217	-.1097	.5120	-.1764

7	.2377	-.0331	.2046	-.1392
8	.6556	-.1428	.5128	-.2178
9	.0020	.0735	.0755	36.7499
10	.1640	-.0735	.0905	-.4482
11	.4455	.1428	.5883	.3205
12	.1681	.0331	.2012	.1968
13	.4139	.1097	.5236	.2650
14	.7010	-.1066	.5944	-.1521
15	.2369	-.0362	.2007	-.1528

- LEAST-SQUARES REGRESSION ANALYSIS :

SUM OF SOURCE	DEGREES OF SQUARES	MEAN FREEDOM	SQUARE	F-RATIO
REGRESSION	.58480	9	.06498	3.1
RESIDUAL	.10317	5	.02063	
PURE ERROR	0.00000	2	0.00000	
LACK OF FIT	.10317	3	.03439	*****
TOTAL	.68797	14	.04914	

ADJUSTED R2 : .58
CALCULATED REGRESSION = .58480 AND TOTAL = .68797

If you intend to map out the fit answer yes (Y) to this request :

- SAVE FIT IN MAP.IN (Y/N) ? Y

- ENTER 'END' TO STOP
END
- END PROGRAM LSIFIT.

As a final option you may repeat another fit with the same data file by entering anything but END (caps import). If you do so, your next entry consists of choosing what response must be fitted as demonstrated above under "- ENTER NUMBER OF DEPENDENT PARAMETER :". LSIFIT output values are displayed using the F format therefore if a calculated value is too large for its allocated format stars are printed in place of digits.

d) LSIFIT output files :

LSIFIT creates an output file containing basically what appears on the screen plus the correlation matrix. The output file status is 'UNKNOWN'. Computers such as Macintosh™ or Microvax™ give the output file a default name ('00000000' on Macintosh, 'fort.4' on Microvax).

If you have saved one or more fits during the execution of LSIFIT, you have also created an output file named MAP.IN which contains almost all the information that MAPPING.F needs for mapping out contour plots. In order to actually use this file as MAPPING.F input data, you must complete it according to the example given under iv) b). Typically, you will have to specify the number of model coefficients on the second line and the number of responses. Depending on the response function used in MAPPING.F you may have to insert a few zeros between the model coefficients as shown in the example.

e) Correlation matrix :

The correlation matrix includes intercorrelation coefficients between model terms, correlation coefficients between responses and model terms as well as intercorrelation coefficients between responses. If there are less than 4 independent parameters, the cubic model terms are also included, otherwise only second order terms are displayed.

f) Customized model function :

Model functions other than standard polynomial functions can be defined in FUNCTION FUNCTN. A customized function is reached using option 0 when the order of polynomial is required. To define your own function assign the variable FU the fortran expression of your function. The model coefficients are stored in the array A(K) while the independent variables are in X(H,I) where H identify the H^{th} process parameter and I the I^{th} experimental observation. The customized function is declared in the ELSE branch of the most nested IF statement of function FUNCTN, after label 20. In the example below it appears in bold characters.

LSIFIT's FUNCTION FUNCTN :

```
      FUNCTION FUNCTN(X,I,A,NPAR,NOD)
      DIMENSION  X(28,100),A(28)
      IF (NOD.EQ.3) THEN
        FU=A(1)+A(2)*X(1,I)+A(3)*X(1,I)**2+
     1       A(4)*X(1,I)**3+
     1       A(5)*X(2,I)+A(6)*X(1,I)*X(2,I)+A(7)*X(2,I)**2+
     1       A(8)*X(2,I)*X(1,I)**2+A(9)*X(1,I)*X(2,I)**2+
     1       A(10)*X(2,I)**3+A(11)*X(3,I)+A(12)*X(1,I)*X(3,I)+
     1       A(13)*X(2,I)*X(3,I)+A(14)*X(3,I)**2+A(15)*X(3,I)*
     1       X(1,I)**2+A(16)*X(1,I)*X(3,I)**2+A(17)*X(3,I)*
     1       X(2,I)**2+A(18)*X(2,I)*X(3,I)**2+
     1       A(19)*X(1,I)*X(2,I)*X(3,I)+A(20)*X(3,I)**3
         ELSE
       IF (NOD.EQ.2) THEN
        FU=A(1)
        DO 10 K=1,NPAR
        DO 10 L=1,K+1
        IF (L.EQ.1) THEN
         XC=1.
        ELSE
          XC=X(L-1,I)
        END IF
          N=(K+1)*K/2+L
10      FU=FU+A(N)*X(K,I)*XC
       ELSE
        IF (NOD.EQ.1) THEN
         FU=A(1)
         DO 20 K=2,NPAR
20         FU=FU+A(K)*X(K,I)
       ELSE
                FU=A(1)+A(2)*X(1,I)*X(2,I)+A(3)*X(2,I)**2+
     1       A(4)*X(2,I)**3+A(5)*X(1,I)*X(3,I)+A(6)*X(3,I)*X(2,I)+
     1       A(7)*X(3,I)**3
```

```
      END IF
   END IF
  END IF
  FUNCTN=FU
  END
```

g) Dimensions of vectors and matrices :

LSIFIT's original code accepts up to 100 data points of up to 28 independent parameters X(28,100) and 10 responses Y(10,100). Up to 38 correlation matrix terms can be defined T(38,100) while the number of model coefficients is limited to 28 A(28). Those arrays can be expanded or reduced by modifying the fortran DIMENSION statements at the beginning of the main program block as well as at the beginning of each subroutine or function. Of course expanding those arrays implies expanding similarly the other arrays. For instance if you need 12 responses and 29 model coefficients replace all occurences of 10 by 12 and all occurences of 28 by 29.

h) CPU times :

Running a fit with designed parameters values (Box-Behnken or so) is faster than with non designed values. Typically, for about 20 model coefficients and 30 data points, the iteration loops take about one minute (order of magnitude).

j) Formats :

output	label	block	format
Input file	611	main	E9.3
Normalization-standardization coefficients	136	main	E10.3
Correlation matrix	110	CORR	F3.1
Model coefficients	7777	main	E11.4
Partial F-ratios	7777	main	F6.1
Data, residuals, fit, relative residuals	9330	STAT	E10.3
Regression sum of square and mean square	90	STAT	F9.4
F-ratio	90	STAT	F7.1
Residual sum of square and mean square	9311	STAT	F9.4
Pure error sum of square and mean square	92	STAT	F9.4
Lack of fit sum of square and mean square	94	STAT	F9.4
Lack of fit to pure error F-ratio	94	STAT	F5.1
Total sum of square and mean square	93	STAT	F9.4
Adjusted R^2	95	STAT	F4.2
Calculated regression and total sum of square	100	STAT	F9.4

iv) Contour plots : <u>MAPPING USER-GUIDE</u>

a) Introduction :

Fortran program MAPPING displays 2-dimensional contour plots of the response surface obtained with LSIFIT. MAPPING is not limited to the drawing of polynomial functions. It can draw 2-D contour plots of any function. When LSIFIT and MAPPING are used together, LSIFIT outputs serve as MAPPING inputs. MAPPING converts automatically the parameters X_k in actual units into their transformed value X_k. Thus, the user does not have to worry about units. Up to 10 response functions can be seen simultaneously versus 2 parameters. Parameter ranges and fixed parameter values are defined interactively. As MAPPING deals

with Macintosh's toolbox it is not possible to implement it on other computers.

b) MAPPING input file :

Type the number of independent parameters on the first line and the number of model coefficients on the second line. On the following lines type the parameter's names with no more than 20 characters. The first character string corresponds to the first parameter in LSIFIT etc... Then copy from LSIFIT's output file the minimum, maximum average and variance values associated with the transformation of each parameter. Next declare the number of responses that a single run can handle. Then type the first response's name (20 characters maximum) followed by the model coefficients values A(1,K). Repeat this operation as many times as there are responses. See the example given in the next page.

c) Model function :

MAPPING's model function is defined in function POLY. Assign the variable FU with the fortran expression of your model function. The H^{th} process parameter value is stored in the X(H) vector while model coefficients are in A(J,K), where J refer to the J^{th} response and K is the model term index. If you wish to define different functions for each response you may program a conditional statement using the value stored in variable ND. ND identifies what response is currently selected.

d) Tricks :

- Incomplete model : it is not always necessary to change the model function every time you change of model. For instance if you are dealing with 3 process parameters you may define a third order polynomial function. Thus you can plot linear, quadratic or cubic functions without having to actually modify MAPPING's model function. Just assign the value 0.0 to those coefficients that are not part of the model as shown in the example below for a quadratic fit using a cubic polynomial.
- Non normalized-standardized parameters : assign the maximum a value 1.0, the minimum a value -1.0, the variances the value 1.0 and the averages the value 0.0 .
- Responses with different model functions and uneven number of model coefficients : declare the highest number of model coefficients and assign the value 0.0 to model coefficients which are not used in their corresponding model.
- No model coefficients : declare 0 model coefficient. Type only the response descriptor(s).

e) Dimension statements :

Make sure that MAPPING array dimensions can handle your variables. Model coefficient dimension statements appear in the main program block A(10,28), in subroutines PLOT2, DRAWING, OMBRE and function POLY. Normalization-standardization coefficients are stored in R(28,4) declared in the main program block and in subroutine PLOT2. Parameter values are held in the XX(28) array declared in subroutines PLOT2, DRAWING and OMBRE. In function POLY they are stored in the X(28) array. You may change values in bold characters.

```
MAPPING input file :
3
20
Power (KWatt)
Pressure (Torr)
Helium flow (%)
0.8     1.0     1.0  0.0
1.0     3.0     1.0  0.0
0.0     0.5     1.0  0.0
2
Etch rate BOX(µm/mn)
 5.4063E-01 = A( 1) +/-  8.1650E-07
 2.0900E-02 = A( 2) +/-  1.1180E-06
-6.9629E-02 = A( 3) +/-  1.1180E-06
 0.
 2.2612E-02 = A( 4) +/-  1.1180E-06
-2.2850E-02 = A( 5) +/-  1.5811E-06
-2.9095E-01 = A( 6) +/-  1.1180E-06
 0.
 0.
 0.
 1.5113E-02 = A( 7) +/-  1.1180E-06
 2.0300E-02 = A( 8) +/-  1.5811E-06
 2.3377E-01 = A( 9) +/-  1.5811E-06
 6.7096E-02 = A(10) +/-  1.1180E-06
 0.
 0.
 0.
 0.
 0.
 0.
Uniformity BOX (%)
 8.8147E-02 = A( 1) +/-  5.7534E-01
 1.7884E-02 = A( 2) +/-  3.5338E-01
 1.0349E-01 = A( 3) +/-  5.1945E-01
 0.
-3.4398E-01 = A( 4) +/-  3.5338E-01
 5.5325E-02 = A( 5) +/-  4.9975E-01
 3.8579E-01 = A( 6) +/-  5.1945E-01
 0.
 0.
 0.
 1.1183E-01 = A( 7) +/-  3.5338E-01
 1.0058E-02 = A( 8) +/-  4.9975E-01
-2.8888E-01 = A( 9) +/-  4.9975E-01
-1.3106E-01 = A(10) +/-  5.1945E-01
 0.
 0.
 0.
 0.
 0.
 0.
```

f) Running MAPPING :

Use of MAPPING is pretty straightforward and does not require much explanations. First of all enter the input file name then follow the instructions given in the upper left rectangle.

- Define graph size : press down the mouse where you want to have the upper left corner of your graphic then drag the mouse in the down position. The size of the drawing window is displayed in pixels in the upper right rectangle. Make sure to manage enough room around your drawing window to allow text and labels to be typed in.
- Define labeling : press down the mouse and drag the tick mark where desired. The difference between the parameter's value at the tick mark and at the origin is displayed in the upper right rectangle. Tick marks and labeling will appear regularly spaced while the mouse is released. If the mouse is released at the left or at the right, respectively above or below, the horizontal, respectively vertical, axis, tick marks and labels are not recorded.

The response to be plotted is selected by clicking the mouse in the upper left rectangle. When the desired response appears ratify your choice by clicking OK. Then choose the resolution. Low resolution plots (response tested every 3 pixels) take less than one minute to be completed. Standard resolution (response tested every other pixel) takes between 1 and 5 minutes depending on the size of the drawing window. High resolution drawing (response tested at every pixel) takes between 5 and 15 minutes. A typical output is illustrated below :

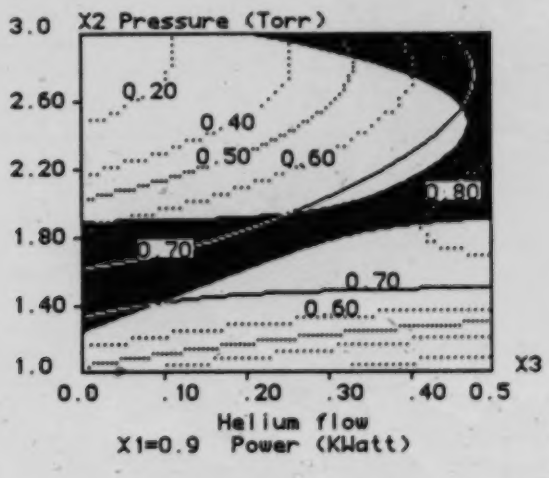

FIG. 1) Typical output from MAPPING.

This graphic shows etch rate contour plots as a function of helium flow and pressure while the power is fixed at 900 watts. Contours have been labeled using option LEVELS. Response contour interval must be assigned when "DY =" appears in the upper left rectangle. The contour labeled 0.50 (µm/min) is in standard resolution, contours labeled 0.70 (µm/min) are in high resolution while remaining contours are in low resolution. The area where the uniformity is below 5% (0.05) has been blackened. The resolution of a highlighted area depends on the previous resolution used during plotting. It may be changed by requiring a plot in another resolution and by cancelling the calculation. Once a plot is completed you have to click the mouse where you want the contour plot title to be written. Click it above the frame if you do not want any title.

Then come the following options : NEW MAP, ADD ON, LEVELS,MORE, SHADE, CLEAR, QUIT. NEW MAP clears the screen. ADD ON allows you to draw in the current window on top of what has been already drawn. LEVELS is used to label contours. MORE starts a new drawing

window. SHADE allows to highlight area where the selected response in comprised within a defined range. CLEAR clears the drawing window only. Clicking QUIT gets you out of the LEVELS mode or the drawing mode when applicable. Otherwise it gives the run an end.

g) Printing results :
Pressing simultaneously BUTTERFLY KEY-SHIFT KEY-4 makes a hard copy of the screen.

h) Saving results :
Pressing simultaneously BUTTERFLY KEY-SHIFT KEY-3 creates a Macpaint document containing the current screen. This option has been used for pasting graphics in this text.

j) Useful features :
The LEVELS mode is useful for checking response values as a function of two parameters. When you click the mouse on the response surface, the horizontal and vertical coordinates in actual units, as well as the response are displayed in the upper rectangles. As long as the mouse is down the response value will not be printed on your drawing. This procedure allows you to check predicted response values for given operating conditions. If you release the mouse button inside of the drawing window, it will print the response value at the point where is the dot of that value if its magnitude is below 9.995. Response values of magnitude greater than that correspond on the plot to the pixel which is at the bottom of, and between the first two digits.To avoid printing drag the mouse, button down, out of the currrent window and then release it.

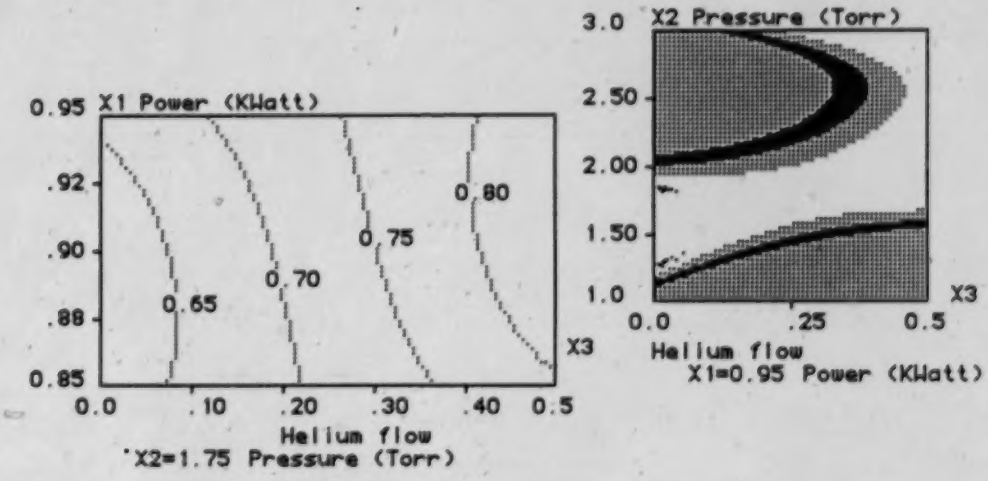

FIG. 2) Other MAPPING's outputs.

5) SIMPLEX, an optimization technique

The Response Surface Methodology is not appropriate for searching of an optimum process when the experimenter has no idea about where is the optimum in the parameter space. Optimum does not necessarily mean maximum but rather a set of operating conditions for which one or several responses meet the experimenter's specifications referred to as the target. SIMPLEX is a designed experimental method that allows the user to reach the target no matter where he starts almost. The basic principle is the following. To begin with, determine

your target. For instance regarding our example of plasma etching, we might target 6000 Å/min with uniformity less than 5% and selectivity oxide to polysilicon 8:1.

The method consists of maximizing, or minimizing, a so called response function RF, which accounts for all responses. The target is the value taken by the RF when responses meet the specifications. For the oxide etching example the RF might be :

$$RF = (1-e^{-ER/6000}) + (1-e^{-SL/8}) + 2\cdot e^{-UN/5}$$

where ER, SL and UN represent the measured oxide etch rate, the selectivity oxide to poly and the uniformity. The RF target value is therefore 2 and it is a maxima. Responses can be weighted depending on their importance. In the example the uniformity is affected a weight of 2.

Assuming that the process depends on N independent parameters, the experimenter now has to calculate the RF for N+1 different combinations of N parameters called a SIMPLEX. The worse RF, which is the one which value is the farthest from the RF target value, is rejected. The coordinates (N in the parameter space) of the corresponding point are then reverted with respect to the other points. The RF is measured and calculated at the reverted point and so on.

As we said the SIMPLEX requires initially N+1 experimental points, but then only one point has to be measured per new SIMPLEX. To illustrate this method let us assume that a single response which depends on two parameters must be maximized. It is easy to imagine the SIMPLEX path on a contour plot :

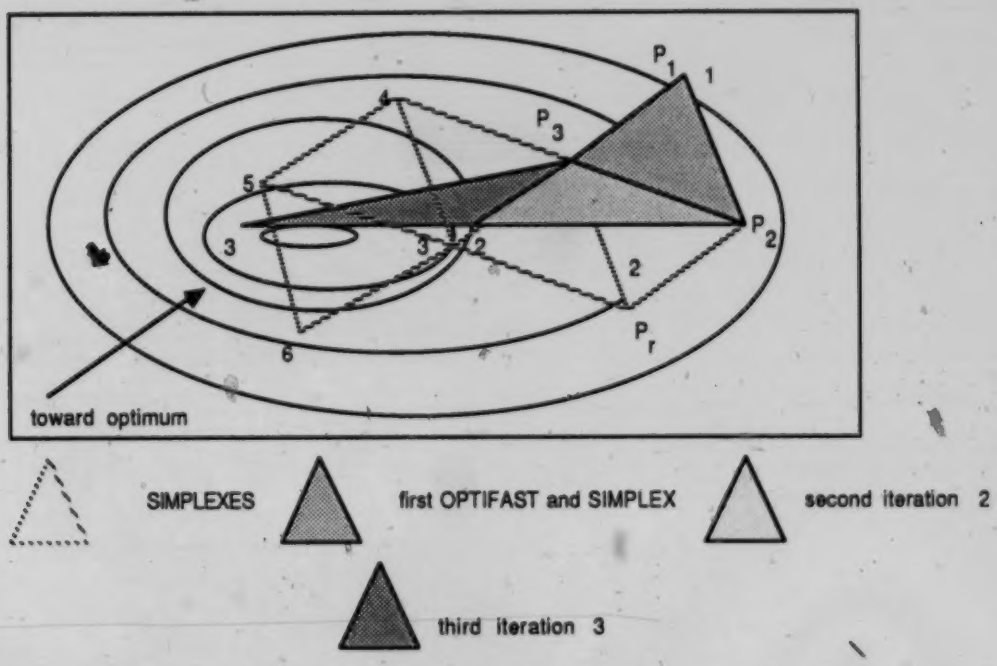

FIG. 3) SIIMPLEX search toward the optimum. OPTIFAST consists of flipping the worse point with respect to the best, it is sometimes faster than SIIMPLEX, when far from the optimum.

The first SIMPLEX has 2+1=3 points, it is a triangle numbered 1. The worse response is at

triangle 1 top corner. This point is reverted in P_r etc.

The coordinates of the starting SIMPLEX are determined with respect to the center point with coordinates $(c_1,c_2,...,c_N)$ as follows :

Point #	X_1	X_2	X_3	X_N
1	$-a_1$	$-a_2$	$-a_3$	$-a_N$
2	a_1	$-a_2$	$-a_3$	$-a_N$
3	0	$2a_2$	$-a_3$	$-a_N$
4	0	0	$3a_3$	$-a_N$
:	:	:	:	:
N+1	0	0	0	$N\cdot a_N$

Where a_i i=1,...,N is parameter X_i 's increment. For more details see reference [4]. Let us call P_j the N-dimensional vector of coordinates $(X_{1j},X_{2j},...,X_{Nj})$. In our illustration : $RF(P_1)< RF(P_2)< RF(P_3)$ therefore P_1 is rejected and reverted with respect to the centroid : $P' = (1/N)(P_1+ P_2+ P_3)$ where + is the standard summation of vectors. The coordinates of the reverted point P_r are given by : $P_r = P' + \beta(P' - P_1)$, where β is a scaling factor.

At the beginning of each step β=1, if the new response is not better than the worse do $\beta=\beta-1/4$ until $\beta= -1$. If a better reponse has not been obtained yet, leave the worse point at his original place and try to revert the second worse point and so on.

A set of rules takes care of the situations where those simple operations fail to work properly. It is not the purpose of this document to expose the theory for searching of an optimum therefore you are invited to read references [4,5] if you want to use this method.

Clearly it would be more efficient to revert the worse RF along the steepest ascent rather than flipping it over the centroid. Such procedure is described in reference [4].

6) Remarks

Here come a couple of observations about RSM based on the characterization of plasma etching processes. RSM is a statistical method, therefore one must be very careful in drawing conclusions based on contour plots.

Statistical criteria for judging the quality of a fit do not tell you if the fit is physically significant. This ultimate decision requires the experience and knowledge of the experimenter.

For example, let us consider a 5-parameter process : X_1 = power, X_2 = pressure X_3 = helium flow rate, X_4 = C_2F_6 flow rate and X_5 = gap. A designed was used (not the one given in this document) in which the model term X_1^2 was highly correlated to X_4^2. The uniformity as a function of X_1 and X_4 is shown in Fig. 4. This type of symmetrical contour plot may be the result of significant correlations between model terms. Such a contour plot should not be trusted unless experimental proof is made that the response really behaves like this.

The C_2F_6 process has been characterized with 25 measurements. Fits of etch rate, uniformity and selectivity oxide to poly were all statistically good, yet subsequent measurements along various sections of the parameter space proved bad predictions even in terms of major trends. Those sections showing that a second order fit could suit well, one concludes that either the process is unstable or not enough data points have been collected.

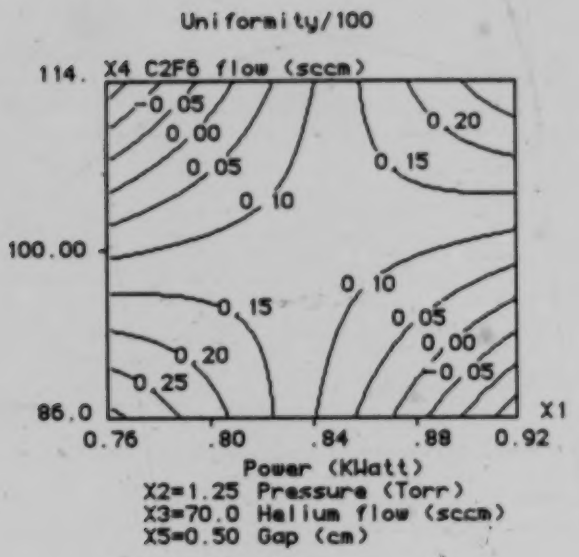

FIG. 4) Uniformity of etch.

Fig. 4 shows regions of negative uniformities but according to its definition, the uniformity is a positive quantity. This is a common problem when the response to be optimized is close to zero. If the uniformity does not take values below -0.05 (-5%) say, the fit may eventually still be regarded as significant as far as trends are concerned. However, when the uniformity takes large negative values as shown in Fig. 4, it indicates a lack of experimental points. One can also argue that the definition of the uniformity:
U=100(maximum etch rate - minimum etch rate)/(maximum etch rate + mimimum etch rate), is not suitable for RSM since it has a discontinuity when maximum and minimum etch rates are zero.

Practically it is very unlikely to happen, but what usually happens with non-etching recipes is that negative minimum etch rates result from differentiation of film thickness before and after etch. Consequently, very high uniformities (>100%) are often associated with slow-etching or non-etching recipes. Furthermore, those uniformity values may vary greatly from one run to another. Since it is easier reducing X^2 by approaching values of large magnitude, non-etching processes may wreck a uniformity least-squares fit. For example a uniformity of 15.0 (1500%) may take a fitted value of 12.0 (1200%) while most of the other values lie between 0.05 (5%) and 0.20 (20%). Somehow, the surface must dip from 12.0 down to 0.05. One can imagine that nothing can then stop it dipping far below zero. In that case, one can assign the uniformity a value of 1.0 (100%). This is not an arbitrary method since it means that the variation of the etch rate across the wafer is of the same order as the etch rate itself.

A better way to overcome this problem is simply to fit the inverse of the uniformity.

The optimization of a process does nor necessarily consist of finding the maximum or the minimum of a single response function, sometimes several responses must meet certain specifications. Provided you have collected data on the responses to be optimized for the same experimental design, you can define a specification response function, in the way it is done with the SIMPLEX method, fit it with a quadratic surface and map it out. If you choose your

specification response function appropriately, that is in such a way as the target corresponds to a maximum, LSIFIT will tell you whether a maximum exists in the window and where it is. The specification response function is a mathematical combination of observed responses. For example, let us say that our target is to reach 5000 Å/min etch rate with less than 5% uniformity of etch. Let us define the specification response function as follows :

$$Spec = \exp(-(ER-5000)^2/2\cdot10^6) \cdot \exp(-(UN-2)^2/50)$$

Since we have requirements on the etch rate ER AND the uniformity UN, the PRODUCT of two gaussians is used. Spec equals 1.0 (maximum) when ER=5000 Å/min AND UN=2%. Note that Spec decreases too if ER is much larger or much smaller than 5000 Å/min, or when UN is far from 2% both ways. For this reason 2% instead of 5% has been used in Spec. The coefficients of the gaussians must be chosen adequately depending on what weight you want to give to each response. If you want to improve a response OR another, use a SUM of gaussians instead of a product.

7) Quick reference manual

i) - Create an input file for LSIFIT according to the example given in paragraph 4) iii) a).
- Do not forget to assign a weight even if you do not use it.
- The magnitudes of the parameter values should not exceed 999.95 to be compatible with MAPPING.
- The magnitudes of the response values should not exceed 99.95 to be compatible with MAPPING.

ii) In LSIFIT's code :
- Make sure the arrays are large enough to handle your data (see & 4) iii) g)).
- If you intend to use a customized model function, check function FUNCT (& 4) iii) f)).

iii) If you have modified LSIFIT's code, compile it.

iv) - Create an input file for MAPPING according to the example given in paragraph 4) iv) b) .
- Do not forget that the model coefficients are only valid for the transformation specified.
- Check the model function in function POLY (see 4) iv) c)).

v) If you have modified MAPPING's code, compile it.

vi) TROUBLES ?
With LSIFIT :
- stars instead of numbers in LSIFIT's outputs ====> check formats in & 4) iii) j).
- no partial F-ratios =====> use a larger relative accuracy on chi-square (& 4) iii) c)).
- overflow error ====>
  · your design may lead to divisions by zero in subroutine CURFIT.
  · the arrays are too small to handle your data.

With MAPPING :
- plot is going crazy ====>
  · check input file (see & 4) iv) b)).
  · check dimensions of arrays (see & 4) iv) e)).
  · check MAPPING's function POLY.
  · did you compile MAPPING ?
  · the drawing window is too large and you run out of memory.

Other problems ?

Call :

Dr. Roger Patrick, MS J201
LSI LOGIC Corp. 3115 Alfred St.
Santa Clara, CA
Tel : (408) 433-6261

Philippe Schoenborn
Department of Electrical Engineering
The University of Alberta
Edmonton, Alberta
Canada T6G 2E1
Tel : (403) 432-3914

8) Reference example

Here is a complete example taken from reference [6]. If you have modified the source code of a program and you have some doubts about your results, you may use it as a reference fit. If you want to map it out, make sure that the function POLY in MAPPING is adequate.

LSIFIT input file :

```
3
1
17
Power (Watts/cm2)
Pressure (Torr)
Fraction of CF3Cl
Etch rate (µm/min)
.315    .6   .865    .088    1.
.315    .6   .865    .081    1.
.315    .6   .865    .081    1.
.315    .6   .865    .094    1.
.315    .6   .865    .104    1.
.087    .3   .865    .039    1.
.715    .3   .865    .1      1.
.715    .9   .865    .356    1.
.315    .3   .738    .052    1.
.715    .6   .738    .217    1.
.315    .9   .738    .062    1.
.087    .6   .738    .045    1.
.315    .3   .956    .11     1.
.087    .6   .956    .042    1.
.315    .9   .956    .045    1.
.715    .6   .956    .392    1.
.087    .9   .865    .042    1.
```

LSIFIT output file '00000000' :

```
- LSIFIT.FOR BEGIN
- EXPERIMENT : REFERENCE
- DATE 07/01/87
- INPUT FILENAME :
 X( 1) <= Power (Watts/cm2)
 X( 2) <= Pressure (Torr)
 X( 3) <= Fraction of CF3Cl
 Y( 1) <= Etch rate (µm/min)

  X( 1)   X( 2)   X( 3)   Y( 1)
  .3150   .6000   .8650   .0880  1.0000
  .3150   .6000   .8650   .0810  1.0000
  .3150   .6000   .8650   .0810  1.0000
  .3150   .6000   .8650   .0940  1.0000
  .3150   .6000   .8650   .1040  1.0000
  .0870   .3000   .8650   .0390  1.0000
  .7150   .3000   .8650   .1000  1.0000
```

```
 .7150  .9000  .8650  .3560 1.0000
 .3150  .3000  .7380  .0520 1.0000
 .7150  .6000  .7380  .2170 1.0000
 .3150  .9000  .7380  .0620 1.0000
 .0870  .6000  .7380  .0450 1.0000
 .3150  .3000  .9560  .1100 1.0000
 .0870  .6000  .9560  .0420 1.0000
 .3150  .9000  .9560  .0450 1.0000
 .7150  .6000  .9560  .3920 1.0000
 .0870  .9000  .8650  .0420 1.0000

- MINIMUM   MAXIMUM    VARIANCE  AVERAGE PARAMETER
  .087000  .715000    .721011   -.144998 1
  .300000  .900000    .707107   0.000000 2
  .738000  .956000    .712193    .087426 3

- CORRELATION MATRIX :

 1.0
 0.0 1.0
0.0 0.0 1.0
 0.5  0.0 0.0 1.0
 0.0 0.0 0.0 0.0 1.0
0.0  0.0 0.0 0.0 0.0 1.0
0.0  0.0 0.0  0.1 0.0 0.0 1.0
0.0 0.0 0.0 0.0 0.0 0.0 0.0 1.0
0.0  0.0 -.3  0.1 0.0 0.0  0.1 0.0 1.0
1.0  0.0 0.0  0.6 0.0 0.0 0.0 0.0 0.0 1.0
0.0  0.7 0.0 0.0  0.4 0.0  0.0  0.1 0.0  0.0 1.0
 0.7  0.0 0.0  0.4 0.0  0.1 0.0  0.0 -.1  0.7  0.0 1.0
0.0 1.0  0.0 0.0 0.0 0.0  0.0 0.0  0.0  0.0  0.7 0.0 1.0
0.0  0.0  0.7 0.0 0.0  0.4  0.1 0.0 -.2 0.0  0.0 0.0 0.0 0.0 1.0
 0.7 0.0 0.0  0.4 0.0 -.3 -.1 0.0 0.0  0.7 0.0 0.0 0.0 -.1 1.0
 0.0 0.0  0.7  0.1 0.0 -.1 0.0 0.0 -.2 0.0 0.0 0.0 0.0 0.0 0.0 0.0 1.0
 0.0  0.7 0.0 0.0 -.1 0.0 0.0 -.3 0.0 0.0 0.0 0.0  0.7 0.0 0.0 0.0 1.0
 0.0  0.1 0.0  0.0  0.5 0.0  0.0 -.8  0.0  0.0  0.2 0.0  0.1 0.0 0.0 0.0 0.0  0.2 1.0
 0.0  0.0 1.0  0.0  0.0 0.0 0.0 0.0  -.4  0.0  0.0 0.0 0.0 0.7 0.0 0.7  0.0 0.0 1.0
  0.8  0.2  0.2  0.6  0.3 0.2 -.1 -.1 0.0  0.8  0.4  0.5  0.2  0.2  0.8  0.1 0.0  0.2  0.2 1.0
 X 1 X 2 X 3 1* 1 1* 2 1* 3 2* 2 2* 3 3* 3 1^32*1^21*2^22*33*1^21*3^23*2^22*3^21*2*33^3 Y 1

- ENTER ORDER OF POLYNOMIAL :
  2
- WEIGHTING MODE : NO WEIGHTING
- ALL COEFFICIENTS SET TO  1.0000E+00
- ENTER RELATIVE ACCURACY REQUIRED :
  1.000E-05
- ENTER MAXIMUM NUMBER OF ITERATIONS :
       9

-  3 ITERATIONS
```

- ELAPSED TIME : 13 SEC

- MODEL COEFFICIENTS	STD ERROR	F-RATIO
.099585 = A(1) +/-	.020138	24.5
.070826 = A(2) +/-	.012808	30.6
.025285 = A(3) +/-	.011996	4.4
.017576 = A(4) +/-	.010757	2.7
.036516 = A(5) +/-	.010770	11.5
-.016019 = A(6) +/-	.010478	2.3
.020388 = A(7) +/-	.011471	3.2
.022447 = A(8) +/-	.010774	4.3
-.006900 = A(9) +/-	.010763	.4
.006829 = A(10) +/-	.011000	.4

- CHI SQUARE = 1.8528E-03

- EXTREMUM IS NOT IN WINDOW.

POINT #	DATA	RESIDUAL	FIT	RELATIVE RESIDUAL
1	.0880	.0016	.0896	.0182
2	.0810	.0086	.0896	.1062
3	.0810	.0086	.0896	.1062
4	.0940	-.0044	.0896	-.0468
5	.1040	-.0144	.0896	-.1385
6	.0390	.0170	.0560	.4349
7	.1000	.0442	.1442	.4418
8	.3560	-.0002	.3558	-.0006
9	.0520	-.0359	.0161	-.6906
10	.2170	-.0108	.2062	-.0498
11	.0620	.0151	.0771	.2441
12	.0450	.0316	.0766	.7020
13	.1100	-.0252	.0848	-.2294
14	.0420	.0124	.0544	.2948
15	.0450	.0460	.0910	1.0225
16	.3920	-.0332	.3588	-.0846
17	.0420	-.0609	-.0189	-1.4507

- LEAST-SQUARES REGRESSION ANALYSIS :

SOURCE	SUM OF SQUARES	DEGREES OF FREEDOM	MEAN SQUARE	F-RATIO
REGRESSION	.1691	9	.0188	10.1
RESIDUAL	.0130	7	.0019	

PURE ERROR	.0004	4	.0001	
LACK OF FIT	.0126	3	.0042	44.5
TOTAL	.1821	16	.0114	

ADJUSTED R2 : .84
CALCULATED REGRESSION = .1691 AND TOTAL = .1821
- END PROGRAM LSIFIT.

MAPPING.F input file (with second order polynomial function POLY)

```
3
10
Power (Watts/cm2)
Pressure (Torr)
Fraction of CF3Cl
    .087000    .715000    .721011   -.144998  1
    .300000    .900000    .707107   0.000000  2
    .738000    .956000    .712193    .087426  3
1
Etch rate (µm/min)
  .099585 = A( 1) +/-   .020138
  .070826 = A( 2) +/-   .012808
  .025285 = A( 3) +/-   .011996
  .017576 = A( 4) +/-   .010757
  .036516 = A( 5) +/-   .010770
 -.016019 = A( 6) +/-   .010478
  .020388 = A( 7) +/-   .011471
  .022447 = A( 8) +/-   .010774
 -.006900 = A( 9) +/-   .010763
  .006829 = A(10) +/-   .011000
```

MAPPING.F contour plot :

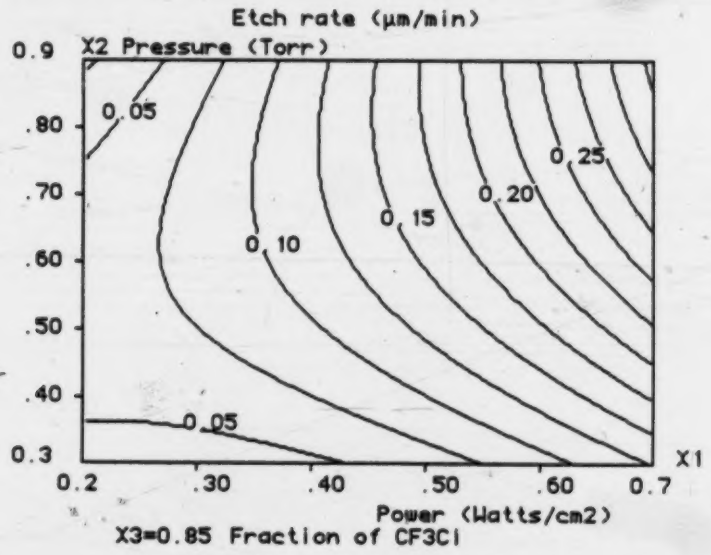

9) References

[1] "Statistics for Experimenters", George E.P. Box, William G. Hunter, J.Stuart Hunter, John Wiley & Sons N.Y., 1978

[2] "Data Reduction and Error Analysis for the Physical Sciences", Philip R. Bevington, McGraw-Hill N.Y., 1969

[3] "Applied Regression Analysis, Second Edition", Norman Draper, Harry Smith, John Wiley & Sons N.Y , 1966

[4] "Process Improvement With "Simplex" Self-Directing Evolutionary Operation", B.H. Carpenter, H.C. Sweeny, Chemical Engineering, July 5, 1965

[5] Analytical Chemistry, Vol 45, No. 3, March 1973

[6] "The Modeling of Plasma Etching Processes Using Response Surface Methodology", Solid State Technology, April 1986, pp. 175-182

APPENDIX B, FCC & NESTED FCC-BOX-BEHNKEN DESIGNS

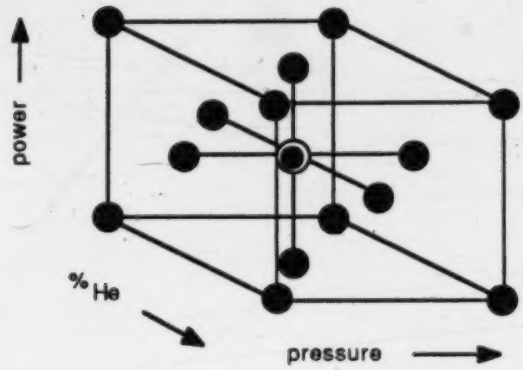

FCC design
15 points

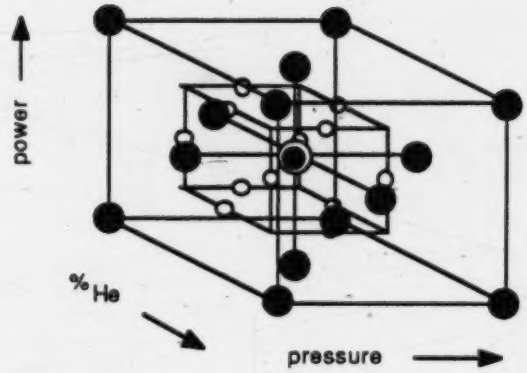

Nested
FCC-Box-Behnken
designs
27 points

APPENDIX C, GLOW DISCHARGE LUMINESCENT INTENSITY

Derivation of the expression relating the spectrometer readings with the luminescent intensity of the glow discharge. The glow discharge as seen by the optical sensor is depicted in the drawing of Fig. C1.

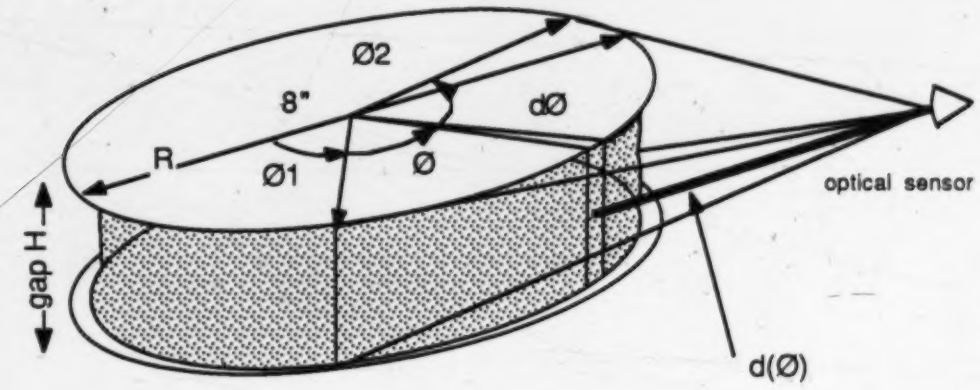

Fig. C1) Position of the tip of the fiber optic (optical "sensor") with respect to the glow region (dotted area) contained between two parallel plates.

The detector receives light from a portion of the glow surface which angle is Ø2-Ø1. The intensity of an infinitesimal element of the glow surface is :

$$\Delta i = \Delta I_{\mu}\, H \cdot R \cdot d\emptyset \quad [\text{Watts}] \qquad (C1)$$

where ΔI_{μ} is the flux of energy ($J \cdot m^{-2} \cdot sec^{-1}$) crossing the glow surface, H the glow height and R the glow radius. At d(Ø), the distance from the glow surface to the sensor at an angle Ø, the intensity emitted from the element of surface is spread over the area of the sphere of radius d(Ø) given by $4\pi d(\emptyset)^2$. Therefore the intensity received by the detector is now given by :

$$\Delta i_{d(\emptyset)} = \Delta I_{\mu}\, H \cdot R \cdot d\emptyset / (4\pi\, d(\emptyset)^2) \qquad [\text{Watts} \cdot m^{-2}] \qquad (C2)$$

It is assumed that $d(\emptyset) \gg H/2$ so that $d(\emptyset)$ is pretty much constant along the glow height. Otherwise Δi should be restricted to a portion dH of the height and the integration over the surface should be carried out along the height as well. The total intensity the detector receives is therefore given by :

$$I_\mu = (\Delta I_\mu \, H \cdot R / 4\pi) \int 1/ d(\emptyset)^2 \, d\emptyset \qquad [Watts \cdot m^{-2}] \qquad (C3)$$

where the integral expands from $\emptyset 1$ to $\emptyset 2$. The intensity received by the detector is also related to the number of photon counts :

$$I_\mu = N_\mu \, h\mu/(At_s C(\mu)) \qquad (C4)$$

where N_μ is the number of counts at frequency μ when the background is subtracted. A is the sensor sensitive area, t_s the sampling time and $C(\mu)$ the detector response in counts per photon at frequency μ. As a result, the flux of photons escaping the plasma at the glow surface at frequency μ is given by :

$$\Delta I_\mu = \left[4\pi h\mu/(HRAt_s C(\mu) \int 1/ d(\emptyset)^2 \, d\emptyset) \right] N_\mu \qquad [Watts \cdot m^{-2}] \qquad (C5)$$

Let us calculate the integral for the Lam etcher. The detector is placed behind the reactor rear quartz window as shown in Fig. C2. The parameters used to locate the sensor with respect to the glow region are : the distance D between the electrode and the line parallel to the window and passing by the sensor position, and E the distance the sensor is off-center. $d(\emptyset)$ must be related to D and E and the electrode radius R. The sensor "sees" a portion of the glow delimited by the angles $\emptyset 1$ and $\emptyset 2$ also related to D, E and R.

$d(\emptyset)$ is part of a triangle defined by $L=(D^2 + E^2)^{1/2}$, $P = 2 \cdot R \cdot tg((\emptyset - \pi/2)/2)$ and $\Omega = \pi - \beta - ((\pi - (\emptyset - \pi/2))/2) = \pi/4 - arctg(E/D) + \emptyset/2$ (see Fig. C3), furthermore :

$$d(\emptyset) = (L^2 + P^2 - 2 \cdot LP \cdot \cos \Omega)^{1/2}$$
$$= (D^2 + E^2 - 4 \cdot R(D^2 + E^2)^{1/2} \, tg((\emptyset - \pi/2)/2) \cdot \cos(\pi/4 - arctg(E/D) + \emptyset/2))^{1/2} \qquad (C6)$$

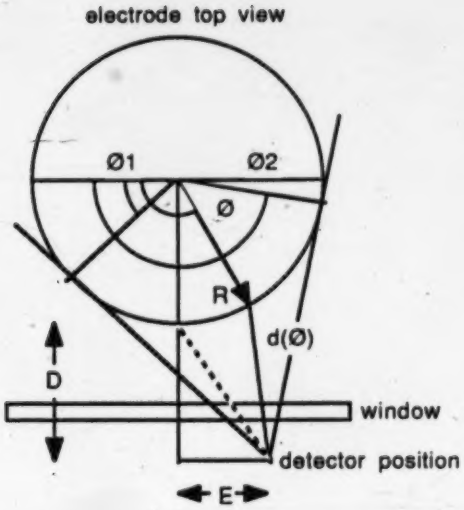

Fig. C2) Top view of the reactor showing the position of the optical sensor with respect to the electrodes.

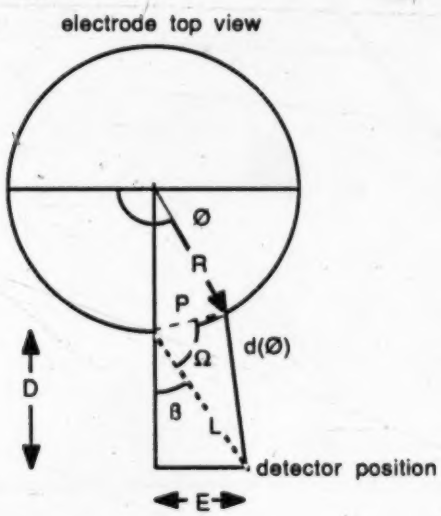

Fig. C3) Top view of the reactor showing the position of the optical sensor with respect to the electrodes.

Ø1 and Ø2 are determined as follows. The angle a is given by (Fig. C4) :

$$a = \text{arctg}(E/(D+R)) \quad \text{(C7)}$$

$$Ø1 = \pi/2 + a - \arccos(R/(R+d(a))) \quad \text{(C8)}$$

$$Ø2 = \pi/2 + a + \arccos(R/(R+d(a))) \quad \text{(C9)}$$

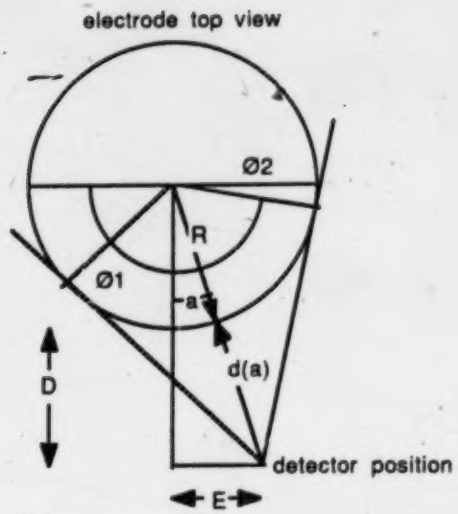

Fig. C4) Top view of the reactor showing the position of the optical sensor with respect to the electrodes.

Let us define S the integral :

$$S = \int 1/d(\emptyset)^2 \, d\emptyset \qquad \text{(C10)}$$

where the integration is taken from Ø1 to Ø2. d(Ø) (equ. C6), Ø1 and Ø2 (equ. C7-C9) have been expressed in terms of D, E and R. The integration can be advantageously calculated numerically for any particular position of the detector. Typically, for an 8 inch electrode, D=7 cm and E=4 cm, one finds S=2283 m^{-2}.

APPENDIX D, CHEMICAL KINETICS REACTION SCHEME

Input data for FORTRAN program "chemk" [40]. Relations 1 to 49 are the reactions from Plumb and Ryan [32]. The other relations are the feeding and pumping parameters.

#	reactants		products	rates A	parameters S, F, A1, S1
1	CF4	-e->	CF3 + F	1.7359	0.0 -1.0 259.4 900.
2	CF4	-e->	CF2 + F + F	4.0504	0.0 -1.0 259.4 900.
3	CF3	-e->	CF2 + F	5.7863	0.0 -1.0 259.4 900.
4	CF2	-e->	CF + F	5.7863	0.0 -1.0 259.4 900.
5	CF3 + CF3	-M->	C2F6	2.8e-23	0.0 0.32 8.3e-12
6	CF3 + F	-M->	CF4	7.7e-27	0.0 0.63 2.0e-11
7	CF2 + CF2	--->	C2F4	5.e-14	
8	CF2 + F	-M->	CF3	3.0e-29	0.0 0.73 1.3e-11
9	CF + F	-M->	CF2	3.2e-31	0.0 0.72 1.0e-11
10	C2F6	-e->	CF3 + CF3	5.7863	0.0 -1.0 259.4 900.
11	C2F4	-e->	CF2 + CF2	5.7863	0.0 -1.0 259.4 900.
12	F + C2F4	--->	CF3 + CF2	4.e-11	
13	CF2 + CF3	-M->	C2F5	2.3e-26	0.0 0.39 1.0e-12
14	C2F5+F	--->	CF3 + CF3	1.e-11	
15	CF + CF2	--->	C2F3	1.e-12	
16	C2F3+F	--->	C2F4	1.e-12	
17	O2	-e->	O + O	1.8805	0.0 -1.0 259.4 900.
18	O2	-e->	O + OD	2.1699	0.0 -1.0 259.4 900.
19	O2	-e->	OM + O	1.7359	0.0 -1.0 259.4 900.
20	OD + O2	--->	O + O2	4.e-11	
21	OD + CF4	--->	O + CF4	1.8e-13	
22	OD + COF2	--->	O + COF2	5.3e-11	
23	OD + COF2	--->	F2 + CO2	2.1e-11	
24	OD	-w->	O	2.e3	
25	O + OM	--->	O2	3.e-10	
26	O	-e->	OM	1.447e3	0.0 -1.0 259.4 900.
27	CF3 + O	--->	COF2+F	3.1e-11	
28	CF2 + O	--->	COF + F	1.4e-11	
29	CF2 + O	--->	CO + F + F	4.e-12	
30	COF + O	--->	CO2 + F	9.3e-11	
31	COF + F	-M->	COF2	6.5e-29	0.0 0.68 1.4e-11
32	CF3 + O2	-M->	CFO2	3.5e-29	0.0 0.49 8.0e-12
33	CF3O2 + O	--->	COF2+F + O2	1.e-11	
34	CF3O2	-e->	CF3 + O2	5.7863	0.0 -1.0 259.4 900.
35	F2	-e->	F + F	5.7863	0.0 -1.0 259.4 900.
36	COF2	-e->	COF + F	5.7863	0.0 -1.0 259.4 900.
37	CO2	-e->	CO + O	11.573	0.0 -1.0 259.4 900.
38	F + CO	-M->	COF	8.1e-32	0.0 0.73 9.4e-11
39	F + O2	-M->	FO2	1.6e-32	0.0 0.70 3.0e-11
40	F + FO2	--->	F2 + O2	5.e-11	
41	O + FO2	--->	FO + O2	5.e-11	